UNIVERSIDADE DE SÃO PAULO
ESCOLA DE ENGENHARIA DE SÃO CARLOS

Ícaro Ostan

Haptic Feedback through Lower Limbs Exoskeleton for Rehabilitation Robotics with Virtual Reality

São Carlos

2021

Ícaro Ostan

Haptic Feedback through Lower Limbs Exoskeleton for Rehabilitation Robotics with Virtual Reality

Master's Thesis submitted to the São Carlos School of Engineering, University of São Paulo, in partial fulfillment of the requirements for the degree of Master of Science - Mechanical Engineering Graduate Program.

Research Area: Dynamics and Mechatronics

Advisor: Prof. Dr. Adriano Almeida Gonçalves Siqueira

REVISED VERSION
VERSÃO CORRIGIDA

São Carlos
2021

Catalog card prepared by Patron Service at "Prof. Dr. Sergio Rodrigues Fontes" Library at EESC/USP

O85h

Ostan, Ícaro
Haptic feedback through lower limbs exoskeleton for rehabilitation robotics with virtual reality / Ícaro Ostan ; Thesis directed by Adriano Almeida Gonçalves Siqueira. -- São Carlos, 2021.

Master (Thesis) Graduate Program in Mechanical Engineering and Research Area in Dynamic and Mechatronics -- São Carlos School of Engineering, at University of São Paulo, 2021.

1. Rehabilitation robotics. 2. Virtual reality. 3. Haptic feedback. 4. Presence. 5. Impedance control. I. Title.

Elena Luzia Palloni Gonçalves – CRB 8/4464

FOLHA DE JULGAMENTO

Candidato: Engenheiro **ÍCARO OSTAN.**

Título da dissertação: "*Feedback* háptico por meio de exoesqueleto de membros inferiores para fisioterapia robótica com realidade virtual".

Data da defesa: 07/06/2021.

Comissão Julgadora	**Resultado**
Prof. Associado **Adriano Almeida Gonçalves Siqueira (Orientador)** (Escola de Engenharia de São Carlos/EESC-USP)	APROVADO
Prof. Dr. **Anselmo Frizera Neto** (Universidade Federal do Espírito Santo/UFES)	APROVADO
Prof. Dr. **Eduardo Lázaro Martins Naves** (Universidade Federal de Uberlândia/UFU)	APROVADO

Coordenador do Programa de Pós-Graduação em Engenharia Mecânica:
Prof. Associado **Adriano Almeida Gonçalves Siqueira**

Presidente da Comissão de Pós-Graduação:
Prof. Titular **Murilo Araujo Romero**

ACKNOWLEDGEMENTS

I would like to first thank my mother and my sister, who, despite my detachment from home, provided me with the most support at their range.

I also would like to thank my friends, with whom I could share my achievements. Thanks to them, I could recognize better the results of my efforts.

I am also grateful to Adriano, my advisor, for all the guidance over the years, and for providing me the opportunity to be his teaching assistant over two semesters.

I would like to express my gratitude to my laboratory colleagues, who passed on to me their experience, provided me useful technical advice, and a pleasing working environment.

I wish to acknowledge the financial support provided by CNPq, without which I would not be able to carry out this project.

Finally, I would like to thank the people that direct or indirectly assisted me and was present during the development of this work, such as the undergraduate students I had the pleasure to assist during the control systems courses.

"A aproximação, do que quer que seja, se faz gradualmente e penosamente — atravessando inclusive o oposto daquilo que se vai aproximar." [1]

C. Lispector

[1] The approach, of whatever it may be, happens gradually and painstakingly — even passing through the opposite of what it approaches. (Translation by Idra Novey.)

ABSTRACT

Ostan, Í. **Haptic Feedback through Lower Limbs Exoskeleton for Rehabilitation Robotics with Virtual Reality**. 2021. 147p. Dissertação (Mestrado) - Escola de Engenharia de São Carlos, Universidade de São Paulo, São Carlos, 2021.

Rehabilitation robotics along with virtual reality presents an interesting scenario to improve the physical rehabilitation process. In order to take full advantage of this technology, it is crucial to deliver an immersive experience. To perform this task, visual, auditory and haptic, or, in general, multisensory feedback interfaces are implemented. While the virtual reality equipment provides visual and auditory stimuli, usually a robotic device provides the haptic stimuli. This work describes the design and implementation of a multisensory feedback system for infinite walk inside virtual reality. A lower limbs robotic exoskeleton was adapted to function as a haptic interface device, at the same time it assisted the user to perform a pre-recorded trajectory. A virtual environment was modeled and created in order to distract the user. Motion tracking was implemented in order to ensure embodiment, thus, a greater feeling of presence. Tests with ten healthy subjects were performed in order to assess the user experience and evaluate the current setup. Three controllers were tested: an impedance controller, which only delivered haptic assistance; a cascade admittance-impedance controller that delivered haptic assistance and feedback, helping the user to perform a trajectory but restraining its range; and a transparency controller, which simply followed the user's movements. Results showed that the cascade controller could track the reference trajectory with similar accuracy as the impedance controller, at the same time it modulated the trajectory to deliver haptic feedback. Furthermore, most physical side effects reported by the users after the experience were due to the exercise rather the exposure to virtual reality; even though this exposure was relatively short, results suggested that the current virtual reality setup is safe and comfortable for an infinite walking task. Regarding immersion and the feeling of presence, spatial presence was the attribute with best results, whereas the involvement and realism were hampered, mainly due to moments of break-in-presence.

Keywords: Rehabilitation Robotics. Virtual Reality. Haptic Feedback. Presence. Impedance Control.

RESUMO

Ostan, Í. **Feedback Háptico por meio de Exoesqueleto de Membros Inferiores para Fisioterapia Robótica com Realidade Virtual**. 2021. 147p. Dissertação (Mestrado) - Escola de Engenharia de São Carlos, Universidade de São Paulo, São Carlos, 2021.

A reabilitação robótica e a realidade virtual apresentam-se como ferramentas diferenciadas que podem assistir na recuperação de pacientes. Para usufruir destas tecnologias ao máximo, é crucial que uma experiência imersiva seja entregue ao usuário. Para tal, interfaces de retroalimentação multissensorial, como visual, auditiva e, menos frequentemente, háptica, são desenvolvidas. Enquanto o equipamento de realidade virtual fornece estímulos visuais e auditivos, geralmente um dispositivo robótico fornece o estímulo háptico. Este trabalho descreve o projeto e implementação de um sistema de retroalimentação multissensorial para caminhada infinita sobre esteira ergométrica dentro de realidade virtual. Um dispositivo robótico de membros inferiores para fisioterapia de marcha foi adaptado para funcionar como uma interface de retroalimentação háptica ao mesmo tempo que fornece assistência para realizar um movimento pré-determinado. Um ambiente virtual foi modelado e criado de forma a distrair o usuário. Técnicas de captura de movimento foram implementadas para garantir incorporação e maior sensação de presença dentro do ambiente virtual. Em sequência, testes com dez indivíduos hígidos foram realizados, de forma a avaliar a configuração de testes atual e a experiência do usuário. Três controladores foram testados: um controlador de impedância, que assistia durante a marcha; um controlador em cascata, que assistia no movimento e também o restringia de forma a simular a interação com o ambiente virtual; e um controlador de transparência, que somente seguia os movimentos do usuário. Resultados mostram que o controlador em cascata segue a trajetória com tanta precisão quando o de impedância, ao mesmo tempo que modula a trajetória para considerar a interação virtual, fornecendo retroalimentação háptica. Além disso, a maioria dos efeitos colaterais relatados durante a experiência restringiram-se à atividade física; embora o tempo de exposição à realidade virtual tenha sido curto, os resultados sugerem que a configuração atual é segura e confortável para caminhada infinita. Em se tratando da imersão e da sensação de presença, o atributo de presença espacial foi a sensação mais forte durante a experiência, ao passo que o envolvimento e o realismo foram as componentes mais prejudicadas, devido aos momentos de quebra de presença.

Palavras-chave: Reabilitação Robótica. Realidade Virtual. Retroalimentação Háptica. Presença. Controle de Impedância.

LIST OF FIGURES

LIST OF TABLES

LIST OF ABBREVIATIONS AND ACRONYMS

AC	Admittance Controller
AIP	Autonomy, Interaction and Presence
AR	Augmented Reality
AV	Augmented Virtuality
BIP	Break-in-Presence
CAAE	Certificado de Apresentação de Apreciação Ética
CAN	Controller Area Network
CAPES	Coordenação de Aperfeiçoamento de Pessoal de Nível Superior—Brazil
CAVE	Cave Automatic Virtual Environments
CCD	Cyclic Coordinate Descent
CEAS	Centro de Engenharia Aplicada à Saúde
CNPq	Conselho Nacional de Desenvolvimento Científico e Tecnológico
CoM	Center of Mass
CVA	Cerebrovascular Accident
DLR	Deutsche Zentrum für Luft- und Raumfahrt
DoF	Degrees-of-freedom
EESC	Escola de Engenharia de São Carlos
FAPESP	Fundação de Amparo à Pesquisa do Estado de São Paulo
FES	Functional Electrical Stimulation
FIR	Finite Impulse Response
FOV	Field of View
GVRFQ	Gaming and Virtual Reality Familiarity Questionnaire
HFQ	Haptic Feedback Questionnaire
HMD	Head-Mounted Display

HTC	High Tech Computer
IC	Impedance Controller
IK	Inverse Kinematics
IPD	Interpupillary Distance
IPQ	iGroup Presence Questionnaire
KF	Kalman Filter
LWR	Light-Weight Robot
MS	Motion Sickness
MSSQ	Motion Sickness Susceptibility Questionnaire
MT	Modes of Transportation
PGPTA	Pesquisa Científica e Tecnológica em Tecnologia Assistiva
PID	Proportional-Derivative-Integrative
ReRob Lab	Rehabilitation Robotics Laboratory
rSEA	Rotary Series Elastic Actuator
SCI	Spinal Cord Injury
SEA	Series Elastic Actuator
SPI	Serial Peripheral Interface
SRPAR	SEA-based Robotic Platform for Ankle Rehabilitation
SSQ	Simulator Sickness Questionnaire
SUS	Slater, Usoh and Steed
TC	Transparency Controller
USP	Universidade de São Paulo
VE	Virtual Environment
VR	Virtual Reality
WHO	World Health Organization
WS	Witmer & Singer

LIST OF SYMBOLS

s	Laplace variable
$Z(s)$	Impedance transfer function
$Y(s)$	Admittance transfer function
$F(s)$	Force transfer function
$X(s)$	Position transfer function
$\mathbf{e}$, e	Error
$\mathbf{M_d}$, M_d	Desired inertia
$\mathbf{B_d}$, B_d	Desired damping
$\mathbf{K_d}$, K_d	Desired stiffness
$\mathbf{M_{adm}}$, M_{adm}	Admittance controller inertia
$\mathbf{B_{adm}}$, B_{adm}	Admittance controller damping
$\mathbf{K_{adm}}$, K_{adm}	Admittance controller stiffness
$\mathbf{M_{imp}}$, M_{imp}	Impedance controller inertia
$\mathbf{B_{imp}}$, B_{imp}	Impedance controller damping
$\mathbf{K_{imp}}$, K_{imp}	Impedance controller stiffness
$\mathbf{M_{env}}$, M_{env}	Environment inertia
$\mathbf{B_{env}}$, B_{env}	Environment damping
$\mathbf{K_{env}}$, K_{env}	Environment stiffness
M_r	Conceptual model robot inertia
B_r	Conceptual model robot damping
$\mathbf{x}$, x	Measured end-effector position in Cartesian coordinates
$\mathbf{x_{env}}$, x_{env}	Environment position in Cartesian coordinates
$\mathbf{x_d}$, x_d	Desired end-effector position in Cartesian coordinates
$\mathbf{x_e}$, x_e	Position error in Cartesian coordinates

$\mathbf{x_r}$, x_r	Admittance control output displacement
$\mathbf{F_a}$, F_a	Actuator force
$\mathbf{F_{ext}}$, F_{ext}	External forces
$\mathbf{F_{env}}$, F_{env}	Environment forces
$\mathbf{F_d}$, F_d	Desired force at end-effector
$\mathbf{F_e}$, F_e	Force error
$\mathbf{F_r}$, F_r	Impedance control output force
$\mathbf{q}$, q	Exoskeleton joint displacements
$\mathbf{q_e}$, q_e	Joint error
$\mathbf{q_d}$, q_d	Desired joint position
$\mathbf{q_r}$, q_r	Admittance control output joint displacement
$\tau_\mathbf{a}$, τ_a	Actuator torque
$\tau_\mathbf{ext}$, τ_{ext}	External torque
$\tau_\mathbf{env}$, τ_{env}	Environment torque
$\tau_\mathbf{d}$, τ_d	Desired torque at joint
$\tau_\mathbf{e}$, τ_e	Torque error
$\tau_\mathbf{r}$, τ_r	Impedance control output torque
$\mathbf{k_p}$, k_p	PID proportional gain
$\mathbf{k_i}$, k_i	PID integrative gain
$\mathbf{k_d}$, k_d	PID derivative gain
$\mathbf{a}$	Exoskeleton links length
$\mathbf{l}$	Exoskeleton links center of mass
$\mathbf{m}$	Exoskeleton links inertia
g	Gravity acceleration
t	Continuous time
t_i, t_f	Arbitrary time interval (initial and final time)

Δt	Discrete time-step
k	Time step index
$\mathrm{L}(\mathbf{q})$	Forward kinematics operation
$\mathrm{L}^{-1}(\mathbf{q})$	Inverse kinematics operation
$\mathbf{H}(\mathbf{q})$	Robot inertia matrix
$\mathbf{C}(\mathbf{q}, \dot{\mathbf{q}})$	Coriolis forces
$\mathbf{G}(\mathbf{q})$	Gravitational forces matrix
$\mathbf{F_v}$	Viscous friction forces matrix
$\mathbf{F_c}$	Coulomb friction forces matrix
$\mathrm{J}(\mathbf{q})$	Jacobian matrix

CONTENTS

1 INTRODUCTION

This Master's thesis investigates the use of virtual reality in the context of rehabilitation robotics by casting a light on the current state of these technologies and their recent applications. Further, the focus is directed towards haptic feedback as a means of enhancing physical therapy. By including haptic feedback together with visual and auditory cues, multisensory feedback systems are envisioned, which are proved to enhance patient recovery through somatosensory feedback. As off-the-shelf virtual reality equipment already provides immersive visual and auditory cues, this thesis focus on haptic stimuli. Herein, a haptic interface system, based on interaction control theory, is proposed by changing the control architecture of a lower limbs exoskeleton already employed for gait rehabilitation research. In this chapter, the motivations behind this thesis, the context in which it is inserted, as well as the objectives and the outcomes that thus far stemmed from the development of this project are presented.

1.1 Motivation

The latest World Health Organization (WHO) report on disabilities states that, as average life expectancy increases, the number of people with disabilities rises. Moreover, the report also states that motor impairment is not restrict to victims of cerebrovascular accident (CVA), also known as stroke, or spinal cord injury (SCI); in fact, most people, at some point in life, can be affected by some sort of temporary disability.

Therefore, both population growth and life expectancy are critical factors that affect health institutions, particularly the ones aimed to physical rehabilitation, due to an increasing demand. As a result, new strategies to enhance the practice of physical therapy, denominated assistive technologies, have been envisioned to offer advantages over the traditional methods, either by leading to better results within the same amount of therapy sessions, or by reducing, substituting or supplementing support devices and services, possibly reducing care costs (ORGANIZATION, 2011).

With that in mind, two kinds of technologies stand out as they explore ways to enhance the practice of physical therapy. On the one hand, there are robotic devices, which can guarantee movement precision; and on the other hand, there are virtual reality applications, which provide an engaging environment for the completion of motor tasks.

Rehabilitation robotics consists of the practice of physical therapy with the aid of robotic devices. The robotic devices do not have to be necessarily wearable, but, in the circumstance they are, they can function as prostheses or orthoses. Exoskeletons are included in this latter category. In general, these robotic devices are capable of not only

Figure 1 – A few rehabilitation robotic devices. (a) LWR KUKA for medical purposes. (b) Lokomat developed by Hocoma, Switzerland. (c) Lower limbs exoskeleton ExoTao developed at EESC-USP ReRobLab. (d) ARMin 7-DOF robotic exoskeleton. (e) SRPAR, also developed at EESC-USP ReRobLab.

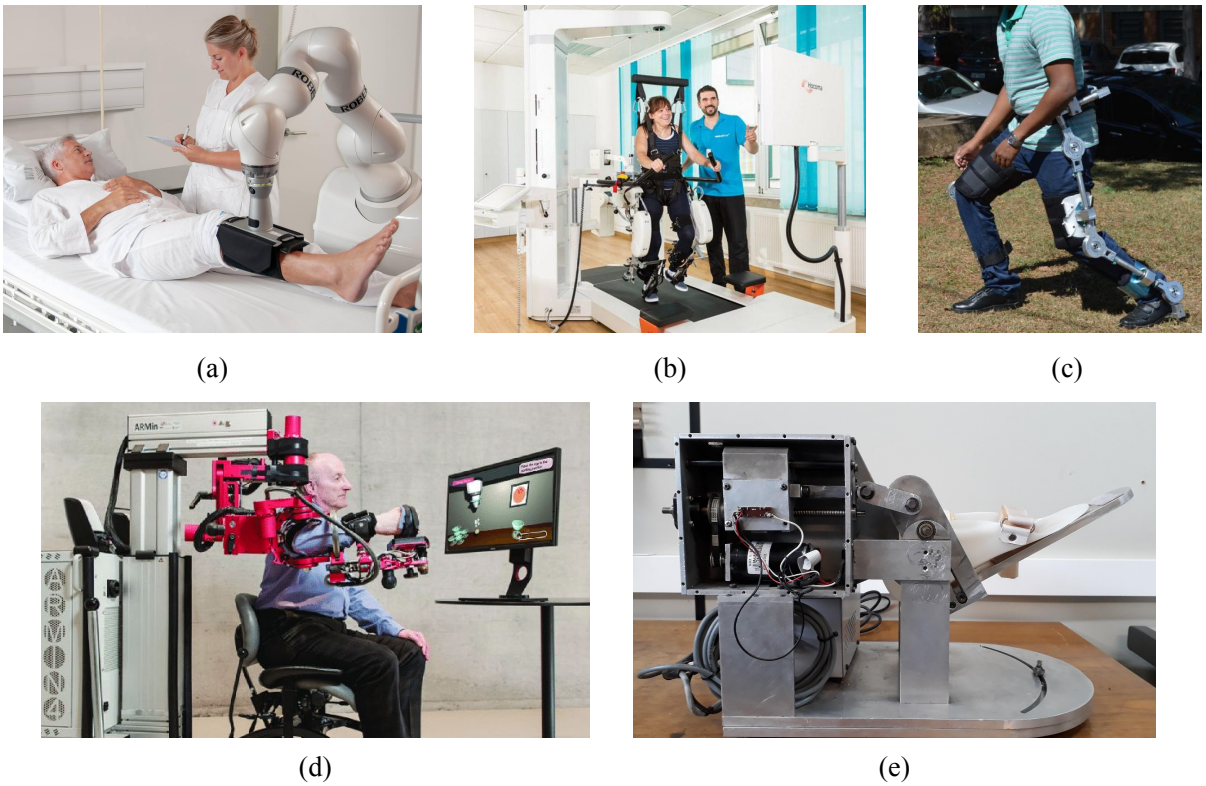

Source: (a) (KUKA AG, 2020). (b) (HOCOMA, 2020). (c) (SANTOS *et al.*, 2017). (d) (MARCHAL-CRESPO *et al.*, 2017). (e) Author (2021).

supporting the body parts of patients, but also of increasing their range of motion and strength (PONS, 2008).

Among the advantages of rehabilitation robotics, one can cite the regularity while performing exercises; continuous data gathering, which guarantees an objective evaluation of the patient progress over time; smaller dependence on human resources and specialized personnel when compared with traditional physiotherapy methods; and finally, the provision of a meaningful and engaging context for physiotherapy, specially in the case rehabilitation robotics is employed with serious or exercising games (also known as exergames), a scenario in which the patient's progress can be both scored and documented, enhancing the therapy (FRISOLI *et al.*, 2007).

Figure 1 presents a few robotic devices aimed for medical purposes. Besides robotic devices from laboratories abroad, the figure also shows robots developed at the Rehabilitation Robotics Laboratory (ReRobLab) located in the São Carlos School of Engineering (EESC), University of São Paulo (USP), as well as commercial solutions. In the first row,

left, a lightweight robot (LWR) KUKA is depicted lifting the leg of a patient, illustrating one of the advantages of using robots in this context: while the robot carries the patient's body weight, the healthcare professional can focus on other tasks. It is important to emphasize that robots do not intent to replace healthcare professionals, but rather help them in tasks in which robots excel. This example also shows how a robot, first designed for industrial purposes, can also be applied to support medical services. In the second figure, in the center, Hocoma's Lokomat robot designed for gait therapy is depicted. The patient wears the robotic exoskeleton while a mechanical structure supports the weight of the human and the robot. At the same time, the user walks on a treadmill, while watching a computer screen. Usually, games or other engagement features are being shown on the screen for the patients, in order to motivate them. In the far right, the lower limbs exoskeleton ExoTao, developed at EESC-USP, is depicted, the robot used in this work. In the second row, left, the ARMin-7-DOF robot, for upper limbs rehabilitation, is shown. This example illustrates how robots are also applied for upper limbs rehabilitation in conjuction with games being displayed to the patients on a computer screen, as with the Lokomat example. Finally, in the right, the SEA-based Robotic Platform for Ankle Rehabilitation (SRPAR), also developed at EESC-USP is depicted. The actuator of this robot is compliant, likewise ExoTao's actuator, and the platform itself was used to test multisensory feedback strategies (VILLAMIZAR *et al.*, 2020), while this present work was developed.

Meanwhile, virtual reality (VR), according to the Merriam-Webster (2020) dictionary, is defined as "an artificial environment which is experienced through sensory stimuli provided by a computer and in which one's actions partially determine what happens in the environment". It is important to notice that VR does not comprise only the virtual environment itself, but also the collection of technologies, regarding hardware and software, crucial to maintain the illusion of being somewhere else (PARISI, 2015). Over the last decade, VR has been extensively used for many applications, mainly due to the availability of consumer-grade VR hardware, such as Oculus Rift[1], HTC Vive[2], and Playstation VR[3]. Nowadays, VR is employed worldwide for a variety of purposes, such as scientific data visualization; architecture and product design; flight simulation; design review; training; entertainment; engineering analysis; and therapy (JERALD, 2016).

Figure 2 depicts some of the aforementioned examples. In the first row, left, VR is employed for data visualization purposes, at the University of California, San Diego (UCSD). In the center, a study performed by the author on how to track the lower limbs movements is depicted (OSTAN; SIQUEIRA, 2019a); the hip and knee joint displacements are estimated by means of an inverse kinematics (IK) algorithm, which

[1] <https://www.oculus.com/>
[2] <https://www.vive.com/us/>
[3] <https://www.playstation.com/en-us/ps-vr/>

Figure 2 – A few VR applications. (a) Scientific visualization of protein molecules. (b) Embodiment of lower limbs and (c) game application for SRPAR at EESC-USP ReRobLab. (d) Training for safety hazard and emergency situations. (e) iLAST (Immersive Leg Coordination and Strength Therapy) project.

Source: (a) (SCHULZE, 2006). (b) (OSTAN; SIQUEIRA, 2019a). (c) (VILLAMIZAR *et al.*, 2020). (d) (TECHNOLOGIES, 2020). (e) (WÜRZBURG, 2018).

uses an approximated position of the user's feet to perform the estimation. In the far right, VR is employed together with the SRPAR, as a means of engaging the user during the exercise, a project implemented by the author and the members of the EESC-USP ReRobLab (VILLAMIZAR *et al.*, 2020). In the second row, left, VR is shown as a means of training for emergency situations; this illustrates how VR can veer from reality and simulate situations which cannot easily be replicated in the physical world, highlighting the versatility of VR. In the right, it is shown that VR alone can also be used as a means of promoting a more engaging lower limbs rehabilitation session. It can be seen that even though there are no robotic devices in this case, tracking the movements is fundamental to use VR for rehabilitation purposes.

In the context of motor rehabilitation, VR has been largely used alone or with robotic devices. The main advantage of using VR in this case derives from the fact that it can engage users in a safe, restrained and controlled environment, while maintaining

experimental control over the stimuli delivered to the patient in real-time. The standardization of assessment and training protocols are also mentioned as an advantage, along with customization of treatment and motivating context for therapy. As with rehabilitation robotics, the data gathered during therapy in the virtual environment (VE) can be instantaneously graded and documented. Moreover, VR can decrease anxiety and increase pain tolerance, an effect yielded also by serious or exergames employed with rehabilitation robots, which enhances the therapy practice (SVEISTRUP, 2005), (MATSANGIDOU *et al.*, 2019).

In order to practice any activity in VR, be it physical therapy or telemanipulation of a robotic arm, the user must be immersed inside the VE. This feeling of being somewhere else, entitled feeling of presence, is fundamental for a comfortable and engaging virtual experience. Generally, sensory feedback interfaces are employed in order to sustain the illusion of presence in the VE while performing a task. However, most of these sensory feedback interfaces consist of visual and auditory feedback only. Haptic feedback, also referred to as tactile feedback, i.e., the sense of touch, granted by haptic interface devices, has been less developed (SVEISTRUP, 2005). This is due to hardware limitations and the emphasis given to the development of new haptic interface designs instead of focusing on existing technology (CLOVER, 1999).

Nevertheless, haptic feedback stands out not only as another source of stimuli for a subject performing exercises in a VE: studies show that sensory feedback in general, capable of increasing presence in VR, can reduce the subject's susceptibility to inconsistencies, which can arise from mechanical limitations of the operated device, while there is also evidence that the strength and robustness of techniques employed to maintain presence correlate positively with dexterous task performance (TOET *et al.*, 2020). In this context, feedback control strategies also intercede to compensate mechanical deficiencies of robotic devices not initially designed for haptic purposes (CLOVER *et al.*, 1997).

1.2 Context

Having in mind the current projects at our facilities, this work plays a role in the "Hybrid Adaptive Control Strategies for Lower Limbs Exoskeleton" research project, as seen in Fig. 3, developed inside EESC-USP ReRobLab, in which VR is to be employed in conjunction with a lower limbs exoskeleton and a functional electrical stimulation (FES) device. The aim is to develop adaptive control strategies based on the muscular activity so that the user's limbs are driven partially by the torque exerted by the robotic exoskeleton device, and partially by the FES signal, which will stimulate specific muscle groups. The aforementioned project is led by Prof. Dr. Adriano de Almeida Gonçalves Siqueira, professor at the Mechanical Engineering Department and head of the Centro de Engenharia Aplicada à Saúde (CEAS). The project team comprises Master's students and

Figure 3 – Diagram of the "Hybrid Adaptive Control Strategies for Lower Limbs Exoskeleton" research project. This Master's thesis focus on the VR block (yellow, top), and presents a control strategy based on the interaction with the VE, so that the haptic feedback generated by the user's avatar interaction with the VE provides a more engaging experience, which is known to enhance physical therapy.

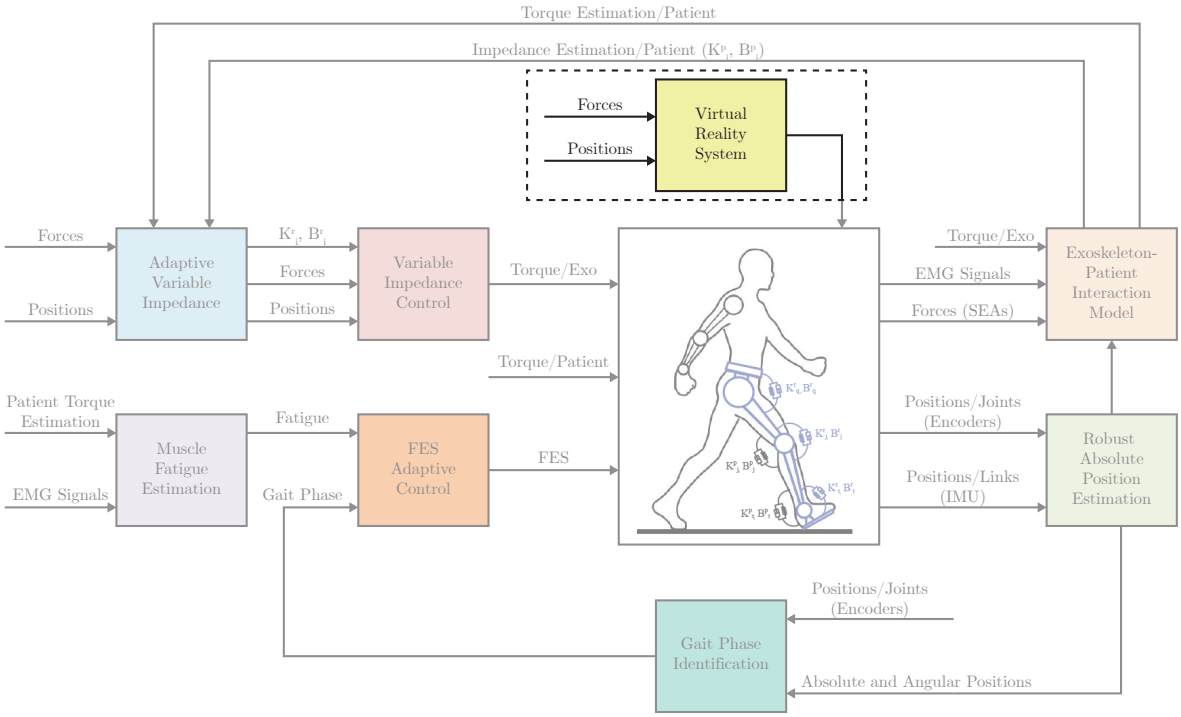

Source: Author (2021).

PhD candidates of the ReRobLab.

This work was developed to study how VR can be used with the existing robotic devices at our facilities. These robots at EESC-USP ReRobLab can respond distinctly according to the control strategy applied to them. Among these strategies, impedance control, for instance, is capable of rendering varying stiffness in respect to the subject's needs. However, there is a lack of applications with causality between the robotic device and the motor task being performed inside the environment where the subject is located. Most applications are restrained to human-robot interaction, i.e., the environment is not contemplated. By including the environment in the context as an agent capable of delivering haptic stimuli, it is expected that the subjects benefit from this new feature, as their presence increases and, consequently, their motor performance.

Over the years of its development, this project was supported by São Paulo Research Foundation (FAPESP) under grant 2019/05937-7, and by Coordenação de Aperfeiçoamento de Pessoal de Nível Superior, Brazil (CAPES) — Finance Code 001, Support Program

for Graduate Studies and Scientific and Technological Research for Assistive Technology in Brazil (PGPTA) and Conselho Nacional de Desenvolvimento Científico e Tecnológico (CNPq).

1.3 General Objective

This work aims at developing a haptic feedback interface to be employed together with VR, creating thus, a multisensory feedback system. Since the lower limbs exoskeleton robot at our facility was not integrated with VR, this project will be an experiment on how this should be executed. Tests with help subjects will elucidate which aspects of the setup must be improved. In practice, it is expected that the multisensory stimuli enhance the feeling of presence in the VE, thus, compensating for eventual limitations of the robotic device. Moreover, there is strong evidence that it will be able to provide a more engaging environment for the practice of physiotherapy, improving it.

1.4 Specific Objectives

In order to accomplish this task, the existing robotic devices aimed for rehabilitation purposes at the facilities of the EESC-USP ReRobLab will be employed as haptic interfaces by means of the proper control system architecture and, in the sequence, will be combined with VR.

With the proper control, the robot will respond to stimuli yielded from its interaction with the VE and virtual objects, at the same time it provides assistance to the completion of a movement. This response should vary according to the physical properties of the modeled environment and the interaction of the subject's avatar with it.

As anticipated, the user will be immersed in VR through a head-mounted display, and will be subjected to visual and auditory cues.

The system will be evaluated directly and indirectly considering the system's response and usual performance criteria, which is either measured, calculated or estimated; and the assessment of the user experience by measuring the user's feeling of presence, side-effects (related to simulator sickness) and the free-form feedback and impressions reported by the subjects during the tests.

These specific objectives are summarized by the items below.

- Review how robots and VR are used together for rehabilitation purposes;
- Adapt the current lower limbs exoskeleton robot at our facilities to deliver haptic feedback, analyzing its performance;
- Develop a VR application which will deliver to the user auditory and visual feedback;

- Test the resulting multisensory (auditory, visual and haptic) feedback system with healthy subjects, analyze results and draw conclusions.

1.5 Contributions

The contributions of this thesis comprise the development of a test setup that combines robotic devices with VR applications, as well as a control strategy that incorporates the VE forces engendered from the interaction of the user's avatar inside VR.

By inserting the user inside the VE with the aid of embodiment techniques, manifold studies can be carried out once the user's kinematic variables (joint angles, center of mass, CoM, coordinates, limbs position) are either measured or estimated based on the variables of the VR equipment being tracked (head and handheld controllers coordinates and orientation). In the case another tracking system is employed (e.g., XSens© Inertial Sensor Modules or the embedded magnetic encoders in the joints of the lower limbs exoskeleton ExoTao, both available at the ReRobLab) the data transmission between external tracking devices is of straightforward implementation, as the visual cues do not require high frame rates, since the head-mounted display through which the user observes the VE refreshes at a frame rate of 90 Hz.

Another more specific contribution is the study of haptic controllers which consider the forces that arise from the interaction between the user's avatar and the VE. In that sense, haptic feedback strategies were studied and an analysis of the robot performance under these circumstances were included. Though it was expected that a robot intended for other purposes rather than to serve as a haptic interface would place some difficulties, the robot performance under some circumstances were satisfactory and technical limitations could be addressed.

1.6 Publications

During the development of this thesis, the author published the following papers as first author that are directly linked to the work here presented:

- **OSTAN, I.**; SIQUEIRA, A. A. G. Motion Capture of a Lower Limbs Exoskeleton for Virtual Reality Application with a Treadmill. *In*: **25th ABCM International Congress of Mechanical Engineering COBEM**. Uberlândia, SP: [*S.l.*: *s.n.*] 2019. DOI: 10.26678/ABCM.COBEM2019.COB2019-0606.

- **OSTAN, I.**; SIQUEIRA, A. A. G. Incorporação de membros inferiores através do algoritmo CCD para prática de terapia física com realidade virtual. *In*: **IV Simpósio do Programa e Pós-Graduação em Engenharia Mecânica da EESC-USP**. São Carlos, SP: [*S.l.*: *s.n.*], 2019. ISSN 2674-8452.

There are other four conference papers and a journal article, in which the author collaborated as second or third author.

- NUNES, P. F.; **OSTAN, I.**; SIQUEIRA, A. A. G. Evaluation of motor primitive-based adaptive control for lower limb exoskeletons. **Frontiers in Robotics and AI**, v. 7,p. 201, 2020. ISSN 2296-9144. Available at: <https://www.frontiersin.org/article/10.3389/frobt.2020.575217>.
- MOSCONI, D.; NUNES, P. F. **OSTAN, I.**; SIQUEIRA A. A. G. Design and validation of a human-exoskeleton model for evaluating interaction controls applied to rehabilitation robotics. *In*: **8th IEEE RAS/EMBS International Conference on Biomedical Robotics & Biomechatronics**. New York, NY: [*S.l.*: *s.n.*], 2020.
- VILLAMIZAR, J. Y. M.; **OSTAN, I.**; ORTEGA, D. A. E. SIQUEIRA, A. A. G. Remote Control Architecture for Virtual Reality Application for Ankle Therapy. *In*: **XXVI Brazilian Congress on Biomedical Engineering, CBEB**. Vitória, ES: [*S.l.*: *s.n.*], 2020.
- NUNES, P. F.; **OSTAN, I.**; DOS SANTOS, W. M.; SIQUEIRA A. A. G. Analysis of Matrix Factorization Techniques for Extraction of Motion Motor Primitives. *In*: **XXVI Brazilian Congress on Biomedical Engineering, CBEB**. Vitória, ES: [*S.l.*: *s.n.*], 2020.
- NUNES, P. F.; MOSCONI, D.; **OSTAN, I.**; SIQUEIRA A. A. G. Control Design Inspired by Motors Primitives to Coordinate the Functioning of an Active Knee Orthosis for Robotic Rehabilitation. *In*: **XXVI Brazilian Congress on Biomedical Engineering, CBEB**. Vitória, ES: [*S.l.*: *s.n.*], 2020.

1.7 Document Structure

Besides this introduction, this work is divided into five more chapters. Chapter 2 presents a literature review on VR, focusing on its applications in rehabilitation and on its aspects related to user experience, e.g., motor task performance, embodiment and comfort. In the sequence, it provides an overview on haptics also in the context of rehabilitation, focusing on haptic interface devices. Some works from the literature are retrieved, and their similarities and differences with this work are highlighted.

Chapter 3 presents the design procedure of the haptic interface. A simplified model of the lower limbs exoskeleton is presented. The model is validated based on experiments on the real hardware under impedance control, the current controller used with the robot. Once the model is validated, a set of virtual environments is described, with which the user wearing the robot will interact. With these interactions in mind, a cascade control architecture is proposed to deliver haptic feedback and assistance to the user. This controller

is tuned, tested on the real hardware, and its performance is compared with the current impedance control architecture.

Thereafter, Chapter 4 lists the hardware and software tools, along with the approaches employed to implement the multisensory feedback system proposed in this work, focusing on the visual stimuli to be delivered by the VR application.

Subsequently, Chapter 5 presents information with respect to the tests results performed on healthy subjects. A discussion of the results obtained is elaborated, considering objective measurements and the personal feedback of each subject.

Finally, Chapter 6 draws some conclusions, summarizes the findings, highlights some particularities of this work and draws future lines of research that may stem from it.

2 LITERATURE REVIEW

This chapter is divided into two parts: virtual reality and haptics. It aims at providing the underlying theory for the comprehension of the present work, along with its terminology and recent applications within the context of physical therapy. Throughout the chapter, many works from the field are retrieved, in order to illustrate how these technologies have been employed by researchers and clinics.

2.1 Virtual Reality Overview

Though it is not a novel technology, the use of virtual reality (VR), or, more generically, extended reality (XR), has been increasing since the last decade, due to the availability of consumer-grade equipment, which is more affordable and can provide a more comfortable experience when compared to former technologies. As it expands, VR has been employed in many fields, where visual feedback plays a significant role, such as rehabilitation. In Section 2.2, some earlier and recent applications of VR within this context are compiled, whether robotic devices are present or not. In Section 2.3, a method to classify and measure qualitatively the components of a VR experience, from a technical perspective, is presented. Following, an overview of the reality-virtuality continuum is elicited in Section 2.4. The continuum was conceived based on a hardware-centric approach, which is employed up to these days. Finally in Section 2.5, in order to comprehend the influence that VR has on the user, some non-technical concepts are presented briefly, together with an explanation on how these cognitive aspects related to VR interplay with robotic devices in order to generate a more engaging physical therapy session, which is the interest of this work.

2.2 Virtual Reality in Physical Rehabilitation

Virtual reality applications[1] aimed for physical therapy have been intensively employed over the last decade along with serious games, i.e., games intended for other purposes rather than entertainment. In VR it is possible to simulate daily tasks such as walking, biking, opening windows, sorting objects, and many other manipulation tasks, everyday activities and even exercises. On the other hand, VR can veer from reality, allowing patients to perform tasks they would not be able to do otherwise. This improves their self-confidence, an important component in healing. Though this work does not intent to study its economic feasibility, VR can reduce costs of rehabilitation through scalability

[1] Virtual reality applications are also referred to as “computer graphics simulations”, “graphics simulations”, “computer simulations” or simply as “simulations”. All these expressions will be used interchangeably throughout this work.

by allowing a single therapist to supervise many remote patients via telerehabilitation (BURDEA; COIFFET, 2003; ORGANIZATION, 2011).

Sveistrup (2005) provides a review on how motor rehabilitation can be enhanced by VR. Her work points out that sensory feedback plays a key role on improving the subject's performance. A more recent review, which considers more extensively the role of robotic devices during physical therapy, was done by Weiss, Keshner and Levin (2014). Besides providing a wide variety of case studies and examples, which are not retrieved in this work to avoid redundancy, they conclude that VR enhances sensory-motor recovery through motivation, engagement and an increased-level of pain resistance, which yield a greater number of repetitions at the same time the application provides salient feedback. As example, a few recent studies confirm these statements (CROCETTA *et al.*, 2017; MATSANGIDOU *et al.*, 2019). Weiss, Keshner and Levin (2014) remark that, if movement quality is desired, a robust movement-tracking system with small latency is a requirement.

As regard to gait, the effects of VR have been studied mainly for two scenarios: treadmill and overground walking. It has been noticed that the gait in VR differs from the gait observed in the real world. These differences dwell on stride length, stride time, stride width, and their respective variances over time, except for stride width. However, as the users familiarize themselves with the VE, most of the discrepancies tend to diminish. Studies also show that the way the gait modifies also varies due to differences among the test setups, e.g., VR equipment used, such as Cave Automatic Virtual Environments (CAVE) or HMD; mode of walking, such as self-paced treadmill, constant-speed treadmill or overground walking; application performance, for instance frame rate, resolution, field of view (FOV); and time given to adapt to the VE. These particularities must be considered when analyzing the user gait performance in VR. The studies conclude that consistent visual depth cues, sufficient FOV and avatar embodiment may help to reduce the gait disparities (MARTELLI *et al.*, 2018).

As mentioned before, when employed together with robotic devices, the latter ones usually play a more significant role during the motor therapy when compared to the former. VR is commonly used as a means of providing visual and, sometimes, auditory feedback (KERN *et al.*, 2019), while the robotic device exerts torque onto the subject's limbs (HAMZEHEINEJAD *et al.*, 2018; HAMZEHEINEJAD, 2019; PARK *et al.*, 2019; BERNARDONI *et al.*, 2019; EISAPOUR *et al.*, 2018; SVEISTRUP, 2005; WEISS; KESHNER; LEVIN, 2014). Moreover, when it comes to performing motor tasks, the most-common approach is to use VR, in spite of mixed or augmented reality. This is due the fact that augmented reality does not provide accurate depth cues as VR does, which can confuse the user during reaching tasks (WENK *et al.*, 2019). Even though lower limbs rehabilitation does not involve explicitly reaching tasks, the depth cues are still relevant and should be present.

Figure 4 – Patient wearing the Lokomat robotic exoskeleton and performing treadmill walking with a HMD, a common setup to achieve infinite straight walking in VR.

Source: Retrieved from (YATES, 2020).

When the users walk on the treadmill inside an infinite VE, they experience what is commonly entitled infinite walking. That seems to be the dominant approach for gait rehabilitation. For treadmill walking, this can be easily implemented. In some cases, the user can perform turns in the VE, which, however, results in a risky approach, as it may trigger motion sickness (MS) (PARK *et al.*, 2015). Figure 4 shows the common setup for this case. Usually, to guarantee better user placement on the treadmill and balance, mechanical structures for partial or total support of the user's weight are employed.

On the other hand, for overground walking, the approach differs. Collision detection and optimal trajectory planning algorithms change the users' point of view imperceptibly in such a way they end up performing a curve in the real world, thus avoiding colliding with the walls of the restrained environment, while having the impression of walking forward in the VE, as depicted in Fig. 5 (SUN *et al.*, 2018). In short, the head of the avatar rotates slightly; in the sequel the user rotates the body to compensate for this undesired (though not constantly perceived) rotation, to keep up walking forward in VR. These slight rotations are performed either when the user experiences brief moments of blindness, e.g., during saccade or blink, or when they are already moving their heads at high speeds, e.g., when they turn aside to depict a virtual object or look for the origin of a foreign ambient sound. In this case, visual and auditory cues are fundamental to stimulate the user's eyes or head motion.

In a similar fashion, this approach is also employed to redirect the users' virtual

Figure 5 – (Left) Visual cues stimulate the user to look at different points, leading to the occurrence of visual saccadic suppresion (momentary blindness). (Right, top) To achieve this, eye tracking is required. (Right, bottom) Virtual (orange) and real (blue) trajectory obtained with redirection algorithm based on saccade and user perspective wrapping.

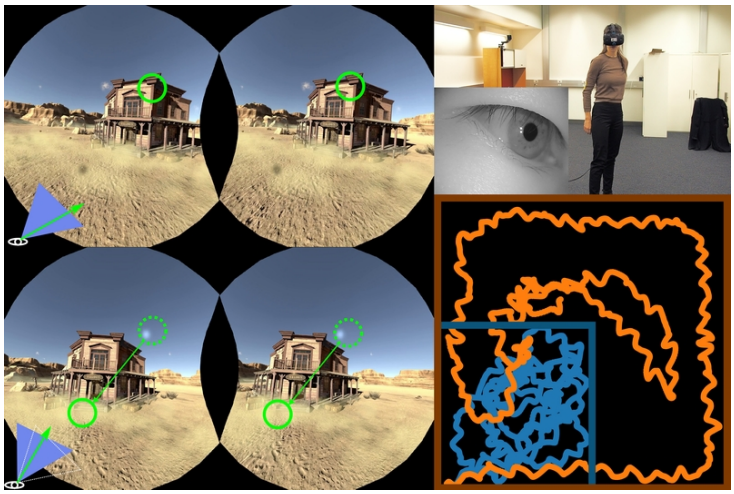

Source: (SUN *et al.*, 2018).

limbs during reaching tasks, so they always grasp the very same physical object whereas, in VR, they see different objects on distinct positions (AZMANDIAN *et al.*, 2016). By doing this, the same physical object provides realistic haptic feedback for different virtual objects, as in Fig. 6. There are, notably, constraints in this approach. All virtual objects must have the same geometric and physical properties, and the physical objects must be tracked in the real world to be placed in the VE, i.e., another tracking system is necessary besides the one tracking the user's body. More haptic feedback techniques are discussed further in Section 2.7.

Studies concluded that the benefits of VR are strongly related to user engagement and immersion. Thus, it is crucial to identify the attributes responsible for motivating and immersing the user. This effort commences by studying the components of a VR experience and end up concluding that haptic feedback, compared to other sensory feedback stimuli, is an overlooked feature up to this day, whose implementation can bring significant improvement to the experience inside VR, including rehabilitation.

2.3 Components of a Virtual Reality Experience

There are distinct ways to classify the components of a VR experience. Though the terminology vary, most definitions match. The taxonomy proposed by Zeltzer (1992) is presented and used throughout this work. It was chosen because it is a fairly broad but accurate way to classify a VE. Recent works in different fields (computer graphics, human-computer interaction, psychology) provide more details that rather complement the overview provided by Zeltzer than outdate it. Though it is a generic, and somewhat

abstract, synthesis, it is a convenient starting point to understand the components of VR.

Zeltzer (1992) proposed three attributes, with which one could classify in a straightforward manner a graphic simulation system (which includes VR). These three attributes are Autonomy, Interaction and Presence, and they form the AIP cube. When considered during the development of an application, these attributes are fundamental to support a consistent VR experience.

Autonomy is defined as the degree at which a computer model act and react to simulated events and stimuli. For example, a simplistic geometric, static model, that does not react when collided with other virtual objects, has no autonomy whatsoever, whilst an ideal physical model, i.e., a virtual object with physical properties such as drag, inertia and stiffness, among other properties, possesses much more autonomy.

Meanwhile, Interaction means the degree of access to model parameters subjected to the user. If one cannot interfere in any properties of a virtual object, there is no interaction. If, for example, the user's actions change shape, position or color of an object, there is some interaction.

Finally, the Presence dimension measures at which degree the input and output channels of the system match the user's channels. That is, the degree of correspondence between what the user experiences in VR and what they feel in the physical world. For instance, if an avatar in VR moves, hears, sees and feels as the user in the real environment, the simulation has a high degree of presence. If the users only see what their avatar sees in VR, then it has a low degree of presence.

However, it is still difficult to measure quantitatively these three components.

Figure 6 – Haptic retargeting experiment. The user perspective and the avatar limbs are redirected so the user has the impression of grasping different objects, whereas there is only one in the real world.

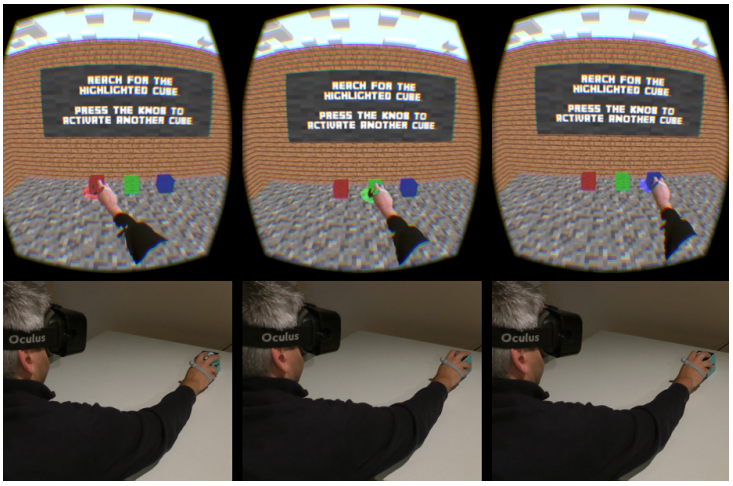

Source: (AZMANDIAN *et al.*, 2016).

Regarding presence, Zeltzer (1992) states that the human sensory system itself and how humans process stimuli and respond to them has to be better understood before implementing better presence techniques.

The Zelter's cube classifies an ideal VR experience by placing it at the coordinates $(1, 1, 1)$, even though most applications fall somewhere near that point, exhibiting some degree of each component. By the way Zelter defines the taxonomy, it seems that only applications that present the outstanding degrees of the three components shall be classified as a VR simulation. However, this is not true. Zeltzer himself mentions that it is impossible, so far, to replicate all real-world features in a computer simulation. Only some degree of fidelity can be attained, which he denotes as selective fidelity.

Thus, the cube should be regarded simply as a tool that helps to identify and measure qualitatively the features of a VR application, rather than a proposal of a "holy grail" to be sought by VR developers. This is supported by the fact that Zeltzer does not propose guidelines for VR implementations when he proposes the classification, he attains only to the taxonomy.

In this work, presence is the most important attribute to be considered. While the other attributes are tight to hardware limitations and rely on programmable features, presence itself must be continuous throughout the whole virtual experience. If no sufficient degree of presence is delivered to the user, all other features and the overall virtual experience are undermined. Thus, presence is more deeply investigated.

Figure 7 – Autonomy, Interaction and Presence (AIP) cube as envisioned by Zeltzer (1992). The corners of the cube present examples to illustrate scenarios where different components are prominent.

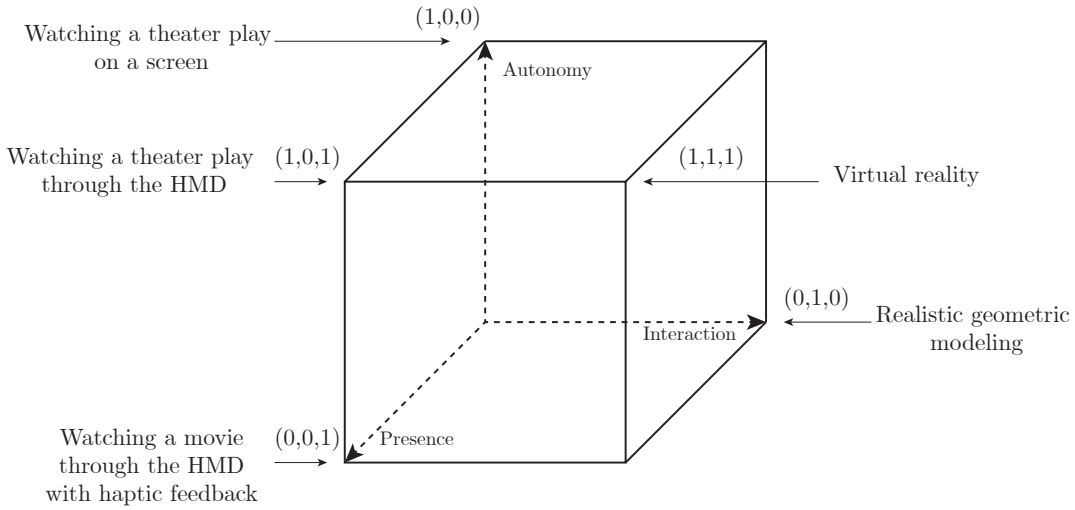

Source: Adapted from (ZELTZER, 1992).

Figure 8 – Simplified representation of the reality-virtuality continuum according to Milgram and Kishino (1994). The recent extended reality definition is included. Some applications are depicted below the continuum, with the HMD commonly used for each application. Microsoft Hololens 2 is depicted for augmented reality applications and the HTC Vive for the others.

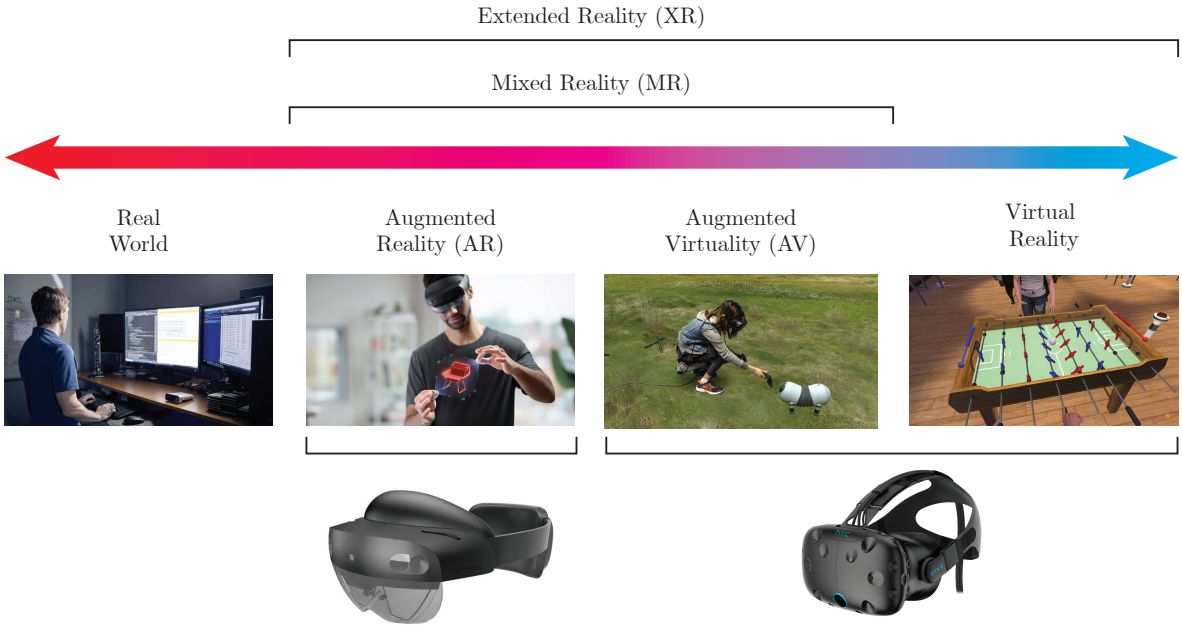

Source: Reconstructed from (MILGRAM; KISHINO, 1994). (From left) the two first images and the Hololens 2 photo belong to (MICROSOFT, 2019); the third and fourth belong to The Lab and Hand Simulator application pages, respectively, available at Steam store (VALVE CORPORATION, 2020). The HTC Vive photo belong to (HTC CORPORATION, 2016).

2.4 Virtuality Continuum

Besides the components that support a VR experience, it is convenient to classify the physical ways, in terms of hardware and displays, employed to render VR, as well as the differences between alternate forms of VR that can be implemented. Along this line, Milgram and Kishino (1994) propose a taxonomy based on the reality-virtuality continuum, as seen in Fig. 8, highlighting also the differences between the experiences that distinct hardware yield, such as flat window screens and head-mounted displays.

The continuum starts with the real, physical environment (or the real, physical world), i.e., the reality. As one moves towards the right, virtuality increases. At some point, there is augmented reality (AR), which consists of real world environments with virtual components. A mobile application which places computer-generated models of furniture in an actual room captured in real-time by the camera is an example of an AR application. More to the right, there is augmented virtuality (AV), which consists of virtual scenarios with real-world components. One common example is elicited by visual-effects techniques such as chroma key compositing. A green screen, for example, is placed in the background

and some real objects are positioned in front of it. The scene, captured by a camera, is edited in the computer, so instead of the green screen a new scenario is rendered. The resulting scene can be rendered to a HMD as well. This way, real objects are placed inside a VE. Far to the right there is the opposite of the physical world, i.e., virtual reality (VR), a virtual environment with virtual objects.

By the time the virtual continuum was presented, the term virtual reality was being misused to refer to all sorts of VR experiences. Though all these graphics simulations still fall somewhere along the virtuality continuum, they differ and should not be mistaken. Besides the far corners (real environments and virtual reality) the continuum encompasses augmented reality, virtuality and their variations, which can be indistinctly named mixed reality (MR). Currently, the novel term extended reality (XR) encompasses indistinctly all simulations along the continuum, being also employed extensively by consumers and developers when they need to refer to VR in a broader way.

Figure 8 shows the reality-virtuality continuum and also provides examples of different applications regarding each simulated reality located along the continuum, together with distinct HMD that can render these simulations.

As mentioned, this taxonomy relies on the display on which the simulation is rendered. Though they are not very immersive, flat screens can be considered VR displays. Nevertheless, there is evidence that a virtual experience with VR and HMD yields a better motorsensory experience without overwhelming the user's cognitive capabilities. Figure 9 shows the setup of the comparative study performed by Wenk *et al.* (2019). A reaching task was performed in three distinct realities: VR with HMD (far left), AR with HMD (center), and VR with flat screen (right). The subjects had to reach virtual objects and count how many were grasped during the session.

Figure 9 – Study performed by Wenk *et al.* (2019) to evaluate the cognitive load and motor task performance in different reality simulations.

Source: (WENK *et al.*, 2019).

2.5 Presence and Embodiment

Presence, also referred to as the illusion of presence or illusion of being present (somewhere or elsewhere), in VR has been extensively studied before and after Zelter published his work. Though it is still not intuitively measured, it has been divided into sub-components and questionnaires have been elaborated to address this issue.

When it comes to the cognitive aspects of the illusion of presence, the works performed by Slater and his team are of fundamental importance, as they provide evidence of the most important aspects to be considered when it comes to VR applications regarding user comfort, immersion and presence (SLATER; USOH; STEED, 1994; SLATER; WILBUR, 1997; SLATER; STEED, 2000; SLATER, 2009a). Thanks to their investigations on VR from the point of view of psychology, some design approaches today can be adopted in a straightforward manner, without the need of discussing and trying other approaches, which could delay and hamper the development process.

Toet *et al.* (2020) state that embodiment is the most significant aspect of presence when it comes to teleoperation. Due to the similarities between a teleoperation task inside VR and rehabilitation robotics inside VR, it is worth noting of which embodiment consists and how it can enhance the experience.

Embodiment is the sense that emerges when an object's properties are processed as if they were the properties of one's own biological body. The rubber hand illusion experiment is a classic example of how it functions. Many researchers replicate and study it up to these days (MOGUILLANSKY; O'REGAN; PETITMENGIN, 2013). A rubber hand is placed in front of a person, in a position the real hand would similarly attain, while the real hand lies slightly disarranged from this position, hidden by a wall, outside its owner's field of view. Another person stimulates both hands simultaneously: first the index finger is caressed by a feather (or any other instrument), then the mid finger, and so on. The hand owners see the rubber hand being stimulated and feel the stimuli in their real hand. Slowly, the subjects incorporate that fake and somewhat unrealistic hand as being their own body. This is confirmed when the other person tries to harm the rubber hand, causing the subject to react immediately.

Toet *et al.* (2020) summarize the sub-components of embodiment as being mainly three: ownership, agency, self-location. The latter is divided into body location and perspective location.

Ownership denotes the illusory perception that non-bodily objects are part of one's own body and are the source of associated bodily sensations. This property is accurately alluded by the rubber hand example. It is engendered by visual and haptic feedback. Regarding rehabilitation robotics with VR, it is intuitive to conclude that the role of ownership is crucial in making the users perceive both the robotic device and their avatars

as part of themselves.

Agency is related to the subjective feeling that the user is the author of an observed action. In this case, if the subject moved the real hand and the rubber hand reproduced the movement, there would be a sense of agency. It is originated by the perception of control over something. This attribute could be crucial to keep an impaired user motivated during a task.

Finally, the sense of self-location is related to the spatial position of the user. It can be either the subjective feeling where their body is in space, i.e., body location, or the subjective feeling where their visual perspective is located in space, i.e., perspective location. The difference between the two dwells on the fact that the former is related to the temporal match between sensed (haptic) and visual stimuli, as from a first-person point of view; whereas the latter is related only to the visual feedback yielded from the perspective of the subject from a third-person point of view. For this work, only the first-person perspective is considered.

Measuring quantitatively the feeling of presence has been difficult because not only presence is a subjective feeling, but also something felt at the moment, i.e. during the VR experience. One way of measuring it is through questionnaires after experiments. Attempts to measure it during the experience can be done by monitoring bodily responses, such as electrodermal activity (galvanic skin response), pupil dilation, skin temperature or heart beat rate (PEREZ-MARCOS, 2018; MATSANGIDOU *et al.*, 2019). However, all these are still indirect measures of the illusion of presence, since it is subjective feeling, also known as qualia (SLATER, 2009a).

Figure 10 – Rubber hand illusion experiment setup. A subject sits in front of a rubber hand, whilst the real hand is hidden.

Source: (MOGUILLANSKY; O'REGAN; PETITMENGIN, 2013).

The moment the presence is broken, however, is easily identified. A break-in-presence (BIP) is a moment when the illusion of being in the VE crumbles down and the users find themselves in the real world, walking around a confined room, wearing a HMD (SLATER; STEED, 2000). These moments, undoubtedly, should be avoided. They are usually triggered by external stimuli, such as people talking outside the VE, phone rings, or stumbling over real world objects such as furniture or cables placed within the virtual rig (JERALD, 2016).

VR, in terms of human experience rather than in terms of any specific technology or hardware, is strictly related to the feeling of presence (STEUER, 1992). Implementing ways to achieve it consists the goal of any VR application (SLATER; WILBUR, 1997). Nowadays, most VR applications aimed for rehabilitation robotics rely only in visual feedback. In a few applications, auditory feedback emerges as a key feature on the rehabilitation process, as a motivation tool (KERN *et al.*, 2019), while tactile or haptic feedback is still overlooked.

The next sections provide an overview on haptics and haptic interface devices, and also support why tactile feedback should be developed along with visual and auditory feedback, emphasizing its importance for the rehabilitation process.

2.6 Haptics

Haptics, or the sense of touch, is an important feature, which is proved to enhance recovery during physical therapy. Despite its benefits, haptic feedback is still an overlooked feature within the context of rehabilitation. In order to render haptic feedback, haptic interface systems based on the user interaction with virtual environments are designed. The functioning of these interfaces rely on interaction control theory, mostly impedance and admittance control. Section 2.7 provides an overview of haptics. Following, section 2.8 presents some off-the-shelf solutions capable of rendering haptic feedback, and highlights the advantages and disadvantages of haptic interfaces in the context of rehabilitation robotics, as well as some approaches utilized to implement a haptic system, which resemble the objective of this work. In the end, Section 2.9 presents the fundamentals of interaction control theory, in order to illustrate the behavior of a haptic interface.

2.7 Haptic Feedback Interfaces

Haptics generically encompasses touch interactions, i.e., physical contact, that occur for the purpose of perception or manipulation of objects. These interactions can be a variety of combinations of human and machine interactions with real, remote or virtual objects (SALISBURY; CONTI; BARBAGLI, 2004). This work handles, a priori, the interaction between human and virtual environments. In order to accomplish this task, a haptic device, also referred to as haptic display or haptic interface (these three taxonomies are interchangeably used in this work) is needed. The function of the haptic

Figure 11 – Haptic devices create a closed loop between user and virtual environments/simulation algorithms. $x(t)$ and $F(t)$ are continuous-time position and force signals exchanged between user and haptic device. $x(k)$ and $F(k)$ are discrete-time position and force signals exchanged between haptic device and virtual environment.

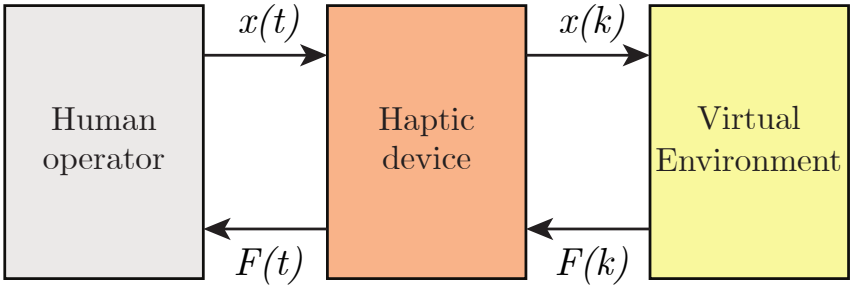

Source: Adapted from (SALISBURY; CONTI; BARBAGLI, 2004).

display is to render a desired dynamic behavior assigned between the operator and the simulated environment. Rendering, in this context, refers to the process of imposing to the user specific sensory stimuli, in order to convey information about the interaction taking place.

Figure 11 shows the three entities involved in haptics and how they relate with one another: the human operator (user), the haptic device (usually a robot), and the virtual environment. In this case, the human operator imposes a movement $x(t)$ to the haptic device in the physical world. This movement will be tracked to the VE as a discrete signal $x(k)$ and generate interactions inside this VE. These interactions will generate discrete force signals $F(k)$ that are propagated as a continuous-time force to be felt by the human operator. Here, since a movement input is resulting in a force output, the haptic interface is said to be of impedance type. In the case the human operator imposed a force as input and the haptic interface generated a movement, it would be of admittance type. Impedance and admittance control schemes are dual. They are the most common approach to design haptic feedback interface systems. These control architectures are discussed in Section 2.9. Besides their mechanical behavior (impedance or admittance), haptic interface devices can also be classified according to the degrees-of-freedom of motion (or force) they can render.

Different from visual and auditory feedback, haptic is bidirectional, as it transmits information and energy from and to the user. This bidirectionality is often referred to as the most important feature of haptic interaction (SALISBURY; CONTI; BARBAGLI, 2004). Moreover, though it is originated from interaction, haptic feedback can be considered a presence attribute, because it contributes to maintain the feeling of being present in the VE, by matching the users' sensory expectation to what they do feel (ZELTZER, 1992).

Salisbury, Conti and Barbagli (2004) list the desirable characteristics that a haptic interface must present. They are: low back-drive inertia and friction; minimal constraints on motion imposed by the device kinematics so free motion feels free; symmetric inertia,

friction, stiffness, and resonate frequency properties (thereby regularizing the device so users do not have to unconsciously compensate for parasitic forces); balanced range, resolution, and bandwidth of position sensing and force reflection; and proper ergonomics that let the human operator focus when wearing or manipulating the haptic interface since pain, or even discomfort, can distract the user, reducing overall performance.

Although many off-the-shelf robots or robots designed for specific purposes do not present these attributes altogether, feedback control can surmount some deficiencies (CLOVER, 1999). Specifically, if the system to be utilized as haptic interface presents high gear-ratio and friction, the admittance approach is the recommended one.

Haptic feedback can also be classified in two categories. It can be either touch feedback or force feedback. The former means that the interaction is restrict to providing information regarding surface roughness and temperature, i.e., it does not involve forces, and neither the robot nor the environment can stop one another. The latter is related to information regarding compliance, weight and inertia, i.e., there are forces being exerted by both the robot and the environment. Thus, the environment can resist to a person's interaction and even stop the person. Moreover, another aspect one must consider while designing a haptic feedback interface is that the forces shall feel real, but not to the point it may harm the user. The design has also to be fail-safe in case of technical problems. Remarks on light and non-intrusive hardware, within the context of the present work, can be deemed with less relevance, as the robotic device already exists (BURDEA; COIFFET, 2003).

2.8 Haptic Interfaces Design and Similar Works

One can think of two ways of approaching the problem of implementing a haptic interface system. One approach would be to develop a novel interface, to be worn or to be in contact with the user. The other would be to acquire an off-the-shelf solution or a robotic device to fufill the haptic feedback purpose. On this matter, Piggott, Wagner and Ziat (2016) summarize many haptic feedback systems for upper-limbs rehabilitation, which comprise laboratory devices designed solely for this purpose, commercial solutions, as well as robotic manipulators adapted to function as haptic interfaces. Following, both approaches are discussed briefly.

Designing haptic interfaces from scratch can be a time-consuming and expensive task. Skidmore, Barkan and Artemiadis (2015) developed a treadmill with variable stiffness, as seen in Fig. 12. Their motivation was to develop a versatile system, which could provide haptic feedback, whose characteristics could be changed in real-time, with accuracy, resolution and robustness, while the subject walked actively on the treadmill, immersed in VR wearing a HMD. The final setup resembles the purpose of this work, as seen in Fig. 13. The studies with the VST investigated the hypothesis that the disturbance caused in the

Figure 12 – Variable Stiffness Treadmill.

Source: (SKIDMORE; BARKAN; ARTEMIADIS, 2015).

human gait by varying the ground stiffness may elicit changes in kinematic patterns and muscle activation that help to elucidate conclusions regarding the human gait mechanisms. Later, Frost *et al.* (2015) show conclusions on this matter, by emphasizing that haptic feedback, along with proprioceptive and visual feedback, might play a key role on providing the user multisensory feedback, which can help further to improve therapy, by providing a better understanding of sensorimotor control and gait.

Acquiring off-the-shelf solutions is an alternative to developing a device from sketch, even though the fact that commercial solutions are somewhat generic and may not fulfill all the user needs is a substantial disadvantage. The Geomagic devices Phantom Premium, Geomagic Touch X, and Geomagic Touch[2] shown in Fig. 14 are examples of 6-DoF haptic interfaces that apply force to the user's hands, providing a sense of touch when in contact with virtual objects. These devices have been used extensively for research purposes.

Still regarding off-the-shelf solutions, another option would be to employ general-purpose robots, such as robotic arm manipulators, to function as haptic interfaces. This work focus on the last approach: on designing a haptic feedback architecture for an already existing robotic device, a lower limbs exoskeleton. As robotic exoskeletons are usually modeled as serial link robotic manipulators, haptic feedback interfaces designed for serial robots were assessed. Works for upper limbs devices were also studied, when they provided a broaden approach on how the haptic interface was designed.

Among the works that employ robotic manipulators as haptic interfaces, force control strategies and impedance control stand out as safe and efficient ways of rendering haptic feedback for robot interaction with virtual environments, humans and objects.

[2] <https://www.3dsystems.com/scanners-haptics>

Figure 13 – Variable Stiffness Treadmill (VST) already developed to emulate different ground reaction forces in VR.

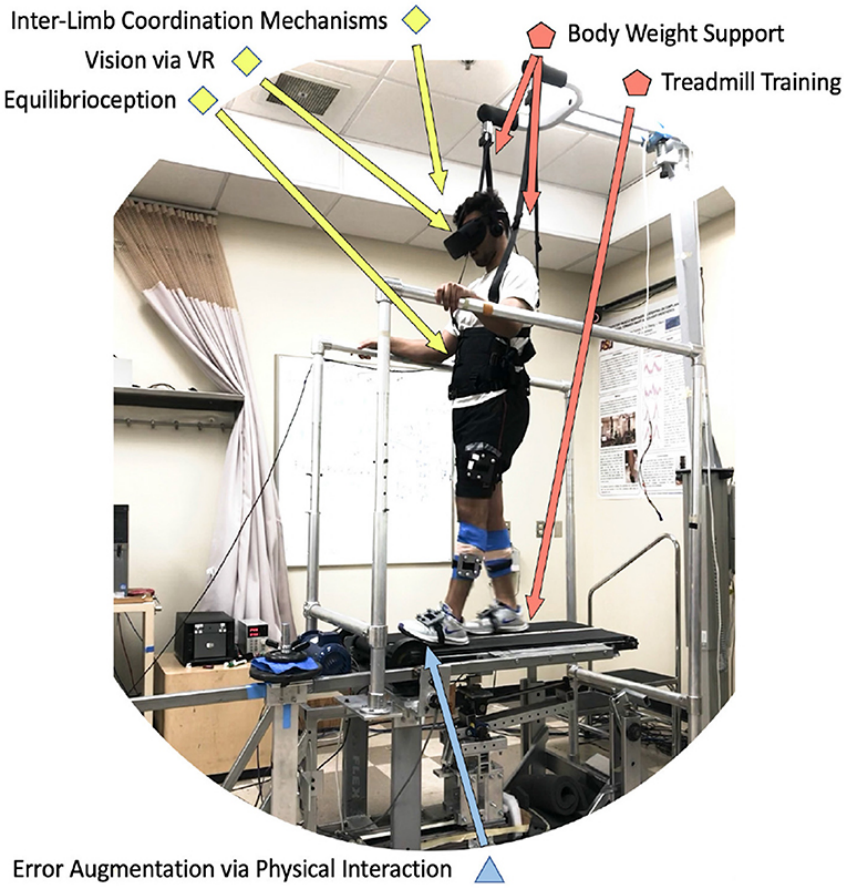

Source: (HOBBS; ARTEMIADIS, 2020).

Figure 14 – Geomagic devices by 3D Systems. From left: Phantom Premium, Geomagic Touch X, Geomagic Touch.

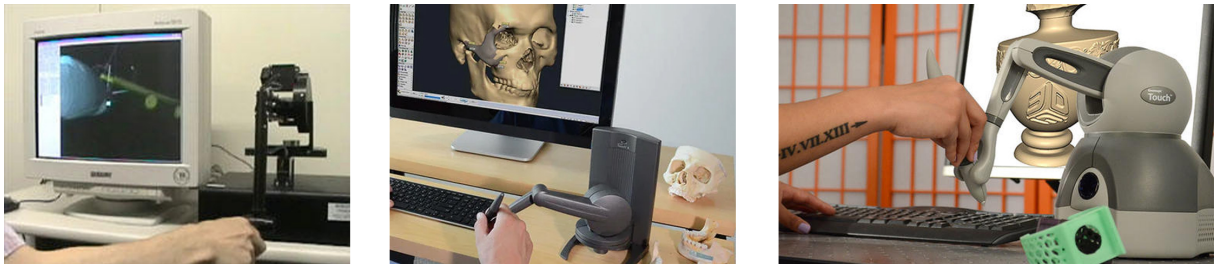

Source: 3D Systems.

Successful applications of this approach are the Iowa State University virtual aircraft control column applied both for Boeing flight simulations (CLOVER *et al.*, 1997) and for John Deer's vehicles (NIESEN; LUECKE, 1999). The same group studied also control strategies that could make the PUMA 560 robot manipulator function as a haptic interface (LUECKE; EDWARDS, 1996). In Luecke and Chai (1997), a force and a position controller are employed. As a means of validating the device, three tests are performed, of which the

Figure 15 – (Left) General-purpose industrial KUKA Light-Weight Robot (LWR). (Right) Two KUKA LWR used at DLR as haptic interface for teleoperation. These two examples illustrate how off-the-shelf general purpose robots can be adapted to function as haptic interface systems.

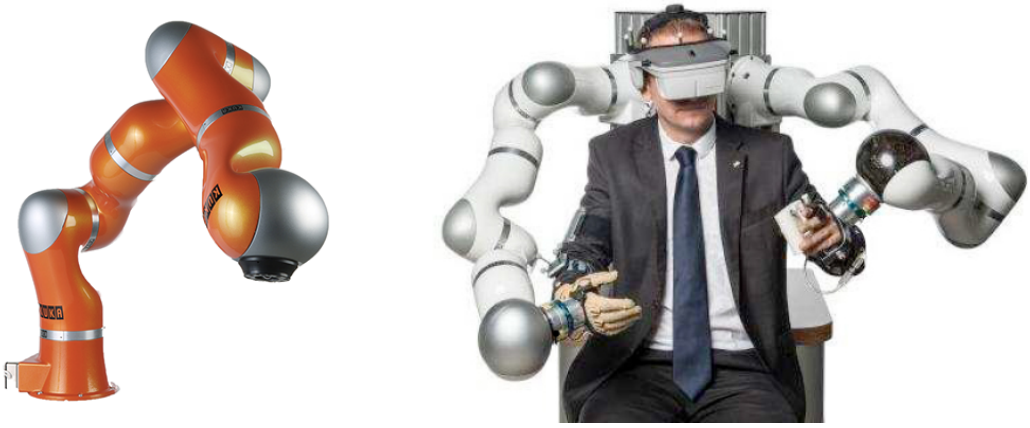

Source: (KUKA AG, 2020), (BALACHANDRAN *et al.*, 2018).

two will be replicated in this work: the position tracking control, as a means of evaluating the position controller performance; and the interaction with a rigid wall, which is the scenario most prone to instabilities. Forces and end-effector position during these tests are monitored and analyzed.

Research performed by the Deutsche Zentrum für Luft- und Raumfahrt (German Aerospace Center) (OTT; NAKAMURA, 2009; OTT; MUKHERJEE; NAKAMURA, 2010), also stand out, as they implement impedance (OTT *et al.*, 2008), admittance, and hybrid impedance-admittance-based control strategies (OTT; MUKHERJEE; NAKAMURA, 2010) so general-purpose robots, such as the DLR-KUKA-lightweight robot (LWR) (ALBU-SCHAFFER *et al.*, 2003), function as haptic interfaces for teleoperation purposes, as seen in Fig. 15.

When it comes to rehabilitation robotics, in which the users already make use of an exoskeleton attached to their limbs or a robotic device with which they are constantly interacting, the fact that another equipment must be attached to them to provide haptic feedback is something that may undermine the experience, as the robotic devices are already bulky and sometimes must be carried by the patient. A perhaps more suitable approach would be to use the exoskeleton itself to provide haptic feedback. With this perspective, Kong *et al.* (2010) developed a force control strategy which applies resisting torques at the user's joints wearing a lower limbs exoskeleton, so the user feels the equivalent effect of practicing physical therapy underwater. Nevertheless, no studied was performed regarding the user perception, the feeling of practing physiotherapy in water, nor visual and auditory cues were provided to replicate the experience. The results were constrained to replicate the forces, thus, the effects on the human limbs. Ayad *et al.* (2018) present an admittance-control strategy to be applied on a robotic Stewart platform, in order to

Figure 16 – (Left) Exoskeleton replicating aquatic therapy forces, without VR; (right) Stewart Platform (still under development).

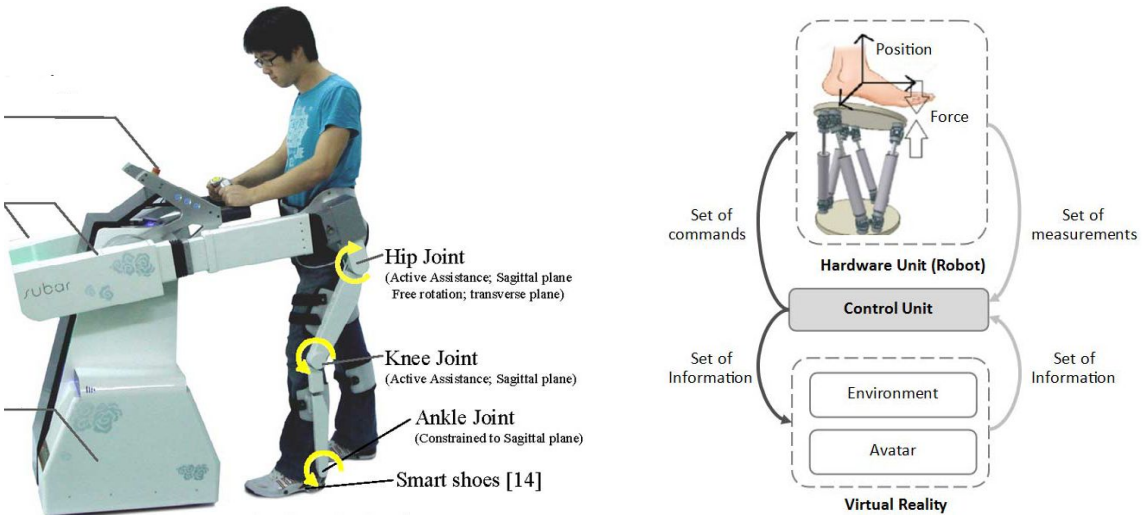

Source: (KONG *et al.*, 2010), (AYAD *et al.*, 2018), (SKIDMORE; BARKAN; ARTEMIADIS, 2015).

render different dynamic behaviors during ankle therapy, to simulate mediums with less (air, water) and more (solid ground) resistance. However, their approach is not very clear, as it is still incipient and the robotic device is still under development. Figure 16 shows these two similar works.

Having in mind the successful applications of general purpose robots as haptic interface systems and the feasibility of implementing haptic interfaces with interaction control architectures, the next sections focus on providing the foundations of interaction control from the point of view of this project.

2.9 Interaction Control

Interaction control can be achieved through force control, in which the force is controlled; through position and force control, in which both variables are controlled, but separately; or through impedance and admittance control, in which the relation between force and position is controlled. Siciliano and Khatib (2008) summarize their applications, benefits and limitations. Here, only the impedance and admittance control schemes are detailed.

Impedance or admittance control is a means of controlling indirectly the contact force between a robot and the environment with which it may interact. As stated initially by Hogan (1985), it aims at rendering the dynamic behavior of a virtual second-order system with adjustable parameters at the robot's port of interaction, i.e., its end-effector. The approach can be expanded in the case the interaction occurs at joint level (SANTOS; SIQUEIRA, 2014). This strategy is known as impedance control, if an inner force control

loop is present, or admittance control, if an inner position control loop is present. A robot under impedance control reacts to motion deviation from a desired trajectory by generating forces, behaving like a mechanical impedance, while the ambient behaves like a mechanical admittance; whereas under admittance control the robot reacts with a motion deviation from the desired trajectory as an interaction force is sensed, behaving like a mechanical admittance, while the ambient behaves like a mechanical impedance (SICILIANO; KHATIB, 2008). For simplicity, the term mechanical is suppressed when referring to mechanical impedance and admittance control.

Using Laplace notation, impedance and admittance are represented by the following transfer functions

$$Z(s) = \frac{F(s)}{sX(s)}, \tag{2.1}$$

$$Y(s) = \frac{sX(s)}{F(s)}, \tag{2.2}$$

where s is the Laplace variable, $F(s)$ is the Laplace transform of the force being computed or sensed, and $X(s)$ is the Laplace transform of the motion being computed or sensed. From 2.1 and 2.3 it can be concluded that there exists a duality relation between impedance and admittance:

$$Z(s) = Y(s)^{-1}. \tag{2.3}$$

As mentioned, a second-order dynamic response is rendered based on adjustable, virtual parameters, such as

$$Z(s) = M_d s^2 + B_d s + K_d, \tag{2.4}$$

$$Y(s) = \frac{1}{M_d s^2 + B_d s + K_d}, \tag{2.5}$$

where M_d, B_d and $K_d \in \mathbb{R}^{1\times 1}$ are, respectively, the inertia, the damping and the stiffness to be rendered at the end-effector.

The interaction between a robot end-effector with a virtual object or environment is shown in Fig. 17. For simplicity, in this drawing, force can refer both to force and torque, likewise the position variables refer both to linear trajectories and rotations.

The end-effector dynamics of the robot is denoted by the subscript r (robot); the actuator dynamics is denoted by the subscript a (actuator). A force sensor is necessary for an admittance control scheme. When it comes to industrial robots, usually, the force

sensor dynamics is reduced to a pure-stiffness element. In this case, as the objects and environment are virtual, the force sensor would be virtual as well. Then, its dynamics can be suppressed. Thus, the external force consists of the virtual object or environment dynamics only. The virtual dynamics to be rendered at the end-effector is given by the virtual mechanical components which will present the desired inertia, damping and stiffness in order to behave as expected. These components take the subscript d (desired), as in Eq. 2.4 and 2.5. The robot is subjected to the actuator force and the external force sensed by the force sensor.

In impedance mode, the end-effector of the robotic device follows a desired trajectory and, in the case a deviation from this trajectory occurs, a force appears at the tip, in order to push the end-effector back to the track. It is as tough the robot tip were attached to the desired path by means of mechanical elements, such as stiffness and dampers, which engender interaction forces to prevent the robot from deviating. This force is, usually, controlled by an inner control loop. A PID controller, for instance, may perform this task.

Figure 18 (top) depicts the block diagram for an impedance control architecture. If a deviation from a pre-established trajectory occurs, $x_d - x$, a force is exerted, F_r. The interaction with the environment, F_{env}, can also be considered in the case backdrivability is present.

In admittance mode, the end-effector of the robotic device follows a desired trajectory according to an inner control loop. Likewise impedance mode, a PID may perform this task. In the case an interaction with an object or the environment occurs, an interaction force is sensed by a force transducer placed at the robot's end-effector. This force will serve as input for the admittance controller, which will generate a displacement that will be further added to the desired trajectory, modifying its value. The greater the sensed

Figure 17 – Schematic of the interaction. The robot (r) is subjected to an actuator force, F_a and interacts with the environment, engendering an interaction force F_{ext}. The impedance/admittance control will render the desired dynamics (d) at the interaction interface, i.e., the dashed vertical line.

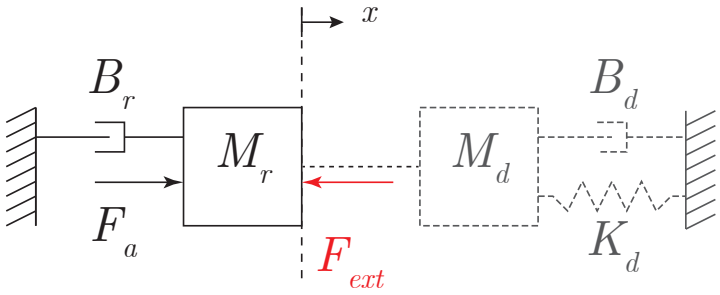

Source: Author (2021).

Figure 18 – General block diagram for 1-DoF linear system under (top) impedance control and (bottom) admittance control. The shaded region denotes the (top) inner force control loop and (bottom) the inner position control loop.

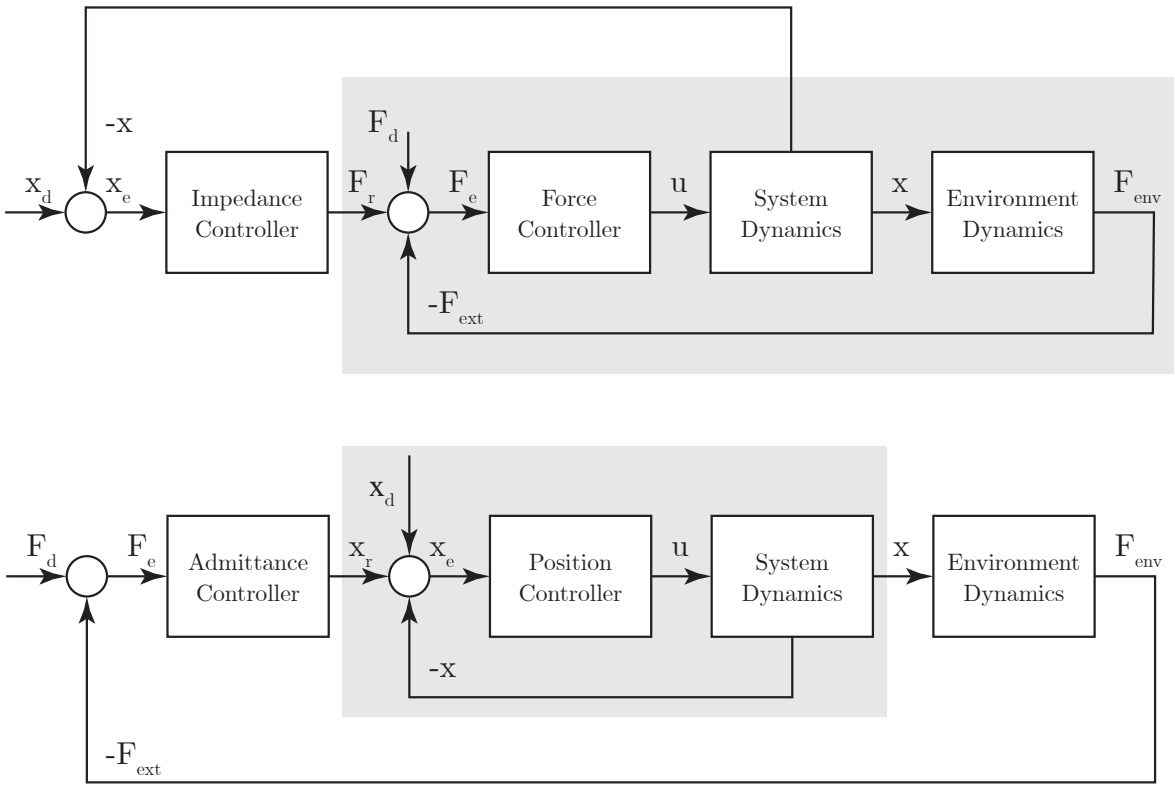

Source: Author (2021).

force, the greater is the displacement needed to correct the desired trajectory, in order to prevent the robot from following the original desired trajectory that leads the robot tip to penetrate deeper into the interface where the interaction occurs. Figure 18 (bottom) depicts the block diagram for an admittance control architecture. When the desired force to be tracked, F_d, is zero, the admittance controller will generate the motion deviation x_r sufficient to keep the force error F_e at zero. As the force error consists only of the external sensed force F_{env}, the admittance controller will prevent the robot from penetrating the surface of the virtual object, as mentioned before. The inner position control loop is depicted. The actuator dynamics is included in the system dynamics block. In this case, the effect of backdrivability is emulated by the control architecture, and the robotic device does not need to be backdrivable.

Both impedance and admittance control architectures can be adapted to handle task-space or joint-space operations. When necessary, the inverse or forward kinematics and dynamics operations are also computed. The architectures presented are in the simplest form, just for illustration purposes. Chapter 3 describes the control in details, considering the characteristics of the robotic device.

3 HAPTIC INTERFACE DESIGN

The haptic interface must be designed with an already existing robot. As a consequence, the mechanical design and the robot development are out of the scope of this project. Hence, the endeavors are focused on achieving the desired robot behavior by means of the proper control architecture, as well as the study of the performance bounds of the system. In Section 3.1 a simplified model of the lower limbs robotic exoskeleton employed in this work is described. Section 3.2 describes the current and most used control architecture applied to this robot in order to provide gait assistance. A set of desired trajectories employed for this task are shown in Section 3.3. Following, the computational model of the exoskeleton is validated by comparing the model and actual robot trajectories for a set of pre-established controller gains in Section 3.4. Once the robot is modeled and validated, the virtual environments with which it may interact are described in Section 3.5. To handle these environments and generate haptic feedback and assistance, two control architectures are described in Section 3.6: the impedance controller and a cascade admittance-impedance controller. The controllers are tuned empirically with the aid of the computational model, as in Section 3.7. To help to evaluate both controllers in terms of efficiency, two performance indicators are introduced in Section 3.8. Section 3.9 describes the tests performed on the real hardware with both controllers. The results are compared and analyzed. Section 3.10 summarizes the findings and presents the advantages and disadvantages for each controller, since their performance are similar and rely mostly on the virtual environment being handled.

3.1 Robot Model

The haptic control architecture will be designed for the modular, wearable, lower-limbs exoskeleton ExoTao, as seen in Fig. 19 (left). The robotic device comprises six rotary, one-degree-of-freedom joints, three for each leg. Magnetic encoders track the movement of the hip, knee and ankle joints on the sagittal plane. For the time being, only the knee joint of the robot is actuated and only the right leg is considered.

The knee joint consists of a module with a rotary Series Elastic Actuator (rSEA) (SANTOS; CAURIN; SIQUEIRA, 2017). The rSEA consists of a worm drive and an elastic element. On the driver side, there is a motor; on the load (or driven) side, there is the robot coupled to the human limb. The rSEA in this case not only ensures safety, by placing a low-rigidity element between the actuator and the human, but also provides a means of measuring the interaction forces between the robot and the human, since the average stiffness of the spring is known. The rSEA motor and encoders are connected to EPOS boards, which communicate with the control algorithm running on a desktop computer

Figure 19 – (Left) Healthy subject wearing the right leg of the lower limbs exoskeleton ExoTao. The blue box denotes the passive joints and the red box the actuated one. (Right) ExoTao modeled as a planar, rigid, serial-link robot manipulator.

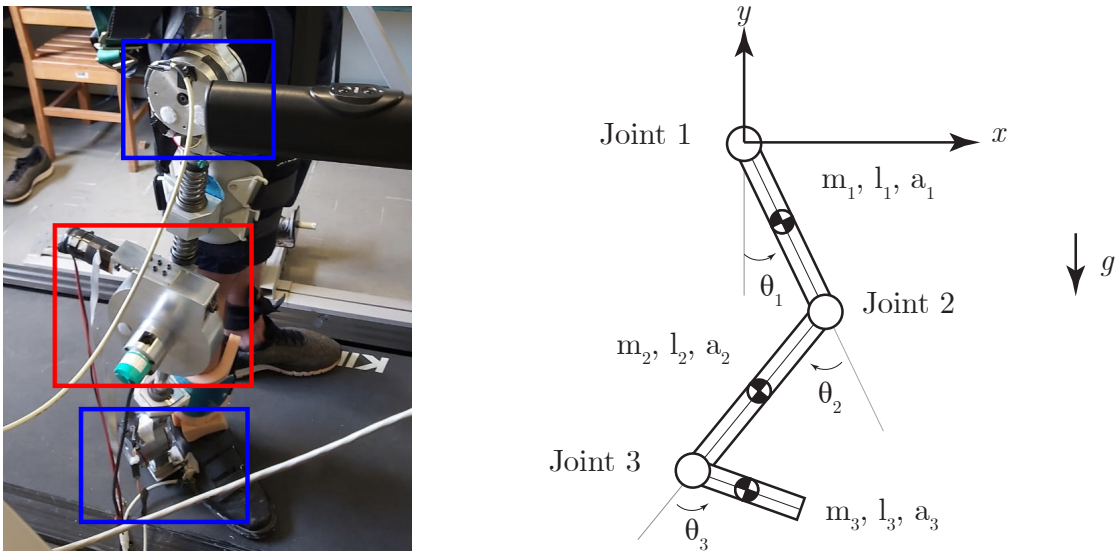

Source: Author (2021).

via Controller Area Network (CAN) ports. The hip and ankle encoders data are acquired through Serial Peripheral Interface (SPI) with the aid of a microcontroller.

The robot can be modeled as a planar, rigid, serial-link robot manipulator, as depicted in Fig. 19 (right). The joints 1, 2 and 3 refer, respectively, to the hip, knee and ankle joints, which perform the angular displacements denoted by q_n where $n = 1, 2, 3$. The robot links 1, 2 and 3 refer to the tight, shank and foot. Their lengths are denoted by a_n, whereas l_n refers to the distance from the origin, which is located at the center of the respective joint, to the center of mass of the link. The robot is subjected to gravity. A metal structure compensates partially for the robot weight, and also prevents the user from slipping while walking on the treadmill.

According to Siciliano and Khatib (2008), the forward dynamics of a robot can be described by

$$\mathbf{H}(\mathbf{q})\ddot{\mathbf{q}} + \mathbf{C}(\mathbf{q}, \dot{\mathbf{q}})\dot{\mathbf{q}} + \mathbf{G}(\mathbf{q}) + \mathbf{F_v}\dot{\mathbf{q}} + \mathbf{F_c}\mathbf{sgn}(\dot{\mathbf{q}}) + \mathrm{J}^{\mathrm{T}}(\mathbf{q})\mathbf{F_{ext}} = \tau_{\mathbf{a}}(\mathbf{q}, \dot{\mathbf{q}}), \tag{3.1}$$

where $\mathbf{q} \in \mathbb{R}^{n\times 1}$ are the joint-space variables and their derivatives. $\mathbf{H}$ and $\mathbf{C} \in \mathbb{R}^{n\times n}$ denotes the robot inertia and Coriolis forces matrix, respectively. $\mathbf{G}$, $\mathbf{F_v}$ and $\mathbf{F_c} \in \mathbb{R}^{n\times 1}$ denote, respectively, the gravitational force, the viscous friction force and Coulomb friction force matrices. $\mathrm{J}^{\mathrm{T}} \in \mathbb{R}^{n\times 2}$ denotes the transpose of the Jacobian matrix, $\mathbf{F_{ext}} \in \mathbb{R}^{2\times 1}$ the external forces matrix and $\tau_{\mathbf{a}} \in \mathbb{R}^{n\times 1}$ the actuator torque.

The robot dynamics can be simulated by isolating the acceleration term and by computing the numerical integration considering the convenient initial conditions

Figure 20 – (Left) Rotary SEA model composed of a motor connected to a worm drive. Between the gear and the robot axis, (right) a rotational spring is present.

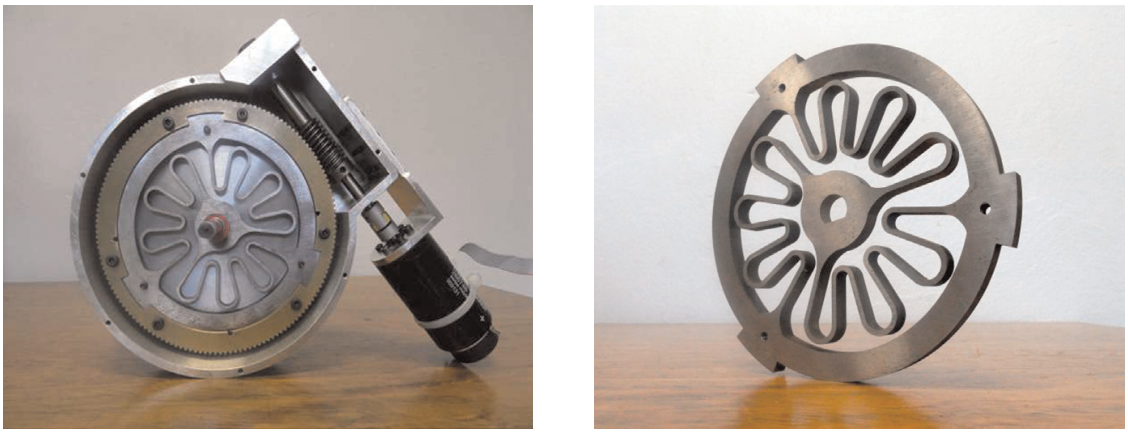

Source: (SANTOS; SIQUEIRA, 2014).

for position and velocity (CRAIG, 2018). Thus, the equation that provide the robot acceleration is given by

$$\ddot{\mathbf{q}}(t) = \mathbf{H}(\mathbf{q})^{-1}(\tau_{\mathbf{a}}(\mathbf{q}, \dot{\mathbf{q}}) - \mathbf{C}(\mathbf{q}, \dot{\mathbf{q}})\dot{\mathbf{q}} - \mathbf{G}(\mathbf{q}) - \mathbf{F_v}\dot{\mathbf{q}} - \mathbf{F_c}\mathbf{sgn}(\dot{\mathbf{q}}) - \mathrm{J}^{\mathrm{T}}(\mathbf{q})\mathbf{F_{ext}}), \quad (3.2)$$

where all terms are evaluated at the time instant t. The velocity in the next instant of time, $t + \Delta t$, is given by the Euler integration method, an explicit integration method, as in

$$\dot{\mathbf{q}}(t + \Delta t) = \dot{\mathbf{q}}(t) + \ddot{\mathbf{q}}(t)\Delta t, \quad (3.3)$$

$$\mathbf{q}(t + \Delta t) = \mathbf{q}(t) + \dot{\mathbf{q}}(t)\Delta t + \ddot{\mathbf{q}}(t)\frac{\Delta t^2}{2}, \quad (3.4)$$

where Δt is the time step.

By doing this, it is possible to simulate the robot, and to test different controllers, which will change the values of the actuator torque τ_a. However, before testing new controllers, the model must be validated, considering its current configuration, which is impedance control.

3.2 Impedance Controller

Currently the robot is configured to work in impedance mode. In this configuration, the robot, attached to the user's leg, measures the angular displacement of the knee joint. The knee angle, θ_k, is read by an encoder. Between the encoder module axis and the worm gear, a torsional spring is placed. The worm gear is in contact with the worm, which is

connected to the motor axis θ_m. This configuration provides a gear ratio of 150:1. In the case the user rotates the knee joint, due to the torsional spring, an interaction torque between the user and the robot is sensed and given by:

$$\tau_{int} = K_{SEA}(\theta_m - \theta_k), \tag{3.5}$$

because of their noisy nature, these torque measurements are subjected to a 2^{nd}-order Butterworth filter with a cutout frequency of 15 Hz. Here, τ_{int} is a scalar. In the circumstance the hip and ankle joints have rSEA actuators, the equation assumes the matrix form:

$$\tau_{\mathbf{int}} = \mathbf{K_{SEA}}(\mathbf{q_m} - \mathbf{q}), \tag{3.6}$$

in which $\mathbf{K_{SEA}} \in \mathbb{R}^{n\times n}$ is a diagonal matrix with the respective stiffness of each joint and $\mathbf{q_m} \in \mathbb{R}^{n\times 1}$, likewise $\mathbf{q}$. Though the real robot only has actuation on one joint, for simulation purposes all joints are ideally actuated, but only the knee joint is controlled.

The impedance control scheme is used as a means of controlling the rSEA so that the sensed human-robot interaction torque is driven to zero. To achieve this, an inner force control loop is implemented, as usual, comprised by a PID controller. The PID control signal serves as input to the innermost control loop, a velocity-based control performed by a EPOS board, a small-sized digital motion controller designed for motors.

When there is no desired trajectory to be tracked, the outermost impedance control loop is inactive and the control architecture is reduced to the PID force controller. In that sense, low-impedance control, sometimes referred to as transparency control, is achieved to a certain extent.

In the case a desired trajectory, $\mathbf{q_d} \in \mathbb{R}^{n\times 1}$ must be tracked, a reference torque, $\tau_\mathbf{r} \in \mathbb{R}^{n\times 1}$ is computed based on the trajectory error, $\mathbf{q_e} \in \mathbb{R}^{n\times 1}$, as in

$$\mathbf{q_e} = \mathbf{q_d} - \mathbf{q}. \tag{3.7}$$

Thus, the reference torque is given by

$$\tau_\mathbf{r} = \mathbf{K_{imp}}(\mathbf{q_d} - \mathbf{q}) - \mathbf{B_{imp}}\dot{\mathbf{q}}, \tag{3.8}$$

in which $\mathbf{K_{imp}}$ and $\mathbf{B_{imp}} \in \mathbb{R}^{n\times n}$ are diagonal matrices with the respective impedance associated to each joint, whereas the torque error, $\tau_\mathbf{error} \in \mathbb{R}^{n\times 1}$, is given by

$$\tau_\mathbf{error} = \tau_\mathbf{d} + \tau_\mathbf{r} - \tau_\mathbf{int} \tag{3.9}$$

and it is driven to zero by the inner torque control loop. In Eq. 3.9, a desired torque profile, $\tau_{\mathbf{d}} \in \mathbb{R}^{n\times 1}$, to be followed by the robot can be included, but it would have similar purposes as $\tau_{\mathbf{r}}$, so it is set to zero.

3.3 Desired or Free Joint Trajectories

A set of hip, knee and ankle trajectories are employed in this work, as seen in Fig. 21. These trajectories are used as desired position, $\mathbf{q_d}$, for simulation purposes, for tests with the exoskeleton alone, and, further, for tests with subjects. These joint trajectories were retrieved from Kirtley's Clinical Gait Analysis Normative Gait Database (KIRTLEY, 2006). The data were collected from 20 adults, 10 younger (15-25 years old) and 10 older (45-55 years). The average gait speed was 1.07 km/h. Data were recorded with a Vicon® motion capture system, comprising 6 cameras. The subjects walked on force plates, in order to measure ground reaction forces. Therefore, subjects walked overground.

In the absence of environment forces, i.e., free movement, these trajectories are the desired trajectories to be achieved by the robot and the human wearing it. For this reason, they are also referred to as free trajectories. If the user is subjected to environment forces, these trajectories no longer establish a desired value; they are used as a reference of what the movement would be if the environment forces were absent.

Figure 21 – Desired, or free, (dashed) hip, (solid) knee and (dotted) ankle trajectories.

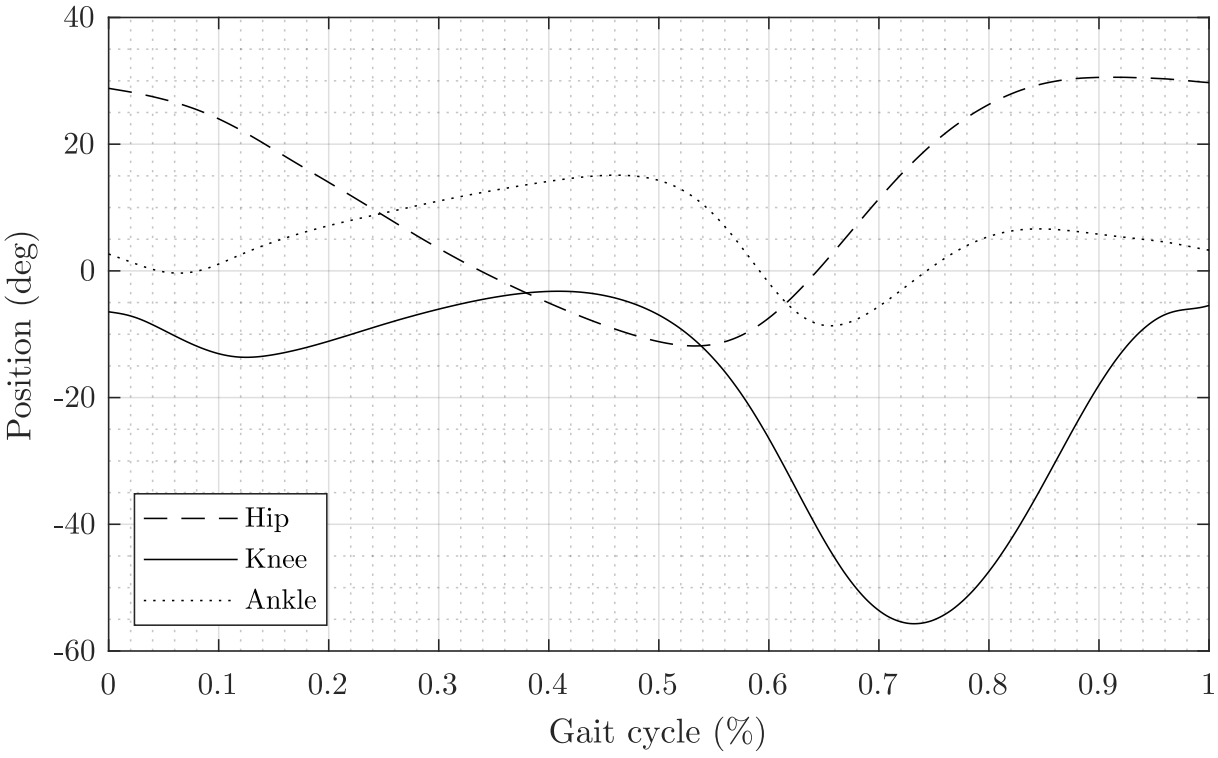

Source: Author (2021).

Figure 22 – Knee joint trajectory and estimated velocity for different values of damping.

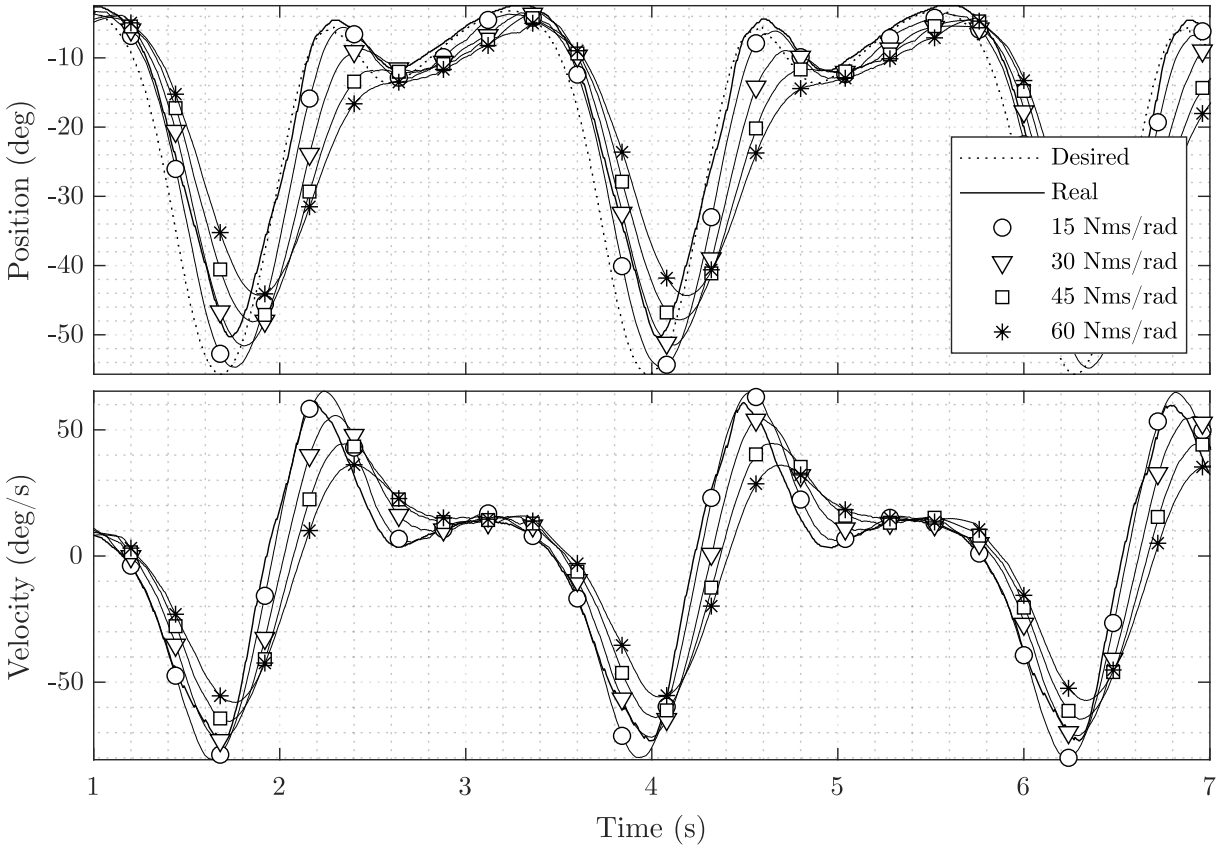

Source: Author (2021).

3.4 Model Validation

In order to validate and adjust the robot model parameters, the robot was set to high impedance mode ($K_{imp} = 100$ Nm/rad, $B_{imp} = 0$ Nms/rad) and a desired trajectory was established based on pre-recorded joint trajectories. In this case, the intent was to mask the impedance controller so that it functioned as a stiff motion controller. The rSEA has a nominal stiffness of $K_{SEA} = 104$ Nm/rad. In theory, a range of virtual impedance varying from 0 to 104 Nm/rad can be achieved, at the same time the system is kept passive (CALANCA; MURADORE; FIORINI, 2016). Tests were carried out with the robot alone.

Figure 22 compares how different damping values affect the simulated trajectory and velocity, which were compared with the real values (solid line), after a desired trajectory was set (dotted line). The SEA damping, once estimated as $B_{SEA} = 60$ Nmrad/s (SANTOS; SIQUEIRA, 2014), had to be adjusted to $B_{SEA} = 30$ Nmrad/s so that the simulation could be closer to the observed results in the real hardware, specially the joint velocities.

The final simulated trajectory and velocity, compared to the real one, are depicted in Fig. 23. It can be noted that the real hardware presents a slight offset compared with the simulation and the desired trajectory (around 3.45 deg). Since no desired velocity

Figure 23 – (Top) Knee joint trajectory and (bottom) estimated velocity. The simulated trajectory (marked) is compared with the desired one (dotted) and the trajectory of the real hardware (solid).

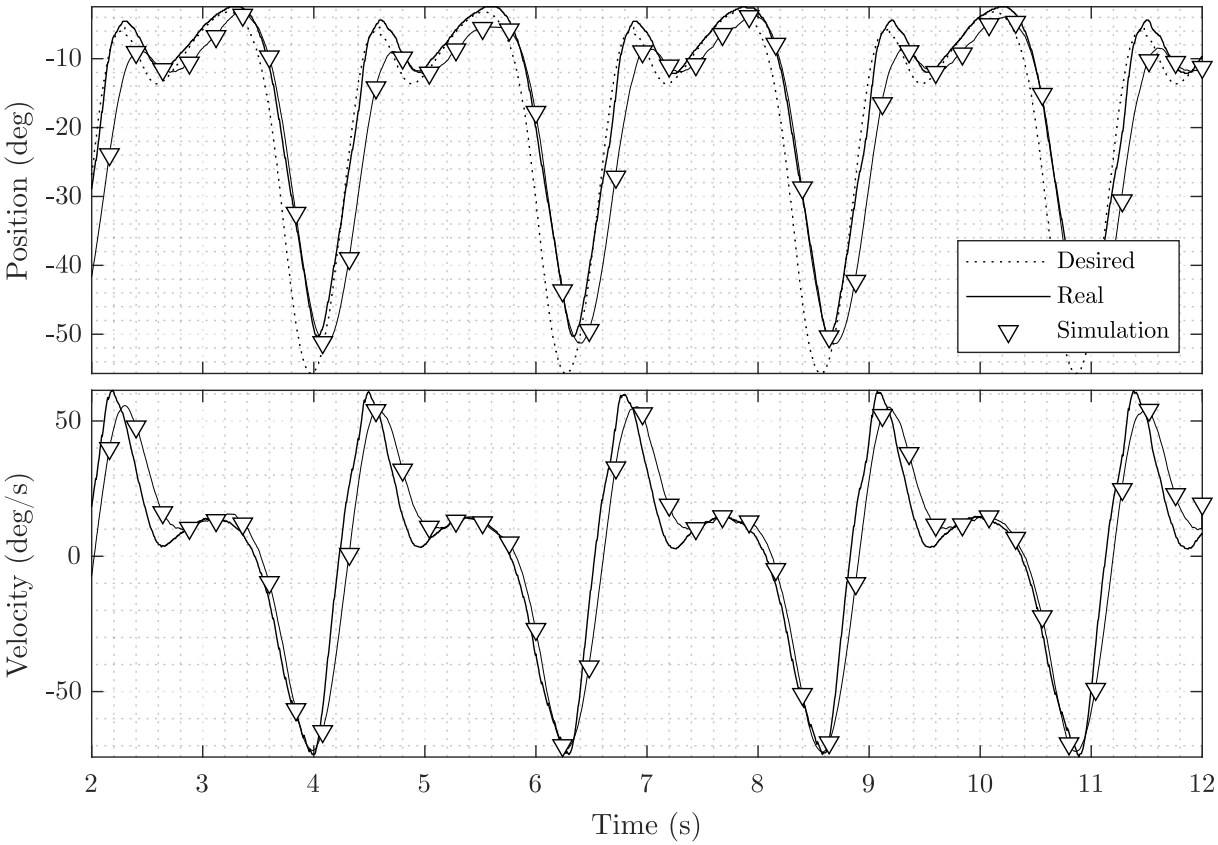

Source: Author (2021).

was established, the velocity values from the simulation could only be compared with the estimated ones from the real system. Over 20 seconds of gait, which comprise around 9 steps, the real system presented a maximum relative trajectory error of 9.1% and the simulated system, 6.7%. The real system presents itself slightly less damped than the simulated one, which can be noted by the greater amplitude of the real signal, compared with the simulated one, as well as the absence of phase, which can be noted in the simulated system. The simulated system was closer to the desired trajectory, presenting a RMS error of 4.46 deg, compared with a RMS error of 5.03 deg presented by the real system.

3.5 Environment Model

Three types of virtual environments are contemplated: (1) a “free”, unconstrained environment, i.e., no environment resistance to the user’s movements is present; (2) soft environments, also referred to as resistive mediums; (3) and rigid environments, also referred to as capacitive environments.

Unconstrained virtual environments offer no opposition force to the user’s move-

Figure 24 – (Left) The user will be immersed in a virtual liquid medium (right) while wearing the lower limbs exoskeleton in the physical world. Lumped impedance parameters model the environment dynamics.

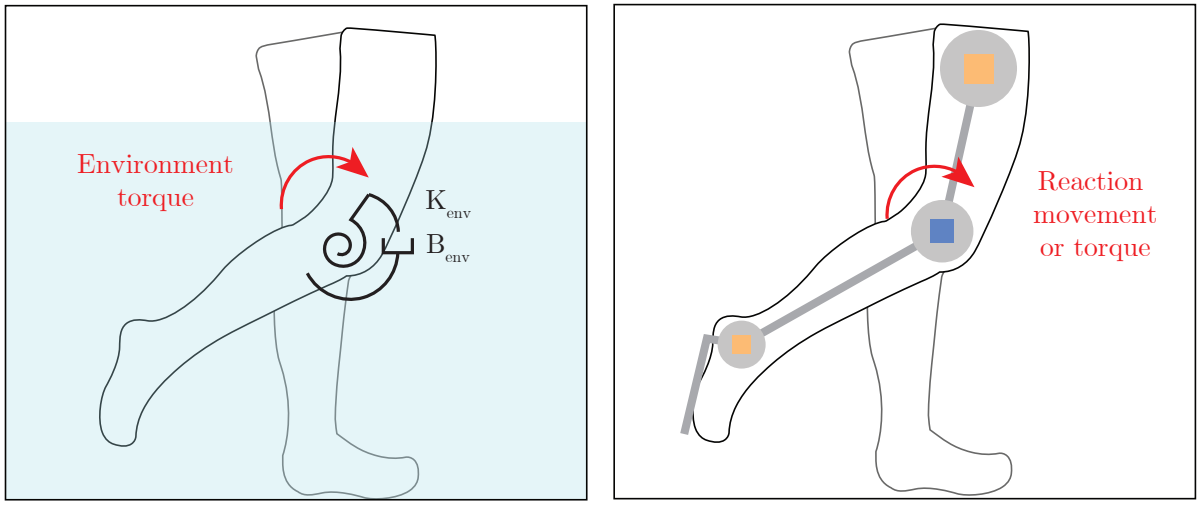

Source: Author (2021).

ments. The environment presents itself merely as a source of visual and auditory stimuli. It has been the approach adopted in most cases, in which there is no haptic interface, and VR works as a means of distraction and engagement. In this case, only movement tracking is mandatory. As the user moves, the robot, in rest, senses an interaction torque through the rSEA, and moves to drive this torque to zero. A low-impedance control loop is used in this case, which is essentially a zero-torque reference controller.

Virtual soft environments encompasses the user's avatar in the form of virtual liquid mediums, as illustrated in Fig. 24. They offer resistance to the user's movements proportionally to angular velocity of the user's joints. The environment resistance is modeled as lumped-impedance parameters rather than by the hydrodynamic equations. This approach is preferred because the aim is to compute an equivalent torque, opposing to the user's movement, instead of computing a realistic torque, which would depend on other factors such as the geometry of the avatar's leg and its surface properties. The interaction takes place only in joint space and is described by the following equation:

$$\tau_{\mathbf{env}} = \mathbf{B}_{\mathbf{env}}\dot{\mathbf{q}}, \tag{3.10}$$

where $\tau_{\mathbf{env}}$ and $\dot{\mathbf{q}} \in \mathbb{R}^{n\times 1}$ are, respectively, the environment torque and the user's joint velocities, and $\mathbf{B}_{\mathbf{env}} \in \mathbb{R}^{n\times n}$ a diagonal matrix with the equivalent environment damping of each joint. In all cases, n is the number of joints being considered.

Virtual rigid environments interact with the user's avatar through the end-effector (the tip toe). They are modeled as lumped-impedance parameters and intent to represent

Figure 25 – Scheme of the interaction with a stiff wall. (Left) The interaction yields an environment force. (Right) The admittance controller yields a motion displacement in order to set the interaction force back to zero, or the impedance controller generates a torque to drive the external sensed torques to zero.

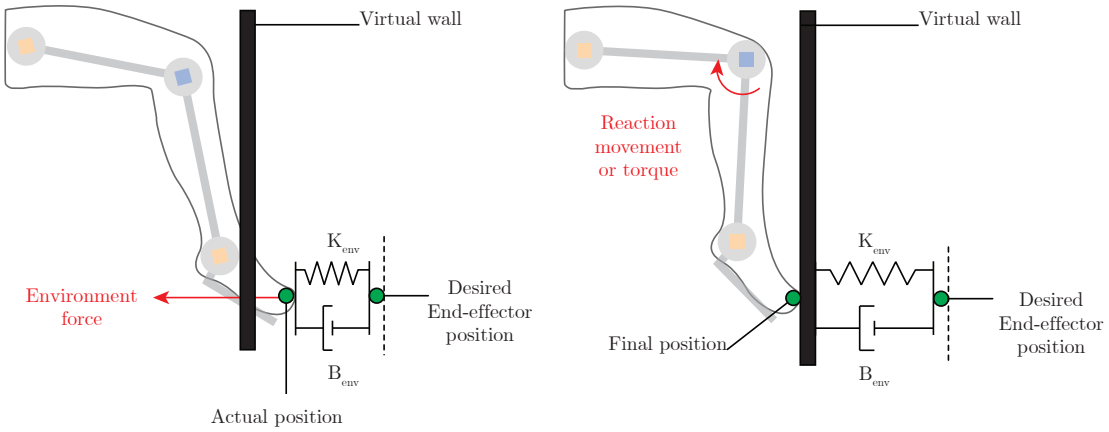

Source: Author (2021).

stiff environments, such as walls. Ideally, when interaction takes place, no penetration into the environment surface should occur. However, this case is still difficult to address for many robots. A preferable approach is to guarantee some level of compliance, and admit that small penetrations beyond the wall threshold may occur. This strategy is adopted, as long as it does not undermine the user experience and guarantees a steadier robot behavior. The environment torque in this case is computed according to:

$$\tau_{\mathbf{env}} = \mathrm{J}^{\mathrm{T}}(\mathbf{K}_{\mathbf{env}}(\mathbf{x} - \mathbf{x}_{\mathbf{env}}) + \mathbf{B}_{\mathbf{env}}\dot{\mathbf{x}}), \tag{3.11}$$

where $\mathbf{x}_{\mathbf{env}}$, $\mathbf{x}$ and $\dot{\mathbf{x}} \in \mathbb{R}^{2\times 1}$ are, respectively, the environment, e.g., wall, position and the avatar end-effector position and velocity, along the X and Y coordinates; $\mathbf{K}_{\mathbf{env}}$ and $\mathbf{B}_{\mathbf{env}} \in \mathbb{R}^{2\times 2}$ are diagonal matrices with the equivalent environment stiffness and damping, respectively, along the X and Y coordinates. One must note that, though the variables are named after the same symbols, $\mathbf{K}_{\mathbf{env}}$ and $\mathbf{B}_{\mathbf{env}}$ have distinct dimensions and units in the case of resistive and rigid environments, since the interaction takes place in different spaces, respectively, joint and task spaces.

3.6 Haptic Feedback Control Architecture

The main approach to design a haptic interface controller is to develop either an admittance or impedance controller. It is known that both schemes are dual. In ideal situations, it means that the engineer can obtain the desired system behavior with both architectures. However, due to limitations that arise from many aspects, one architecture becomes more suitable than the other. For instance, it well-known that the performance

Figure 26 – Impedance and admittance controllers performance according to the environment stiffness.

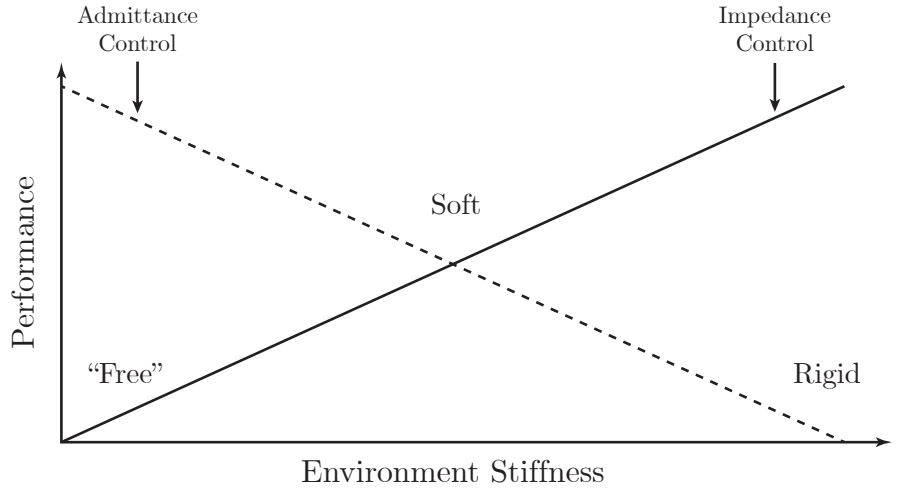

Source: Reconstructed from (OTT; MUKHERJEE; NAKAMURA, 2010).

of the admittance controller deteriorates as the environment stiffness increases, as seen in Fig. 26. Moreover, for the admittance control scheme, force sensing at the end-effector is mandatory to deal with the environment forces, whereas it is not mandatory for impedance control architectures. This, of course, is not a general rule, but illustrates how choosing the proper scheme also depends on the application.

3.6.1 Impedance Control

This architecture handles the human-robot interaction only. Since the robot has a rSEA, to provide haptic feedback based on an impedance control scheme becomes a natural procedure. If one wants to adapt it to function as a haptic interface, one way of achieving it would be to change the impedance parameters, $\mathbf{K_{imp}}$, $\mathbf{B_{imp}}$, with respect to a desired trajectory, so that they render a specific mechanical behavior. In this case, however, the environment is not contemplated, or, rather, the impedance control parameters play both the role of guaranteeing that the trajectory error behaves as a second-order, or simpler, dynamical system, and that the torque felt at the user's joint represents the interaction with some medium, whose characteristics are described by the impedance controller gains. This is a simplistic approach that considers the environment as a force that appears only when trajectory error is sensed. This approach is neither ideal or erroneous; it is, somewhat, oversimplified within the context of this work.

In order to consider the environment contribution more precisely, Equation 3.9

Figure 27 – Impedance control architecture. The environment is included, so that the user feels the forces/torques that arise from the interaction with the virtual environment.

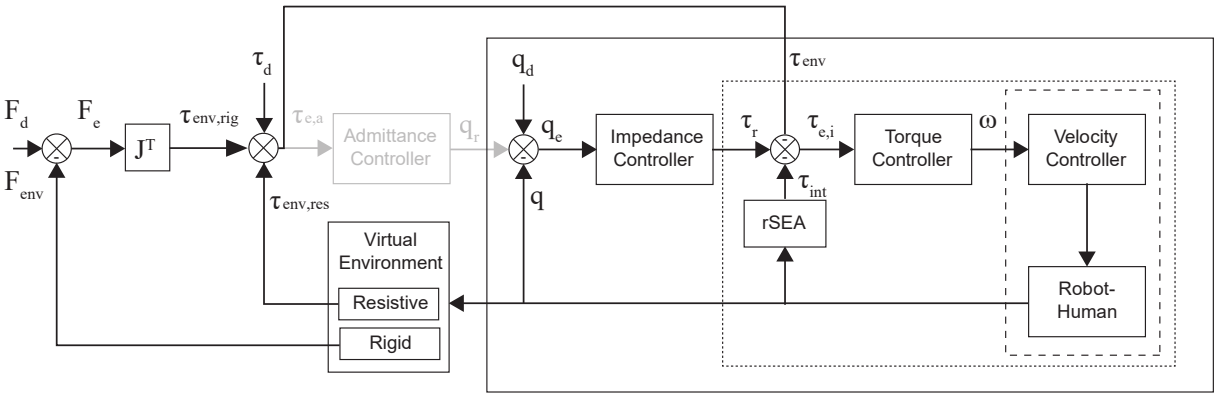

Source: Author (2021).

must become:

$$\tau_{\mathbf{e,i}} = \tau_{\mathbf{d}} + \tau_{\mathbf{r}} - (\tau_{\mathbf{int}} + \tau_{\mathbf{env}}), \tag{3.12}$$

where $\tau_{\mathbf{e,i}} \in \mathbb{R}^{n \times 1}$ denote the torque error of the impedance controller loop.

This scheme can handle the human-robot and the robot-environment interaction at the same time, since both $\tau_{\mathbf{env}}$ and $\tau_{\mathbf{int}}$ are considered in the error equation. This approach, however, presents disadvantages. From a technical point of view, all components of torque, with exception of the desired torque, $\tau_{\mathbf{d}}$, are computed based on the encoders measurements and velocity estimations multiplied by their respective gains, i.e., stiffness and damping. These gains amplify the noise present in these measurements; this generates a noisy error signal and, thus, a noisy control signal, as well as greater control signal variance. Lastly, from a user point of view, the resulting torque acting at the knee joint may not be very comfortable. The reference trajectory torque, tracked by the impedance control loop, $\tau_{\mathbf{r}}$, may be masked by the environment torque $\tau_{\mathbf{env}}$ acting against it, and the resulting torque to be applied at the knee joint may not be enough to drive the user joints according to the reference. Further, if one desired a weaker trajectory tracking, it could happen that the environment torques, $\tau_{\mathbf{env}}$, surpassed the impedance controller torque, $\tau_{\mathbf{r}}$, and led to a weak control action or even a control signal on the opposite direction, when it was not the intent. Therefore, the environment parameters have to be adjusted at the same time as the impedance ones, which is not practical. It is a well-known issue of impedance control the fact that low-gain tuning may lead to poor performance, while high-gain may lead to instability when it there is interaction with high-impedance environments.

It was also noted that, in the case of resistive mediums, i.e., $\mathbf{K_{imp}} = 0$ Nm/rad and $\mathbf{B_{imp}} > 5$ Nms/rad, only impedance control led the system to instability when the robot was attached to the human limbs, due to the occurrence of greater interaction torques,

$\tau_{\mathbf{int}}$, that increase the error, $\tau_{\mathbf{e}}$, and demand more from the torque controller.

Therefore, if one wants to render haptic feedback considering the user interaction inside virtual environments only with the current impedance controller, one must either adopt a simplified approach, that will account for the human-robot interaction and environment torques altogether; or a more precise approach, which would require constant tuning, but may be subjected to instability.

3.6.2 Cascade Admittance-Impedance Control

It is also possible to implement an admittance control architecture in order to render haptic feedback. To do this, an outer admittance control loop will be inserted to the previous architecture. In order to mask the impedance controller, the impedance gains will be set to high values ($\mathbf{K_{imp}} > 50$ Nm/rad), so that the inner loop behave as close as possible to a stiff position control loop. The environment forces are sensed according to Equations 3.10 and 3.11. The torque error now becomes:

$$\tau_{\mathbf{e,a}} = \tau_{\mathbf{d}} - \tau_{\mathbf{env}}, \tag{3.13}$$

where $\tau_{\mathbf{e,a}} \in \mathbb{R}^{n\times 1}$ denotes the torque error with respect to the outermost admittance control loop. Note that the environment torque, either from resistive or rigid environments, is accounted by the $\tau_{\mathbf{env}}$ term.

This torque error functions as input to the outer admittance control loop, which generates a trajectory reference according to:

$$\tau_{\mathbf{e,a}} = \mathbf{M_{adm}}\ddot{\mathbf{q}}_{\mathbf{r}} + \mathbf{B_{adm}}\dot{\mathbf{q}}_{\mathbf{r}} + \mathbf{K_{adm}}\mathbf{q_r}, \tag{3.14}$$

where $\ddot{\mathbf{q}}_{\mathbf{r}}$, $\dot{\mathbf{q}}_{\mathbf{r}}$, and $\mathbf{q_r} \in \mathbb{R}^{n\times 1}$; $\mathbf{M_{adm}}$, $\mathbf{B_{adm}}$ and $\mathbf{K_{adm}} \in \mathbb{R}^{n\times n}$ are diagonal matrices with the respective admittance associated to each joint. The discrete form of Eq. 3.14, evaluated at the k$^{\text{th}}$ instant of time, is given by:

$$\mathbf{q_r}^k = \frac{\tau_{\mathbf{e,a}}{}^k + \mathbf{q_r}^{k-1}\left(\frac{2\mathbf{M_{adm}}}{\Delta t^2} + \frac{\mathbf{B_{adm}}}{\Delta t^2}\right) - \mathbf{q_r}^{k-2}\frac{\mathbf{M_{adm}}}{\Delta t^2}}{\frac{\mathbf{M_{adm}}}{\Delta t^2} + \frac{\mathbf{B_{adm}}}{\Delta t} + \mathbf{K_{adm}}}. \tag{3.15}$$

This computed trajectory reference is added to the desired trajectory, and compared to the current system state, resulting in the trajectory error:

$$\mathbf{q_e} = \mathbf{q_d} + \mathbf{q_r} - \mathbf{q}. \tag{3.16}$$

The error is driven to zero by the inner high-impedance loop.

Figure 28 – Illustration of the control architecture.

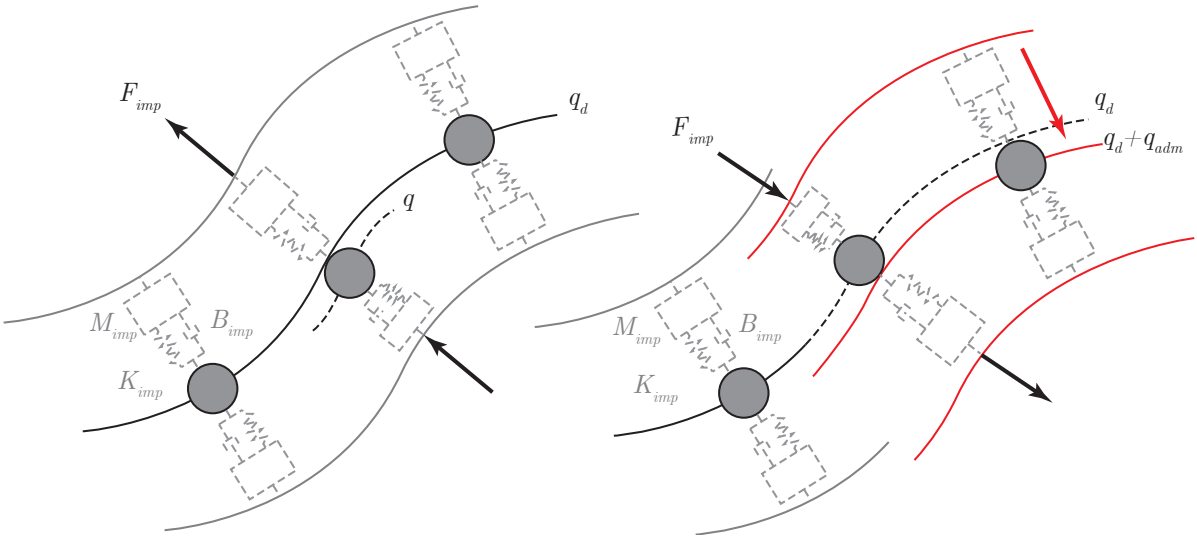

Source: Author (2021).

Figure 29 – Block diagram of the proposed cascade control architecture. The blocks are named intuitively.

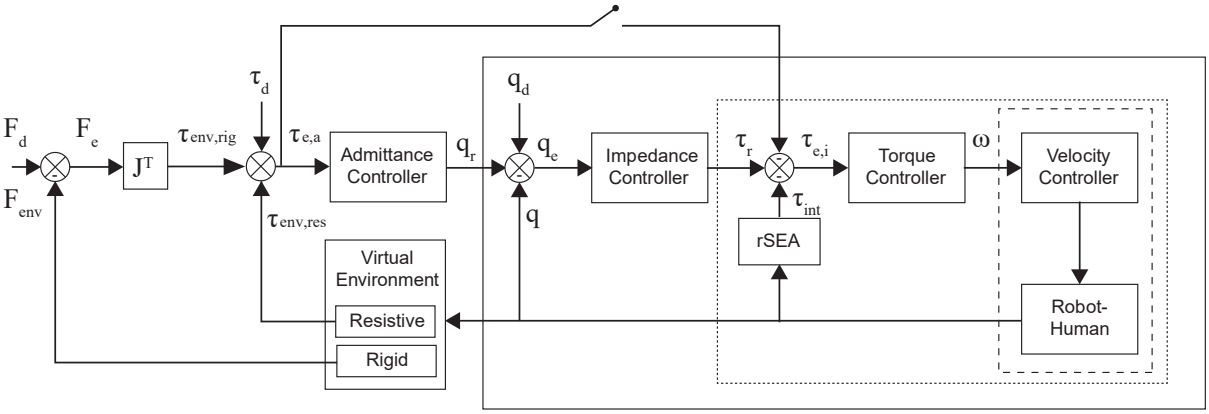

Source: Author (2021).

Figure 28 illustrates how the control architecture functions. An impedance controller ensures reference tracking, by exerting a corrective torque proportional to the trajectory deviation according to the mechanical impedance to be rendered. The higher the impedance, the closer the reference tracking. At the same time, an admittance controller generates a trajectory correction in order to render the effects of environment forces surrounding the user. Figure 29 shows the block diagram of the overall architecture. The torque control loop comprises a PI torque controller, and the outermost control loop consists of an admittance controller. In between, an impedance control loop is shown. The top connection, with a switch, is only present when the admittance controller is removed, so that the impedance controller handles the environment forces instead.

In the absence of environment forces, this architecture is reduced to an impedance controller, which handles only the user interaction torque.

Figure 30 – Robot trajectory under the proposed cascade control architecture. The free trajectory (dotted) is corrected by the trajectory generated by the admittance controller (dash-dotted line), which sum up to create a new desired trajectory (dashed line). The final trajectory of the robot is denoted by the solid line.

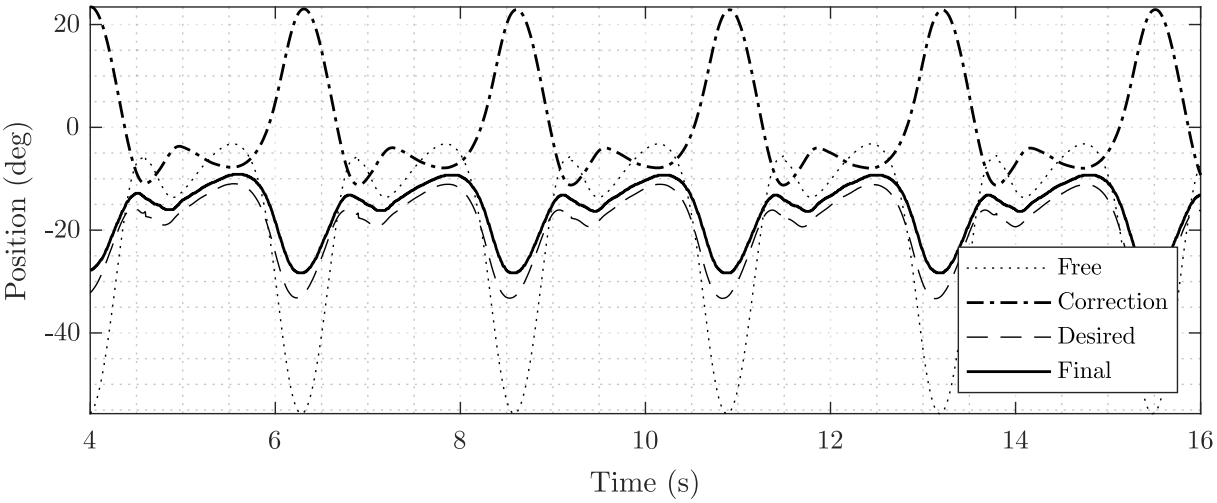

Source: Author (2021).

This approach addresses some issues identified in the previous approach. Since it decouples the human-robot and the robot-environment interaction, the tuning can be done separately; the environment and the admittance controller gains are set according to the sort of environment that one desires to represent, whereas the impedance controller gains are set according to the level of assistance needed to deliver to the users, that is, how closely one would want the controller to drive the human joints to the desired trajectory.

In other words, the robot behavior is "softened" by the admittance controller, whereas the impedance controller gains are kept at values that guarantee a safe and comfortable human-robot interaction, without being too low so that the performance is hampered, at the same time they are not too high, lest there is unstable behavior during interaction.

However, it also presents disadvantages. This approach only functions if a desired trajectory, planned beforehand, is employed. Figure 30 illustrates an example of this controller functioning for a resistive environment ($B_{env} = 50$ Nms/rad, $K_{adm} = 50$ Nm/rad, $B_{adm} = 10$ Nms/rad, $K_{imp} = 100$ Nm/rad). The dotted line denotes the desired trajectory; the dash-dotted line denotes the trajectory correction, generated by the admittance controller; the corrected desired trajectory is given by the dashed line; the final trajectory given by the solid line is more damped than the free one. In this example, the robot could track the corrected desired position with a mean error of 3.08 ± 1.4 deg, RMS 3.38, and a maximum error of 6.72 deg, during the start of the swing phase, moments before the negative peak value. These trajectory errors are of the same order as the ones obtained during the model validation procedure.

3.7 Controller Tuning

The robot alone, without the user, was tuned according to the parameters in Table 1. The integrative gain of the PID controller is set to zero only for the rigid wall environment. The derivative gain k_d was set to zero, because of the noisy nature of the rSEA torque measurements, whose time derivatives, computed numerically, were noisy as well, leading to meaningless interpretation (LYNCH; PARK, 2017). Therefore, the PID controller was reduced to a PI controller. The proportional and integrative force controller gains were tuned based on previous experiments performed on the robot.

The impedance controller was tuned so the joints could follow closely the desired trajectory. Therefore, the chosen virtual stiffness value fell near below the actual stiffness value in order to keep the system passive. The impedance controller deals with the user-robot interaction only. Its values can be adjusted, further, for the case in which the human wears the robot, according to comfort criteria. For the tests performed here with healthy subjects, it was later tuned to $K_{imp} = 80$ Nm/rad, a reduction of 20% of its original value. Likewise, damping was increased to $B_{imp} = 10$ Nms/rad during tests with human subjects.

The admittance controller was tuned based on the environment model. In the case of resistive mediums, the admittance controller gains were reduced to a stiffness value only. This can be induced based on the causal duality principle and the final value theorem (LEWIS; DAWSON; ABDALLAH, 2003). For rigid environments, the admittance controller must present at least a virtual stiffness, along with some damping. The tuning values were chosen based on the simulation results and tests on the real hardware. Since they were tuned with respect to the environment model only, during tests with human subjects they remained the same, since the environment was the same.

Table 1 – Control gains after tuning for a first evaluation of the control architecture performance.

Mode	Environment (K_{env}, B_{env}, M_{env})	Admittance (K_{adm}, B_{adm}, M_{adm})	Impedance (K_{imp}, B_{imp}, M_{imp})	Torque Controller (k_p, k_i, k_d)
Free	(0, 0, 0)	(0, 0, 0)	(0, 0, 0)	(385, 35, 0)
Trajectory	(0, 0, 0)	(0, 0, 0)	(100, 0, 0)	(385, 35, 0)
Resistive	(0, 50, 0)	(50, 10, 0)	(100, 0, 0)	(385, 35, 0)
Rigid	(100-500, 5, 0)	(30, 0, 0)	(100, 0, 0)	(385, 0, 0)

[1] Stiffness, damping and inertia parameters units are, respectively, N.m/rad, N.m.s/rad and kg.m^2/rad.

[2] The inner-force controller parameters units are, respectively, N.m/rad, N.m/rad/s and N.m.s/rad.

3.8 Controller Effort

Because the impedance and cascade control architectures may present similar kinetic and kinematic robot behavior, an energetic analysis of the controllers is performed.

For this, two indicators are calculated. First, the usual definition of controller effort (Q) is computed, which consists of the integral of the controller output squared, as in:

$$Q = \frac{1}{Q_{ref}} \int u(t)^2 dt. \tag{3.17}$$

The controller effort is normalized by the values obtained for the case in which there is no environment forces (Q_{ref}), i.e., only indirect trajectory tracking by means of impedance control (as described in Section 3.2).

Then, the cumulative controller effort (Q_K) is computed. Bartyś and Hryniewicki (2019) present the cumulative controller effort, whose discrete form definition is provided here, as a means of measuring the controller effort of a motor by analyzing the control signal.

$$Q_K = \frac{1}{\Delta t} \frac{1}{\Delta u} \sum_{k=1}^{T-1} \mid u^k - u^{k-1} \mid, \tag{3.18}$$

where

$$\Delta v = \mid u_{max} - u_{min} \mid .$$

Both indicators in Equations 3.17 and 3.18 will be employed in the performance analysis of the control architectures. The advantages of Equation 3.18 compared with Equation 3.17 relies on the fact that the former normalizes the control value, leading to more straightforward conclusions.

3.9 Tests on the Real Hardware

Here, pre-recorded joint trajectories were employed, as in Fig. 21, and the robot was tested alone. In the absence of environment forces, the admittance controller does not affect the desired trajectory. This way, the controller is simplified to an outer impedance control loop with an inner torque control loop. Only the robot-human interaction must be handled by the control architecture.

For resistive environments, the admittance controller adjusts the desired trajectory continuously, based on the sensed environment forces and the admittance controller parameters. In turn, the impedance controller simply considers the environment a component of the inner torque control loop error, according to Equation 3.12. The controller responses are compared.

In the case of rigid environments, the admittance controller generates a trajectory offset to prevent the robot from going further into the rigid environment interface. In turn, the impedance controller simply senses an environment torque which increases the inner

torque loop error, which is driven to zero by the torque controller. These two controller responses are also compared.

3.9.1 Resistive Environment

With respect to the interaction with resistive environments, an example is provided in Figure 31. The environment damping was set to $B_{env} = 50$ Nms/rad and all other environment parameters were null. The controller gains were the same as described in Table 1. The environment resistive force is computed as in Equation 3.10. Since there is more damping, it is observed that both cascade (solid) and impedance (dash-dotted line) controllers result in a robot position and velocity with a smaller amplitude and phase shift when compared to the desired trajectory (dotted line).

The cascade controller follows the corrected desired trajectory with a mean error of 3.08 ± 1.4 deg, RMS 3.38 deg, likewise the example in Fig. 30, since both figures refer to the same data. Furthermore, the final trajectory RMS value is 33.22% smaller than the original free trajectory, with a peak value about 49.19% smaller as well. This denotes that the cascade controller generates a more damped trajectory in the end. The impedance controller cannot be analyzed from the trajectory error perspective. The final trajectory RMS value is 28.27% smaller, and the peak value about 34.35% smaller. The cascade controller generates trajectory which is 17.51% more constrained when compared with the impedance controller trajectory, for the same environment.

The cascade controller presented a normalized controller effort $Q = 0.21$ and a cumulative controller effort $Q_K = 1.84$. These values for the impedance controller were 0.57 and 2.89. For comparison, since the controller effort is relative, the impedance controller without environment forces presented a controller effort of 1 and a cumulative controller effort of 1.66.

Compared with the free trajectory, when a resistive environment is present the cumulative controller effort increased by 10.84% and 74.10% for the cascade and impedance controller, respectively. It can be concluded that the presence of environment forces demands more from the controllers. This can be explained by the fact that more signals are being processed during each time step, and the controllers have to account for errors from different sources, e.g., the environment, the user interaction, as in Eq. 3.12.

The normalized controller effort decreased by 79% and 43% for the cascade and impedance controllers, respectively. Since the final trajectory is more damped than the reference one, over the test the control signal in general was smaller, which explains the observed behavior.

Both architectures seem to render steadily the haptic feedback originated from the user interaction with resistive virtual environments, which can be noted through the

Figure 31 – (Top) Knee position and (bottom) velocity for the cascade (dash-dotted line) and impedance (dotted line) controllers in contact with a resistive medium of $B_{env} = 50$ Nms/rad.

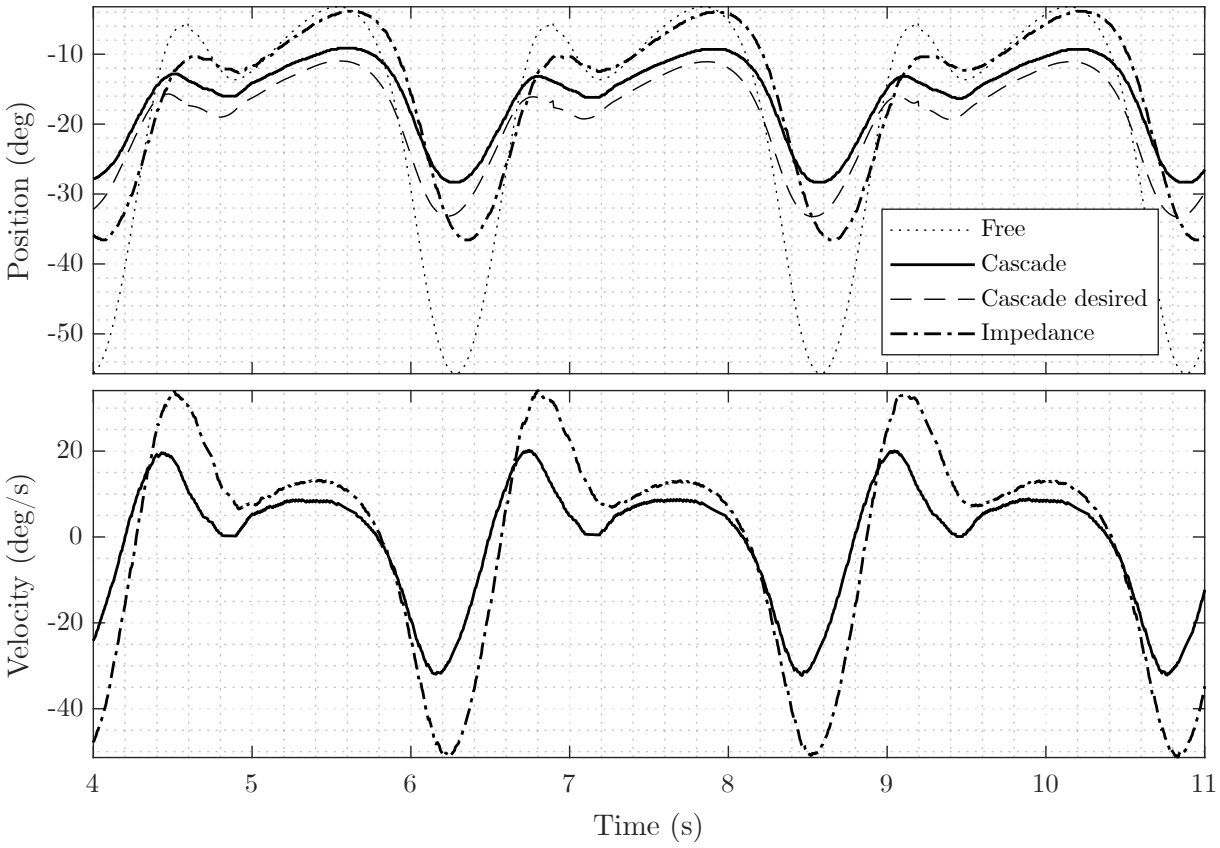

Source: Author (2021).

smaller amplitude of the final trajectory. It is important to remember, though, that the impedance controller becomes unstable for this scenario, once the human is coupled to the robot.

3.9.2 Rigid Environments

Figures 32 and 33 show the robot position, velocity and end-effector distance to the virtual wall for the impedance and cascade controller, respectively. A rigid, virtual wall was placed at 0.25 m in front of the robot, which corresponds to a hip angle around 30 deg. As the robot knee joint performed the desired trajectory, its end-effector interacted with the wall. The environment was modeled according to Equation 3.11, and its parameters were set to $K_{env} = 500$ N/m for the impedance controller, and $K_{env} = 100$ N/m, for the cascade controller. Controller gains were set as in Table 1.

Figure 32 shows the robot in contact with a virtual wall under impedance control. The knee trajectory is constrained, due to the arising environment forces. The movement is only restricted in the direction along which the joint angle increases, because of the virtual wall in front of the robot. In the other direction, the robot matches the desired

Figure 32 – (Top) Knee trajectory and (bottom) velocity for the impedance control scheme, in contact with a rigid wall of $K_{env} = 500$ N/m. Shaded area denotes the moment during which the contact happened.

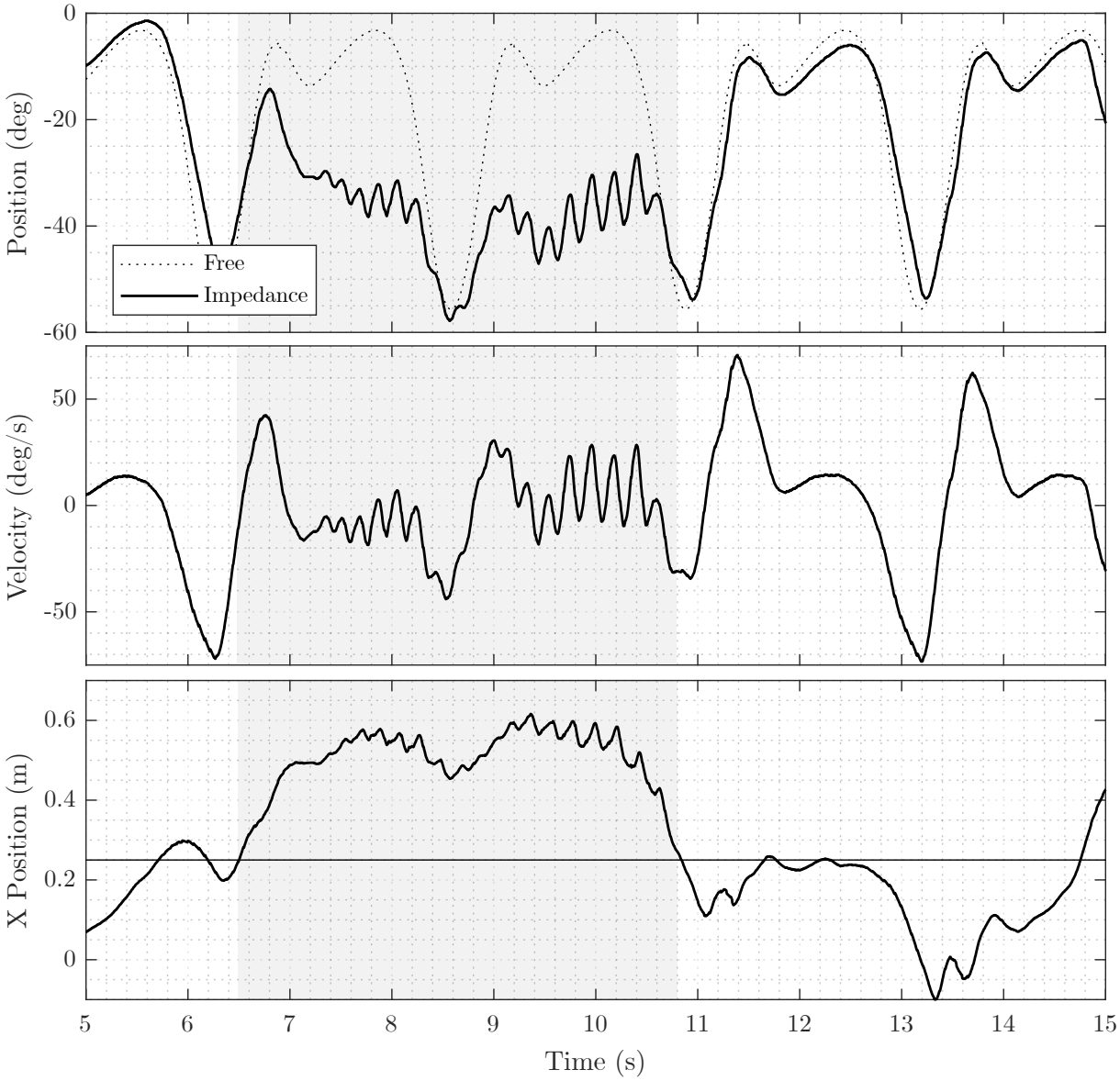

Source: Author (2021).

trajectory. Ripples are present in the final trajectory, and the robot penetrates deep into the virtual wall interface, maximum of 0.37 m.

Figure 33 shows the robot in contact with a virtual wall under cascade control. Likewise the impedance controller, the knee trajectory is constrained, due to the arising environment forces and the movement is only restricted in the direction along which the joint angle increases. In the other direction, the robot matches the desired trajectory. Though ripples are not present, the final trajectory preserves the profile of the desired trajectory, but the robot penetrates significantly into the interface, maximum of 0.43 m.

These experiments with rigid virtual walls are included just for experimental

Figure 33 – (Top) Knee trajectory and (bottom) velocity for the cascade control scheme, in contact with a rigid wall of $K_{env} = 100$ Nm/rad. Shaded area denotes the moment during which the contact happened.

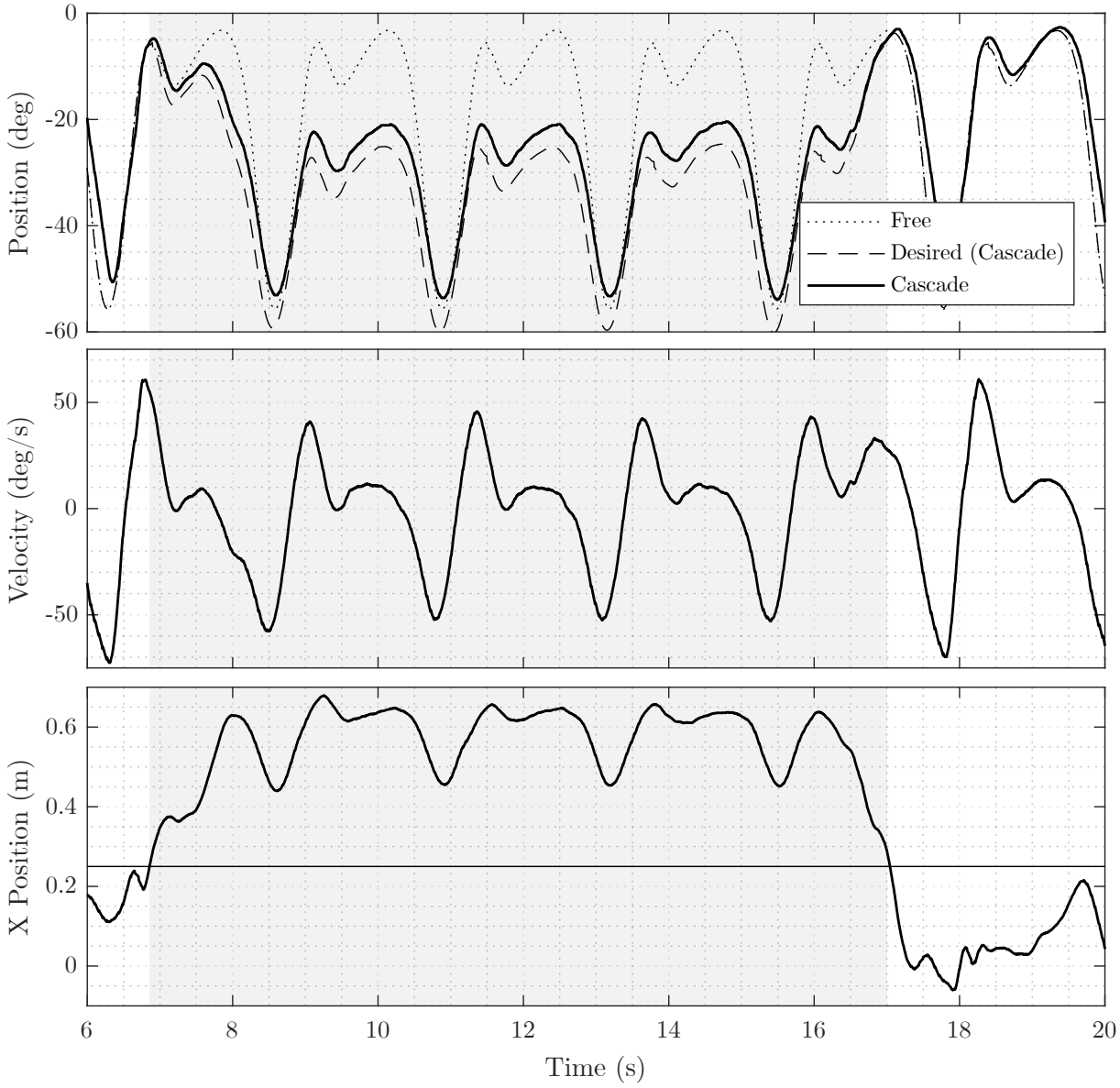

Source: Author (2021).

purposes. Due to their non-optimal behavior (they penetrate too much into the interface), they will not be employed for tests with human subjects.

3.10 Overview on the Controllers Performance

With respect to resistive environments, it is clear that the most suitable architecture is the cascade one, even though the robot alone presented satisfactory performance under impedance control. When preliminary tests with human subjects coupled to the robot were performed, the impedance architecture alone could not handle both the interaction torque and the environment torque and remain stable. Thus, the cascade controller is a

safer option for further tests with human subjects.

When it comes to rigid environments, the impedance controller seems to be the most suitable approach, as it led to smaller penetrations into the interface. Although both architectures require some level of environment compliance in order to achieve steadier responses, the cascade controller only shows stable response when the environment stiffness is five times smaller than the environment stiffness dealt by the impedance controller. In practice, the environment ended up not being much rigid, even though the system responded as if the environment was. Due to their sub-optimal behavior, both controllers will not be employed for tests with humans wearing the robot and interacting with rigid environments, without further study, tuning and stability analysis.

4 MULTISENSORY FEEDBACK SYSTEM IMPLEMENTATION

The design and implementation of the proposed multisensory feedback system comprise three main interfaces, they are: a visual interface; an auditory interface; and a haptic interface. The existing off-the-shelf virtual reality equipment facilitates the implementation of the first two interfaces, whereas the lower limbs exoskeleton present at the laboratory serves as a haptic interface. This chapter is organized as follows: Section 4.1 presents the virtual reality equipment; Section 4.2 presents the software. Further, Section 4.3 presents the auditory feedback and Section 4.4 presents the visual feedback description, which includes all techniques involved in the embodiment process, e.g., movement tracking and velocity estimation. Section 4.5 summarizes the control schemes utilized for the haptic feedback interface and the virtual mediums with which the avatar will be in contact, already explained in detail in Chapter 3. Section 4.6 presents the questionnaires envisioned to assess the experience in virtual reality.

4.1 Virtual Reality Hardware

The HTC Vive was chosen as the virtual reality equipment. It comprises two handheld controllers, two lighthouse stations, and one head-mounted display (HMD), as shown in Fig. 34. The HMD allows the user to experience immersive VR, since it involves most of the visual field of the person wearing it. There is empirical evidence that immersive VR yields stronger feeling of presence and better motor performance, in spite of non-immersive VR (flat screens) and augmented reality applications (WENK *et al.*, 2019).

All components of the HTC Vive (HMD and handheld controllers) can be tracked and their position and orientation in the three-dimensional space is provided through the

Figure 34 – HTC Vive equipment consisting of (from left) one head-mounted display, two handheld controllers, and two lighthouses.

(a) (b) (c)

Source: Author (2021).

SteamVR Unity Plugin[1]. When the controllers are attached to a body part, it can be tracked indirectly. By doing this, the users head and hands are tracked as long as they wear the HMD and hold the handheld controllers.

As the user walks on the treadmill, it is more convenient to track the user's left shank (which is not being tracked by the robot) than the user's hands, since the person will be holding the treadmill handrails instead of the controllers. In order to attach comfortably the controller to the user's shank, an elastic strap is used.

4.2 Virtual Reality Software

Game engine is a software aimed to the development of applications, which provides the necessary and convenient tools in order to build games in an efficient manner (e.g., Unity, Unreal Engine, Amazon Lumberyard, Godot Engine, among others). A built-in physics engine stands out as one of its features. The physics engine is responsible for handling physical simulations in a realistic way inside the virtual environments developed inside the game engines (UNITY TECHNOLOGIES, 2019).

This work makes use of the Unity game engine, which has built-in a NVIDIA PhysX physics engine. In Unity, two and three dimensional models located in a game scene are denominated game objects. Dynamic properties can be attributed to game objects by attaching to them a "Rigid Body" component, a class that provides the developer access to the methods, properties, and other features pertaining the physics engine module. This way, the game objects become subject to forces, and their movement is ruled by the physics engine (NVIDIA, 2019). However, for this work, calculations related to the dynamic behavior between the user avatar and the VE will not be handled by the physics engine. Even though PhysX stands out as one of the best physics engine available, its performance differs for different simulation problems (e.g., integrator performance, material properties, constraint stability, collision system, etc.). Therefore, the physics engine limitations must be considered, and a series of tests and simulations have to be executed, as in Boeing and Braunl (2007), before employing it. The physics engine will handle only the interaction between generic objects in the scene with others game objects.

A virtual environment is a scene inside the game engine; game objects that populate a scene, along with their properties, such as materials, textures, meshes, audio tracks, 2D sprites and C# scripts that add customized behavior and properties to game objects, i.e., all things used to implement a game or application are referred to, generically, as an asset. There is a considerable number of free assets available online. This work rely on these public assets. Only when strictly necessary, new assets are designed from sketch. With this approach, modeling a VE and implementing scripts that handle the user interaction with the surrounding virtual objects becomes an intuitive task within the game engine.

[1] <https://valvesoftware.github.io/steamvr_unity_plugin/>

Figure 35 – (Left) Virtual environment with resistive medium; (center) peaceful forest environment; (right) resistive snow environment. The VEs were developed with free assests from Unity Asset store.

Source: Author (2021).

4.3 Auditory Feedback

The HTC Vive contains a stereo 3.5 mm headphone jack. Auditory feedback is provided through in-ear headphones, included with the HTC hardware. There are two sorts of auditory feedback: (1) background auditory feedback, which consists of ambient sounds; and (2) event-based auditory feedback, which consists of audio tracks that are triggered whenever a specific action takes place. The latter can be environment sounds, based on the elements in the scene, such as the sound of the snow being stomped as the user walks; or sounds unrelated to the environment, such as music audio tracks that are triggered whenever the users score or when their performance declines. Implementing auditory feedback is straightforward, but does require user testing. The virtual environments proposed in this work possess both sorts of auditory feedback. The tests performed with the users in the water environment, detailed further in this Section, were performed with background auditory feedback only.

4.4 Visual Feedback

Visual cues are crucial to maintain the illusion of presence inside VR. As the application is aimed at impaired people, a reduced number of stimuli is developed. The visual cues comprise the environment itself, i.e., the virtual scene and its components, along with the user's avatar. Figure 35 presents the proposed calming virtual environments for straight, infinite walk.

The virtual environments are modeled with 3D models, such as trees, furniture, objects, buildings, and game engine tools, such as terrain modeling and post-processing filters. To name all elements pertaining to a VE is redundant. Only the general characteristics of the environments are mentioned. There are, currently, three environments: (1) the forest environment, which offers no movement restriction to the user, and serves only as a means

Figure 36 – (Left) Avatar placed inside the water environment. (Right) Rendered image on the HMD. The magenta box denotes the virtual panel, through which the subjects can see their real legs in the physical world, as well as the treadmill.

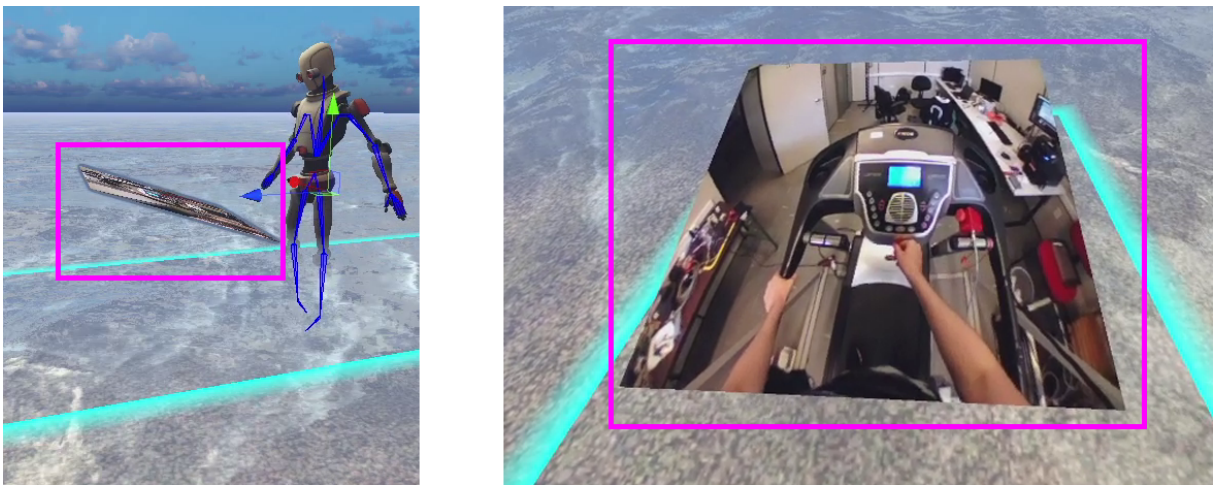

Source: Author (2021).

of distraction; (2) the water environment, a resistive medium, which offers movement resistance according to Eq. 3.10; (3) and the snow environment, which is also a resistive medium, likewise the water environment, but with a greater environment damping. The number of environments can be extended; as this procedure relies on computer graphics design rather than robotics or control theory, it is not the priority of this project.

Rigid virtual walls that would prevent the user from going further are not modeled as a specific VE. Inside the aforementioned environments, some stiff obstacles could be placed, e.g., a tree stomp or a stone, with which the user could interact. However, due to the sub-optimal performance of the controllers for stiff environments, the user interaction with stiff objects is not contemplated for the time being.

In order to improve user comfort and safety, the user will be able to see their feet position in the physical world through the embedded frontal camera of the HMD, as depicted in Fig. 36. The users are given the option to turn off this feature, in order to achieve a greater degree of immersion inside VR.

The user avatar is an important feature. The avatar movements must match to a certain extent the user's movements in order to deliver the feeling of embodiment, one of the most important illusions to guarantee the feeling of presence. To achieve this, movement tracking with low latency is a requirement. Even if the movements of the avatar do not match perfectly a person's movement, the brain can adapt to these changes in limb geometry and location as a result of the embodiment (TOET *et al.*, 2020).

The avatar can be either a realistic humanoid model or an unrealistic cartoonist

Figure 37 – Space robot Kyle developed by Unity Technologies can be employed as an avatar for VR applications. The humanoid bone structure of the avatar is denoted in blue.

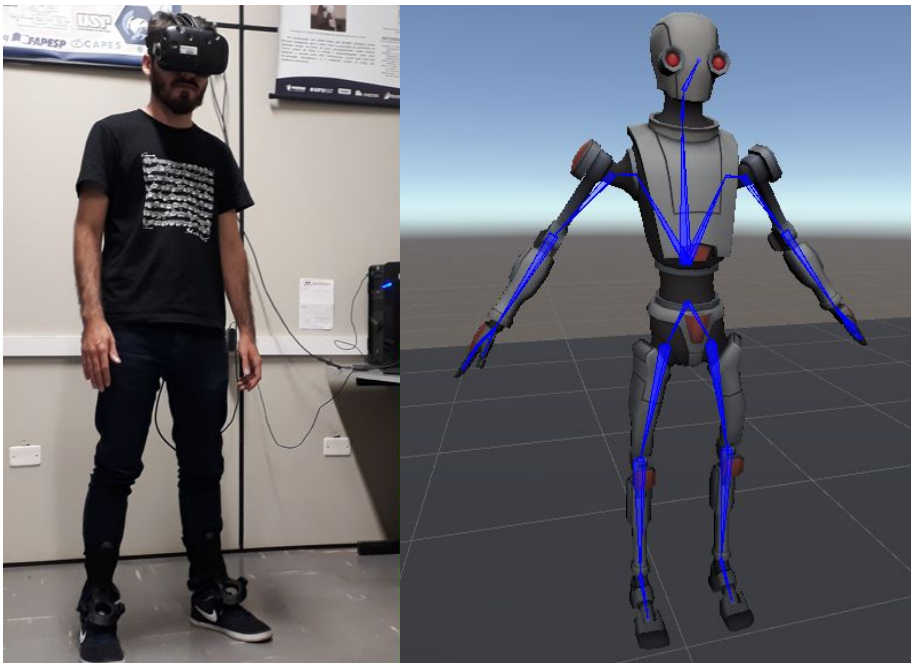

Source: Author (2021).

avatar. Both can be obtained through public assets. Humanoid models can also be developed with Make Human[2], an open-source tool, often employed in VR embodiment research (WENK *et al.*, 2019). When a humanoid avatar is prone to trigger the feeling of discomfort due to the uncanny valley region of human likeness, it is better to employ unrealistic models, such as cartoon-like humanoids or robots (MORI; MACDORMAN; KAGEKI, 2012). For this purpose, the Kyle Space robot developed by Unity Technologies is employed. Both humanoid avatars built with Make Human and the Kyle robot are scaled, rigged 3D models, which means they have a simplified internal bone structure slightly similar to the human one. This bone structure is used to manipulate the model as a puppet and it includes the main lower limbs joints (hip, knee, ankle). Figure 37 shows a subject side-by-side with Kyle. The scale of the avatar can be adjusted to match the user's height.

Head tracking will be achieved through the HMD position and rotation. Though subtle and less noticeable, the head will be treated as a small chain comprised of a link (neck) connected to a base (torso) and an end-effector (head). An iterative inverse kinematics (IK) algorithm based on Cyclic Coordinate Descent (CCD) will be employed to achieve a smooth neck and head tracking (WANG; CHEN, 1991). The CCD algorithm is the common approach to solve the IK problem and it has been employed extensively in the computer graphics industry, specially in gaming and animation applications, in which an adaptation of the original algorithm proposed by Wang and Chen (1991) is presented

[2] <http://www.makehumancommunity.org/>

and utilized in Unity (UNITY TECHNOLOGIES, 2018). It treats IK not as a geometric problem, but as an optimization problem. The algorithm presents some advantages, such as the fact it is not prone to singularities and it can be extended in a straightforward manner for many DoF. Here, a modification of the adapted CCD algorithm is employed. Preliminary studies performed by the author suggested that, by placing a tracker onto the shank the CCD IK algorithm yields satisfactory estimations for the knee and hip joints (OSTAN; SIQUEIRA, 2019a). Figure 38 illustrates the algorithm by showing a few calculation steps.

In short, the algorithm accesses each joint of the kinematic chain, computes the vector from the joint to the end-effector $\vec{u}$, the vector from the joint to a final, or goal, position in the Cartesian space $\vec{v}$, and the vector which represents the subtraction between these two vectors, $\vec{w}$. The joint performs the rotation that minimizes this vector, which is the rotation that makes the vectors $\vec{v}$ and $\vec{u}$ parallel to each other. The algorithm then accesses the next joints successively, performing the same calculation steps and rotating it. The order in which the algorithm accesses the joints can be customized. The algorithm iterates until a tolerance or a maximum number of iterations is achieved.

Tracking the hands can be achieved in a similar manner by means of the same IK algorithm if the user holds the handheld controllers. However, when the users walk on a treadmill, it is not convenient for them to hold the handheld controller, besides the fact that there would not be enough Vive handheld controllers or trackers: for each hand, one controller could be used, but then an additional tracker or controller will be needed for the left leg. Therefore, the tracking of the hands will not be performed and it will be estimated based on the head position of the user. In order to create the illusion that the

Figure 38 – Steps of the IK algorithm based on CCD. The algorithm iterates until an error tolerance or a maximum number of iterations is reached. The subfigures denote the (a) first, (b) second, and (c) third iteration of the algorithm.

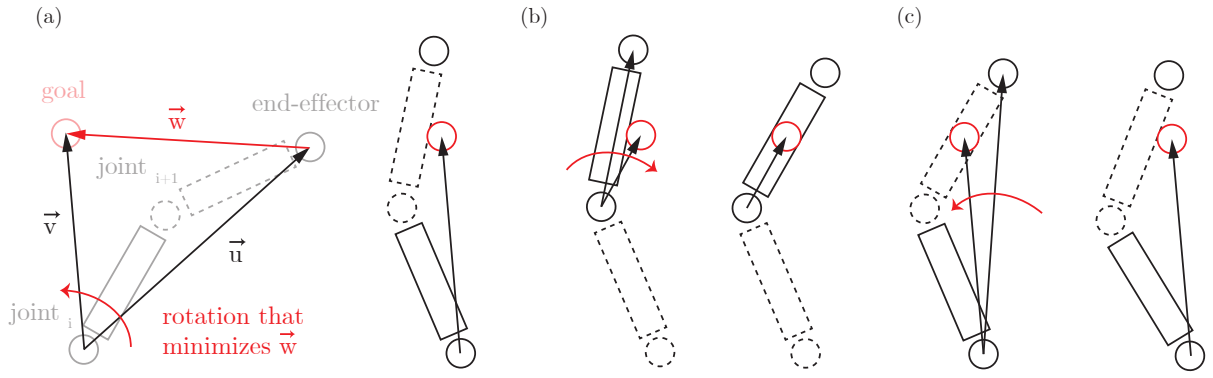

Source: Author (2021).

Figure 39 – The IK algorithm based on CCD can be employed with the Cartesian position of the head, feet or hands to estimate the angle of the joints that compose the human body without the need of additional sensors. In this case, the handheld controllers are attached to the shank, to estimate the hip and knee joint angles. The boxes depict the body parts being tracked.

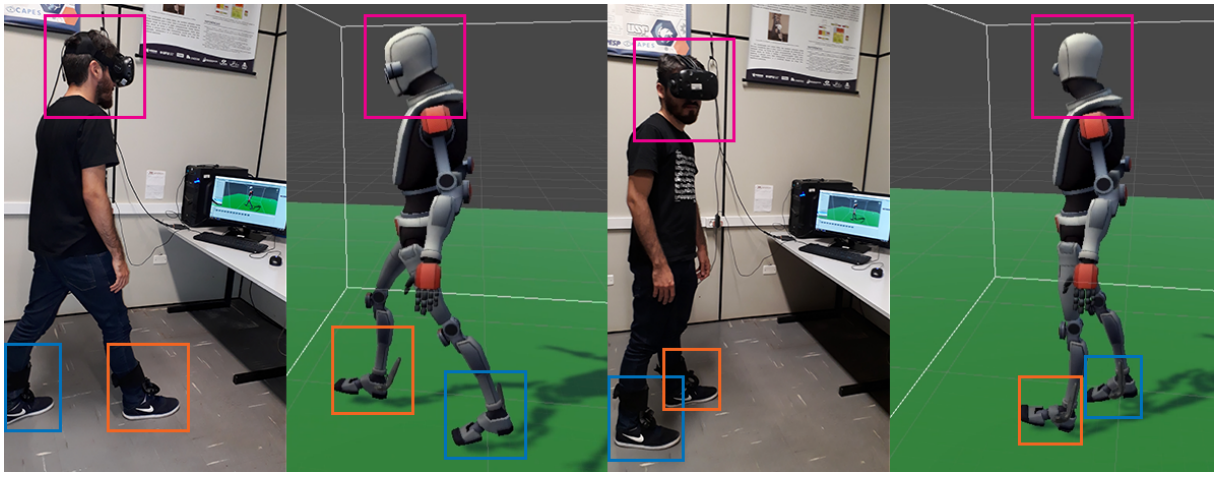

Source: Author (2021).

hands are being tracked, as the user, very likely, during the walk, will not move the hands away from their original position, the hands will be aligned at the same height as the treadmill handrails.

Figure 39 shows the algorithm being tested to estimate the hip, knee and ankle joint displacement based only on the feet Cartesian position, as well as the head and neck rotation. Though the ankle estimations were not accurate, the hip and knee ones were satisfactory. The results can be extended for the upper limbs with no further problems. It is important noticing that the algorithm can track as well the low-range adduction and abduction hip movement on the frontal plane. The algorithm was adjusted to prevent it from estimating joint displacements out of the range of the human joints.

Finally, to match the avatar's linear velocity with the user's, a linear Kalman Filter (KF) is employed. The KF estimates the angular velocity of the hip joint based on the hip joint displacement (OSTAN; SIQUEIRA, 2019b). This velocity is multiplied by the approximate length of the user leg and an augmentation factor. This approach is simpler and more stable than synchronizing the treadmill velocity to the user's and more comfortable than assigning to the avatar a fixed velocity. To match the linear velocity of the avatar and the user can help to prevent motion sickness. In the control algorithm, KFs are used to obtain estimates of all joint velocities.

4.5 Haptic Feedback

To handle the interaction between the human wearing the robot and the VE, the cascade admittance-impedance controller described in Chapter 3 is employed. In the cascade controller, the outer admittance controller guarantees that the desired trajectory is adjusted as environment forces are sensed. Different environments will result in different trajectory adjustments. The impedance controller after the admittance one guarantees that the user's knee joint follows a pre-established trajectory in a compliant manner.

4.6 Questionnaires

In total, five questionnaires are applied. They are: (1) the Motion Sickness Susceptibility Questionnaire (MSSQ); (2) the Gaming and Virtual Reality Familiarity Questionnaire (GVRFQ); (3) the Haptic Feedback Questionnaire (HFQ); (4) the Simulator Sickness Questionnaire (SSQ); (5) and the iGroup Presence Questionnaire (IPQ). The questionnaires are found in the Appendix B−F. They were applied utilizing consolidated translations to Portuguese, whenever available, and with the aid of a computational tool that facilitates to gather the data to be further analyzed in Excel (2016).

4.6.1 Motion Sickness Susceptibility Questionnaire (MSSQ)

The Motion Sickness Susceptibility Questionnaire (MSSQ) is employed, as in Appendix B to evaluate at which degree the user is prone to motion sickness (MS) — the most common adverse effect of VR that may undermine experience during the tests. This questionnaire was proposed by Golding (2006) and is the short version of the questionnaire proposed by Golding (1998). The MSSQ is based on a punctuation-scheme points: the more often the users were subjected to situations prone to be affected by MS — and the more they relate suffering MS symptoms, as nausea or vomiting — the more points they get. The MS susceptibility is scored for their childhood experiences (before 12 years old) and for their experiences in the last ten years, referred to as adult phase. The questions are answered in a Likert-scale from 0 to 3, where: (0) not applicable or never traveled; (0) never felt sick; (1) rarely felt sick; (2) sometimes felt sick; (3) frequently felt sick. As this questionnaire is the first to be filled out, it also contains background information about the subject (age, sex, occupation, self-perception of motion-sickness susceptibility and exercise routine). Though there is no validated Portuguese translation of this questionnaire, the symptoms ("to feel sick" and "to feel nauseated") were translated based on a Portuguese validation of a symptom inventory, which included the symptoms mentioned in the MSSQ (KOLANKIEWICZ *et al.*, 2014). These terms were translated as *sentir-se enjoado* and *sentir-se nauseado ou com náuseas*, respectively. The modes of transportation (MT) of the questionnaire were translated intuitively. Less common MT do not interfere the results, since the user can choose the option "never experienced".

The MSSQ is evaluated in terms of how many points the user scored as follows:

$$\text{MSSQ}_{\text{childhood}} = \frac{\text{MT} \times \text{Total childhood score}}{(\text{MT} - \text{Not experienced MT})}. \tag{4.1}$$

The same is done for second part of the questionnaire, regarding the experiences as an adult. Thus the overall score is simply computed as:

$$\text{MSSQ}_{\text{score}} = \text{MSSQ}_{\text{child}} + \text{MSSQ}_{\text{adult}}. \tag{4.2}$$

According to Golding (2006), the mean score was 12.9 ± 9.9, presenting a positively skewed distribution. The long MSSQ questionnaire (GOLDING, 1998) presented similar results, 12.4 ± 9.4. The subscales (childhood and adult) presented a mean score of 7.75 ± 5.94 e 5.11 ± 4.48, respectively, which suggests that children are more prone to feel MS.

This questionnaire also presents additional questions regarding the medical background of the subject. If the user presents some pre-existing conditions that can be aggravated during the tests, the subject shall be discarded, lest the pre-existing conditions generate more acute collateral effects after the experience. All additional questions not present originally in the MSSQ questionnaire were marked with an asterisk (*) in Appendix B.

4.6.2 Gaming and Virtual Reality Familiarity Questionnaire (GVRFQ)

The second questionnaire to be filled, proposed by the author, is the Gaming and VR Familiarity Questionnaire (GVRFQ), in Appendix C, which should report if the user is familiar or not with VR games and video games in general. This is important because usually people used to VR tends to develop a sense of proprioception (self-body location) in VR, which in turn makes the user less prone to feel MS. It is also important to evaluate the familiarity with VR and gaming in general because as the users get used to these experiences they also tend to feel less motivated or impressed by VR.

4.6.3 Simulator Sickness Questionnaire (SSQ)

To evaluate the occurrence of side effects after the experience, the Simulator Sickness Questionnaire (SSQ), Appendix D, is applied, following the template established by Kennedy *et al.* (1993). The subject must answer this questionnaire through a 4-point Likert scale (0, 1, 2, 3) where 0 denotes no-reported symptom, and numbers from 1 to 3 denote different intensity of symptoms: slight, moderate and severe. Its validated Portuguese translation will be employed (CARVALHO; COSTA; NARDI, 2011), which comprises 16 questions, i.e., symptoms. Table 2 presents these symptoms included in the Portuguese version of the questionnaire, along with the category in which they fall and their respective weight for the score calculation. The SSQ measures whether the user

Table 2 – Symptoms and their respective category, according to the questionnaire proposed by Kennedy *et al.* (1993).

Symptom	**N**	**O**	**D**
General discomfort	1	1	0
Fatigue	0	1	0
Headache	0	1	0
Eyestrain	0	1	0
Difficulty focusing	0	1	1
Increased salivation	1	0	0
Sweating	1	0	0
Nausea	1	0	1
Difficulty concentrating	1	1	0
Fullness of head	0	0	1
Blurred vision	0	1	1
Dizzy (eyes open or closed)	0	0	1
Vertigo	0	0	1
Stomach awareness	1	0	1
Burping	1	0	0
Subscale scores	n	o	d

Source: Reconstructed from (KENNEDY *et al.*, 1993).

feels side effects at the end of the experience and at which degree, with respect to three categories of symptoms (sub-scales): nausea-related symptoms (N); symptoms related to the oculomotor system (O); or disorientation symptoms (D). Hence, it is possible to identify side effects as the cause for a lack of feeling of presence or discomfort during the experiment. The sub-scales can be scored separately as in

$$\mathrm{N} = 9.54 \times \mathrm{n} \qquad \mathrm{O} = 7.58 \times \mathrm{o} \qquad \mathrm{D} = 13.92 \times \mathrm{d}.$$

A total severity (TS) score is computed according to:

$$\mathrm{TS} = \mathrm{n} + \mathrm{o} + 3.74 \times \mathrm{d}. \tag{4.3}$$

4.6.4 iGroup Presence Questionnaire (IPQ)

In order to assess the user's feeling of presence, a questionnaire will be handed at the end of the VR experience. The chosen questionnaire was the iGroup Presence Questionnaire (SCHUBERT; FRIEDMANN; REGENBRECHT, 2001), Appendix E, which

is a miscellaneous of questions based on previous studies and questionnaires, such as the one proposed early by Slater, Usoh and Steed, known as SUS questionnaire (SLATER; USOH; STEED, 1994), and the one proposed by Witmer and Singer (1998), shortened as WS questionnaire. The questions were selected in a way that the three components of presence, as Schubert, Friedmann and Regenbrecht (2001) divide it, could be evaluated: spatial presence, involvement, and experienced realism, which comprise three sub-scales. For tasks in VR, a recent comparative study comparing these three questionnaires was performed by Schwind *et al.* (2019). As there was evidence that the IPQ slightly outperformed the other questionnaires, it was chosen for this study. In this case, the validated Portuguese translation of the IPQ is employed (VASCONCELOS-RAPOSO *et al.*, 2016). The translated questionnaire addressed the user by the second-person singular ("tu"), whereas, in Brazil, it is commonly used the formal pronoun "você". This was the only change made by the author before applying the IPQ.

The IPQ is answered with a 5-point Likert scale: starting at 1 for "totally disaagree" and ending with 5 for "totally agree". The results can be analyzed with respect to each sub-scale or with respect to the overall points at the end of the questionnaire. It is expected that this questionnaire provides some evidence whether the multisensory feedback system proposed by the author can deliver the feeling of being present inside the VE, and what should be improved.

4.6.5 Haptic Feedback Questionnaire (HFQ)

The Haptic Feedback Questionnaire (HFQ), Appendix F, proposed by the author, comprises two 5-point Likert-scale questions, in which the subjects must state whether they agree or disagree with the statement presented at each question, in the same fashion as the IPQ. The HFQ is proposed in this study as a means of measuring the user perception of the haptic feedback system, namely the controller architectures proposed to provide the haptic stimuli. Only two questions are placed for each controller tested. Since three controllers are tested (further explained in Chapter 5), the HFQ consists of 6 questions. The questions comprise the following two statements: "I felt that the environment/robot acted against me/my movement" and "I did not feel the environment/robot resistance".

5 TESTS AND RESULTS

This chapter describes the tests performed with ten healthy subjects and summarizes the findings. Three control architectures are tested. The results are evaluated based on measurements provided by the robot sensors and also on the user perception. Section 5.1 describes the test protocol. Section 5.2 analyzes the results based on the measurements. A discussion is drawn with respect to each controller, and also comparatively. Following, Section 5.3 presents and discusses the questionnaire answers.

5.1 Test Protocol

Ten subjects without motor disabilities participated in this study, 8 male, 26.1 ± 5.1 years, 76.0 ± 16.4 kg, 174.2 ± 8.2 cm. Each subject data are found in Table 7, Appendix A. They were briefed about the objective of this work, the average duration of the test (from 45 to 90 minutes) and the test procedure. Only the subjects who agreed with the test protocol and did not possess any medical condition whose symptoms could be aggravated during the experiment carried on to the next steps. All subjects were undergraduate or graduate students from the EESC-USP. They are referred throughout this text by the letter "S" followed by the number assigned to each of them, e.g., S1 refers to the first subject. The tests were approved by the ethics committee of the University of São Paulo, Escola de Educação Física e Esporte de Ribeirão Preto, EEFERP-USP, CAAE No. 41150620.7.0000.5659, decision statement (approval) No. 4.579.836.

Before the subjects started the test, they answered the MSSQ and the GVRFQ, in this order. In the case any medical predisposition was noted while filling the MSSQ, the user would be discarded.

Following, each subject wore the lower limbs exoskeleton, which was adjusted to the user's body by adjusting the robot links length and its Velcro® straps. To enhance comfort and avoid that the robot was loosely attached to the subject's limb, foams were placed between the robot and the subject. The VR HMD is worn in the sequence. The HMD can be adjusted to the user's head also by means of Velcro® straps. The interpupillary distance (IPD) is adjusted after the HMD is worn by means of a knob on its side. To adjust the IPD reduces eyestrain and helps to obtain a clearer vision of the VE. As the subject holds the treadmill handrails in order to ensure balance, the handheld controllers are not held, but rather used as if they were Vive Trackers®, by attaching one of them with an elastic strap onto the left subject's shank. By doing this, together with an IK algorithm, the left hip and knee joint angles can be estimated, in order to achieve a wider tracking of the lower limbs.

Figure 40 – (Left) Scene view: (red) virtual island, (blue) avatar mirrored image. (Center) Rendered image on the HMD: (green) virtual sky and sun; the water floods the VE. (Right) Distracting virtual elements: (yellow) virtual flock of birds. The perimeter in cyan delimits the area of reach of the VR equipment.

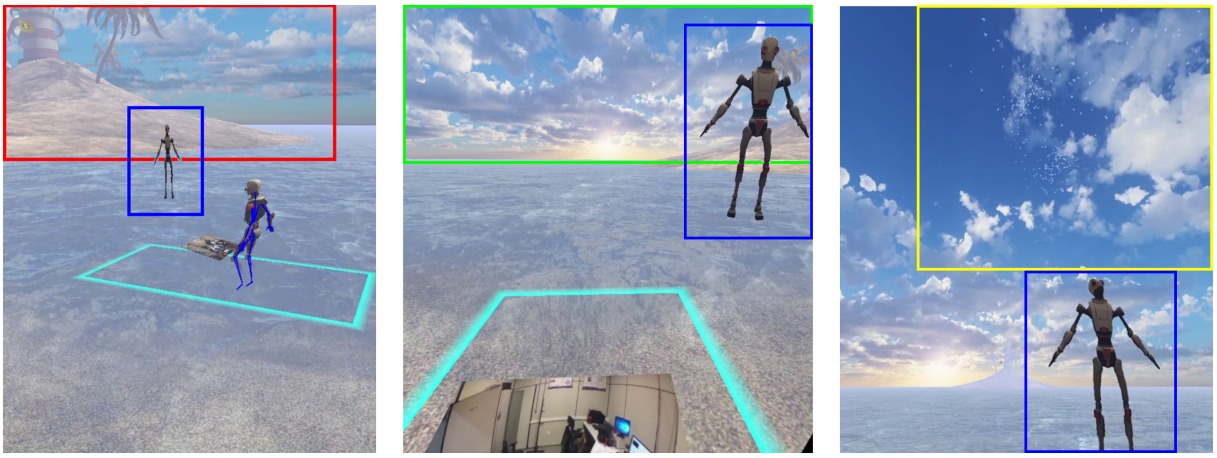

Source: Author (2021).

In the sequence, the VR application is executed. The subject is placed in a calm scenery, inside a shallow and wide ocean, as in Fig. 35. The subject is embodied in a cartoonist robot avatar, which mimics the subject's leg and head movements. On the right upper corner of the subject's FOV, the subject can see the avatar inside a floating window, as though it were a mirror. By doing this, the subjects do not need to look down to see their lower limbs moving. Looking down in VR, specially while wearing the HMD, is a common source of MS.

The avatar's scale is adjusted to the user's head height, so that the avatar's tip toe touches the ground, at the same time the water level is adjusted to be slightly above the avatar's knee joint. A customized algorithm determines the avatar scale for each subject. In addition, the left leg tip toe position is also adjusted, so the IK algorithm can track the leg without the exoskeleton. These adjustments guarantee a better body tracking, a smoother avatar movement and thus a greater level of embodiment.

After the subject is placed on the treadmill, wearing the HMD, and the avatar is adjusted, as in Fig. 41, the tests commence. The subjects must walk on the treadmill, while their avatars move forward and approach a virtual island, as in Fig. 40. Flocks of virtual birds were added to distract the subjects and immerse them, along with a background soundtrack.

The test consisted of three 2-minute walks, approximately, with three different control algorithms, which were not mentioned beforehand to the subject. The controllers were the impedance controller (IC), which delivers haptic assistance only; the proposed cascade controller, which differs from the previous controller by an outer admittance

Figure 41 – Subject wearing the HMD and the lower limbs exoskeleton on the treadmill during the tests.

Source: Author (2021).

controller (AC), and which delivers haptic feedback and assistance; and transparency controller (TC), which does not deliver any sort of haptic feedback nor assistance deliberately. Exceptionally S8 walked only for approximately 1 min, because the subject presented the smallest height and mass (51 kg and 153 cm) compared with the other subjects, and, thus, the robot represented relatively a large inertia to carry during the whole 2-minute walk. Furthermore, the robot could not be adjusted tightly to the subject's limbs, so it was preferred to reduce the test time, rather than excluding the subject from the analysis.

The subjects were instructed to walk at a slow pace following the treadmill velocity, which was set to its minimum velocity, 1 km/h. The subjects could increase the treadmill velocity until they felt comfortable. In general, the speed was kept between 1–1.5 km/h. In between tests, the subject stood still for 1-2 minutes until the controller was changed. During that time, the subject could either remove the HMD and rest the eyes, or contemplate the VE. The controllers were assigned in a pseudo-random order.

In between tests, two questions were placed. These two questions, pertaining to the HFQ, intended to measure the controller behavior from the subject's perspective.

A few remarks about the measurements: only the knee joint measurements are analyzed, since it is the only actuated joint. Some steps were discarded, until the subjects got used to walk on the treadmill with the exoskeleton inside VR. To check the discarded steps, one can refer to Table 10 in Appendix A. Furthermore, the exoskeleton has a fixed shoe, which is rigid to a certain extent, restraining the ankle dorsiflexion and plantarflexion

movements. The shoe cannot be changed according to each subject. For this reason, foams where placed inside the shoe to enhance comfort. However, even after these adjustments, the ankle joint of the robot and the subject's were not aligned. This hampered the ankle joint measurements considerably.

5.2 Controllers Performance Analysis

5.2.1 Impedance Controller

The average knee joint position among the ten subjects is shown in Fig. 42 (top). In all figures, the shaded area denotes the standard deviation of the measurements, $\sigma \in [8.01, 3.23]$ deg. The knee trajectory presented a RMS error of 8.18 deg, maximum absolute error of 19.46 deg. Compared to the desired (free) trajectory, the measured one has a peak and RMS value 30.62% and 27.04% smaller, respectively. It is expected that the robot values did not match the desired trajectory, since the impedance stiffness was reduced by 20%, from 100 to 80 Nm/rad and an impedance damping of 10 Nms/rad was included, to render a more compliant robot-human interaction. This set of impedance gains guarantees that the robot will drive the subject's knee joint to the desired value with greater compliance.

The simulation for the same set of impedance gains resulted in a RMS error of 10.24 deg (maximum absolute error of 21.26 deg), peak and RMS value reduction of 13.69% and 6.64%, respectively. Therefore, the experimental values show maximum and RMS error similar to the ones obtained during the experiment. However, the actual trajectory showed smaller peak values, thus, in general, a smaller amplitude. There are two possible explanations for this.

First, the difference may be explained by the exoskeleton inertia and lack of compensation mechanisms. In this case, there were no mechanisms for full compensation of the gravitational forces; neither the mechanical supporting structure compensates for the robot weight totally, neither the actuator can account for the influence of the weight effectively, for instance, by means of feedforward gravity compensation. Moreover, the desired trajectory was measured on a subject walking overground without a lower limbs exoskeleton; therefore, the desired trajectory does not consider the robot inertia, thus showing a wider amplitude. Second, the desired joint positions were acquired during overground walk, whereas during the experiment the subject walked on a treadmill, and there is some slight differences between treadmill and overground walking. Riley *et al.* (2007), Bennett *et al.* (2008) state that larger positive maxima and more negative minima are noticeable during overground walking compared with treadmill walking, which implies a slightly larger range of motion when the user walks overground. So, smaller range of motion is expected during treadmill walking.

The average interaction torque between the subjects and the robot is show in

Figure 42 – Impedance controller. (Top) Average knee position. (Center) Average interaction torque between the user and the robot. (Bottom) Average torque controller output.

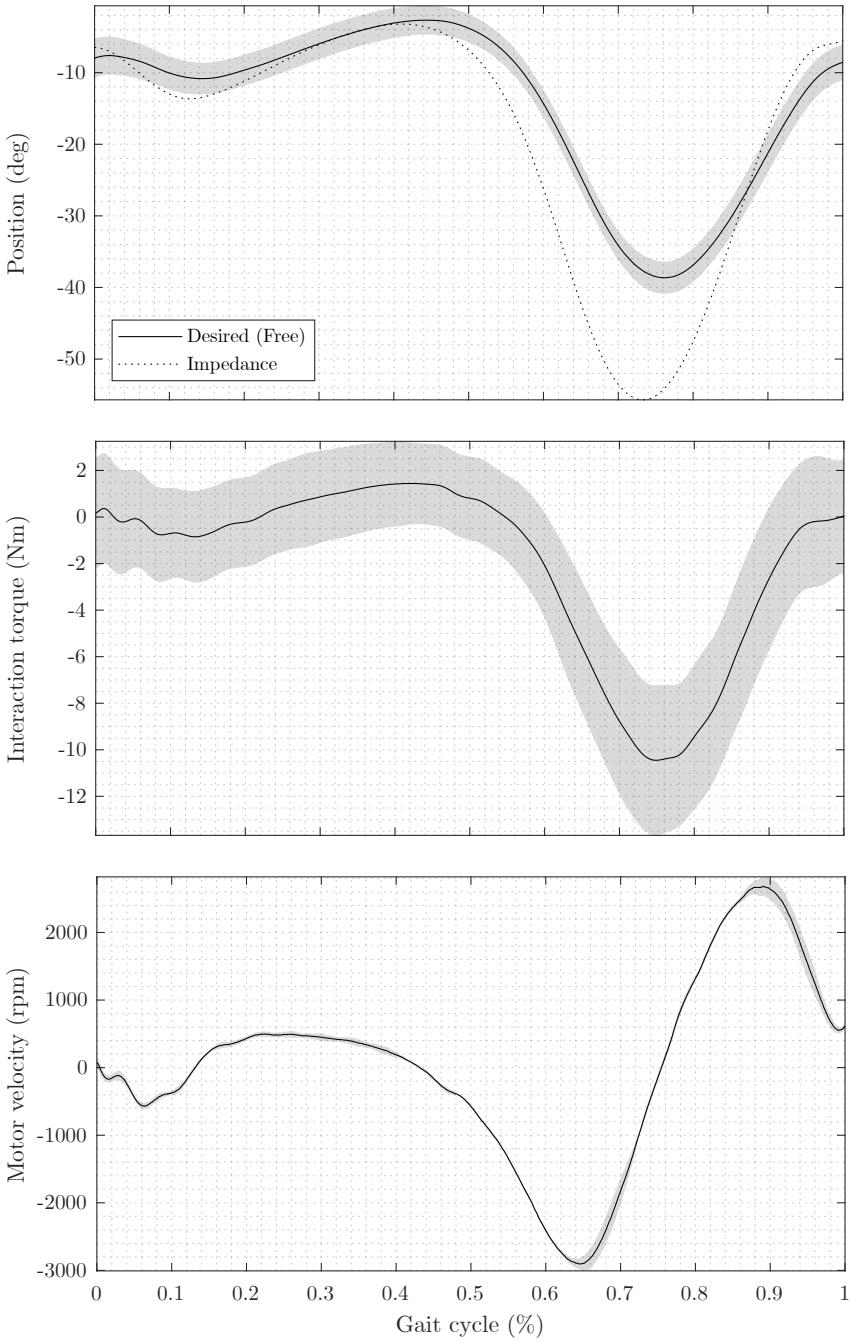

Source: Author (2021).

Fig. 42 (center); it presented a RMS value of 4.30 Nm, $\sigma \in [1.74, 3.23]$ Nm. The torque controller output is shown in Fig. 42 (bottom). It presented a RMS value of 1371.90 rpm, $\sigma \in [10.45, 223.80]$ Nm.

These measurements are analyzed comparatively in Section 5.2.3 after the cascade controller results are presented.

5.2.2 Cascade Admittance-Impedance Controller

The average knee joint position is shown in Fig. 43 (top). It can be noted that the admittance controller consistently generated a trajectory correction that resulted in a more damped reference trajectory for the robot to track, $\sigma \in [2.18, 2.57]$ deg. The knee trajectory presented a RMS error of 5.34 deg, maximum absolute error of 12.19 deg. Compared to the free trajectory, the measured one has a peak and RMS value 53.59% and 37.95% smaller, respectively. Partially, the reduction in the movement amplitude is due to the outer-loop admittance controller, which creates a trajectory reference that is summed to the desired trajectory (dotted line), generating a new reference with smaller amplitude to be tracked (dashed line). The new reference has a peak and RMS value of 34.44% and 19.55% smaller than the free one, respectively. Regarding how well the robot tracked the corrected desired trajectory, the measured one has a peak and RMS value 29.21% and 22.87% smaller, respectively, results similar to the ones obtained for the impedance controller, since it was a matter of position tracking.

The average interaction torque between the subjects and the robot is show in Fig. 43 (center); it presented a RMS value of 3.06 Nm, $\sigma \in [2.46, 4.27]$ Nm. The torque controller output is shown in Fig. 43 (bottom); it presented a RMS value of 671.60 rpm, $\sigma \in [10.89, 112.71]$ rpm.

5.2.3 Cascade and Impedance Controllers Comparison

By comparing the interaction torque in Fig. 42 (center) and 43 (center), it can be noted that the cascade controller resulted in a RMS interaction torque about 28.84% smaller. The cascade controller, however, showed slight greater variation: the difference between maximum and minimum standard deviation values is 21.48% greater. The smaller interaction torque is due to the amplitude of the movement. The impedance controller drives the subject's limbs towards a wider trajectory, generating wider ranges of motion, thus greater interaction torques. However, the cascade controller constrains more the subject's movements, resulting in greater variations in the interaction torque measurements, demanding more of the torque controller due to greater variation of the $\tau_{\mathbf{int}}$ component of the error signal.

Regarding the control signal, when the impedance controller, Fig. 42 (bottom), is compared with the cascade controller, Fig. 43 (bottom), it can be noted that its RMS value was reduced about half its value, being 51.05% smaller. This is explained by the reduction of the amplitude of the trajectory being tracked. The cascade controller must track a trajectory whose RMS value is about half the impedance one, i.e., 53.59% smaller. This will generate a smaller reference torque component, $\tau_{\mathbf{r}}$, compared to the one regarding the impedance controller alone, resulting in a smaller torque error input into the torque controller, demanding less from the controller itself and the actuator.

Figure 43 – Cascade controller. (Top) Average knee position. (Center) Average interaction torque between the user and the robot. (Bottom) Average torque controller output.

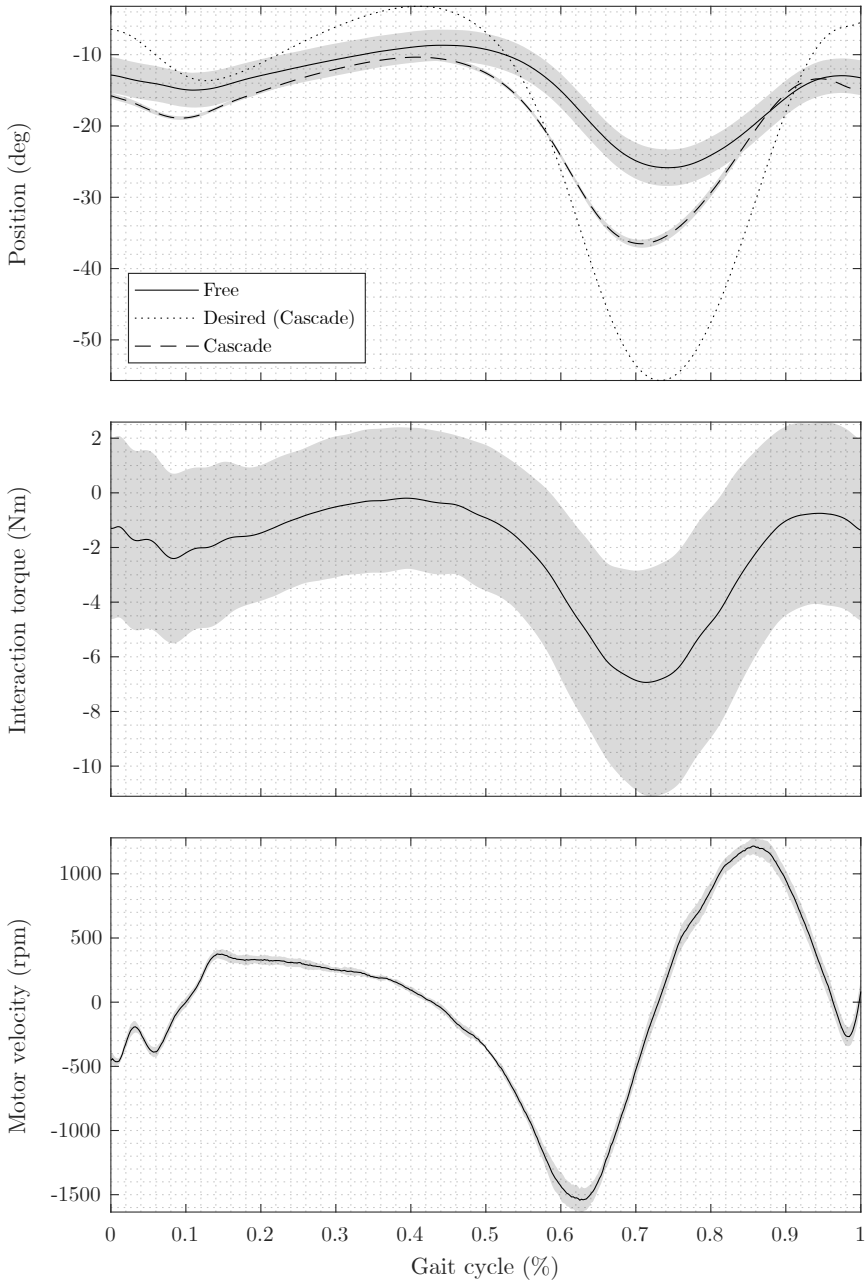

Source: Author (2021).

Figure 44 shows the average knee position error for the cascade (dash-dotted line) and the impedance (solid line) controllers. In general, both controllers showed similar errors with respect to their reference trajectories. Naturally, the trajectory to be tracked affected the error; in the case of the cascade controller, the desired trajectory was smaller; thus, the magnitude of the errors were smaller as well. However, when the position generated by each controller are compared with their respective desired trajectory, the final measured trajectory RMS value is 27.04% smaller for the impedance controller and 22.87% for the

Figure 44 – Comparison between the average knee joint error of a walk under the cascade and impedance controllers.

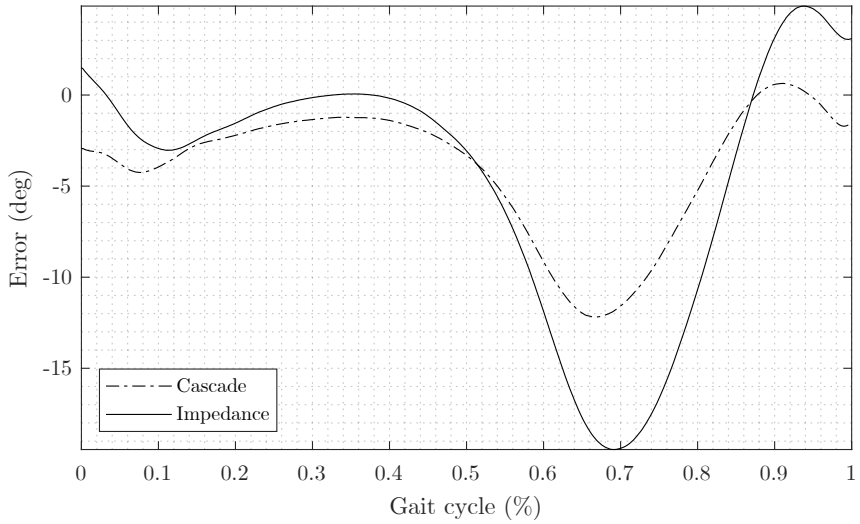

Source: Author (2021).

cascade. The controllers trajectory tracking performance is similar. This was expected, since both controllers share the same trajectory tracking controller gains, i.e., the impedance controller ones.

5.2.4 Transparency Controller

The average knee joint position is shown in Fig. 45 (top). Because the robot was in zero impedance mode, the knee joint was free and the knee trajectory of the robot, as well as the subject, presented great variance, both in amplitude and step length. In order to plot the average knee trajectory, the data were pre-processed. For each subject, the trajectory peaks were identified according to a set of expected characteristics: the minimum distance between two consecutive peaks was set to 200 samples, or 1 second, and the minimum peak height was set to the mean value of the overall trajectory of the knee, with additional 12.5% tolerance in relation to this value. The data were sliced, generating arrays of varying length, one per step. These arrays were resampled using a native MATLAB® function, called `resample`. The resample function essentially calls the `upfdir` function, which uses a polyphase interpolation structure and performs three steps: it upsamples the signal, inserting zeros; applies a finite impulse response (FIR) antialiasing filter, which works as a lowpass filter; and finally it discards samples to downsample the filtered signal. The resample parameter `n` determines the length of the FIR filter. This parameter was set to 5 in order to obtain a smoother signal. Additionally, in order prevent the ripples at the edges, a one-dimensional median filter of order 10 is applied, also by means of another native MATLAB® function, `medfilt1`. To achieve smooth edges, the padding argument of the function is set to `truncate`, so the noisy edges have their median computed, as they are approached. The first steps were excluded from the analysis, by removing samples until

the first peak with the desired characteristics was found. This procedure was repeated with the recorded knee trajectories of all subjects, and an average was taken, resulting in Fig. 45 (top).

The knee trajectory has a RMS value of 10.98 deg, with a standard variation within $\sigma \in [9.12, 14.27]$ deg, and a peak value of -16.24 ± 10.66 deg. The amplitude is considerably smaller, compared with the trajectory profile regarding the previous controllers, likewise the standard deviation shaded areas. Since the controller was not imposing a reference trajectory to be tracked, the subjects walked at their own pace on the treadmill, resulting in distinct trajectories; when the average is taken, due to differences in step length, swing and stance phase duration, and such, the average trajectory is flatter.

The average interaction torque between the subjects and the robot is show in Fig. 45 (center); it presented a RMS value of 1.01 Nm, $\sigma \in [0.31, 1.44]$ Nm. The torque controller output is shown in Fig. 43 (bottom); it presented a RMS value of 350.21 rpm, $\sigma \in [40.95, 533.52]$ rpm.

The transparency controller reveals more interesting insights when the answers given to the HQ by the users with respect to this controller are analyzed, as in the next section.

5.3 Questionnaires

5.3.1 Haptic Feedback Questionnaire (HFQ)

In summary, the HFQ has two questions: in the first question the subjects state if they agree that the robot (or the environment, by means of the robot) is resisting to their movement; in the second, they state if they agree that the robot is not resisting. A clear robot behavior is perceived if the user agrees with the first statement, and disagrees with the second, and vice versa. In terms of score, the higher the score, the greater the perceived robot resistance, as in Fig. 46. Since the second question is a negative sentence, its score was inverted before the analysis. In terms of score distribution, the greater the interquartile distances, the more spread the answers and, thus, the more divergent were the opinions regarding the robot behavior: some subjects felt it was resisting, some did not.

Since the impedance controller only delivers haptic assistance, it is expected that this controller presents the smallest score, i.e., 1–3. On the other hand, the cascade controller, by providing haptic assistance and feedback, is expected to present a higher score, but not the highest, because assistance still takes place, i.e., 3–5. With respect to the transparency controller, in theory, with ideal transparency, the score should be neutral, i.e., close to 3. The subjects are not told beforehand which controller they are going to experience, even though they were briefed about them. Figure 47 shows the boxplot with

Figure 45 – Transparency controller. (Top) Average knee position. (Center) Average interaction torque between the user and the robot. (Bottom) Average torque controller output.

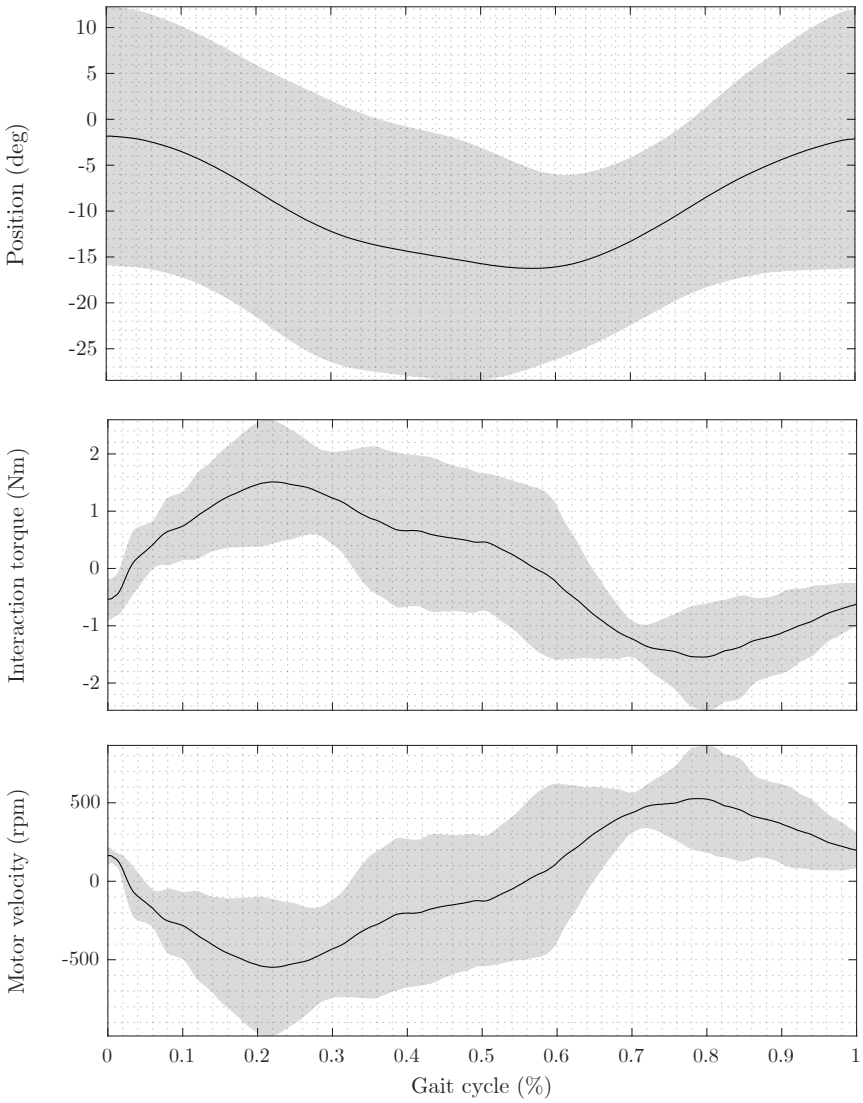

Source: Author (2021).

respect to each question. It can be seen that only the cascade controller hypothesis were verified in practice.

To verify statistically whether the subjects, in general, perceived the three controllers distinctly, paired T-test ($\alpha = 0.05$) were conducted. Regarding the first question, the impedance controller (3.1 ± 1.29) was paired with the answers given to the cascade controller (3.7 ± 1.06) and no significant difference on user perception was found ($p = 0.14$), likewise the impedance and transparency (3.2 ± 1.62) controllers ($p = 0.43$), and the cascade and transparency ones ($p = 0.11$). Regarding the second question of the HQ, the impedance controller (3.5 ± 1.18) was compared with the cascade controller (3.8 ± 1.32) and no significant difference on user perception was found ($p = 0.31$), likewise the

Figure 46 – Answers given to the HFQ. The closer to the right, the greater the perceived resistance from the perspective of the subjects.

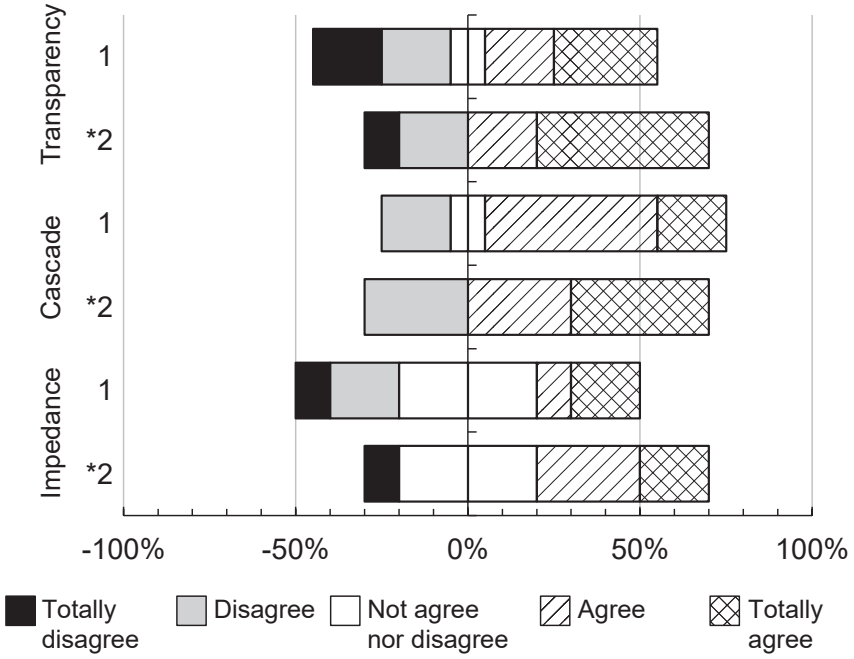

Source: Author (2021).

impedance and transparency (3.8 ± 1.55) controllers ($p = 0.30$), and the cascade and transparency ones ($p = 0.5$). The smallest p-value found were generally related to the cascade controller. Figure 47 shows the boxplot of the scores with respect to each HQ question, regarding each controller.

The HFQ answers are analyzed in the following order: impedance controller (shortened to IC); cascade controller (shortened to AC, in reference to its outer admittance loop); and transparency controller (TC). For each controller, and for each HFQ question, the subject's answers are given together with their free-form feedback, when available. This is important to understand the reasoning behind their answers and, thus, conclude whether, from a user perspective, the controller was being perceived according to the aforementioned expectations.

The controller order that each subject experienced is found in Appendix A, Table 8. The individual answers to each HFQ question by each subject is found in Appendix A, Table 9.

5.3.1.1 Impedance Controller

Regarding the impedance controller, which provided only haptic assistance, it can be seen that the answers for the first question diverged and most subjects reported mixed

Figure 47 – Boxplot of the answers given to the HFQ. The higher the score, the greater the perceived resistance from the subjects' perspective. The larger the interquartile distances, the more divergent the subjects' opinions were.

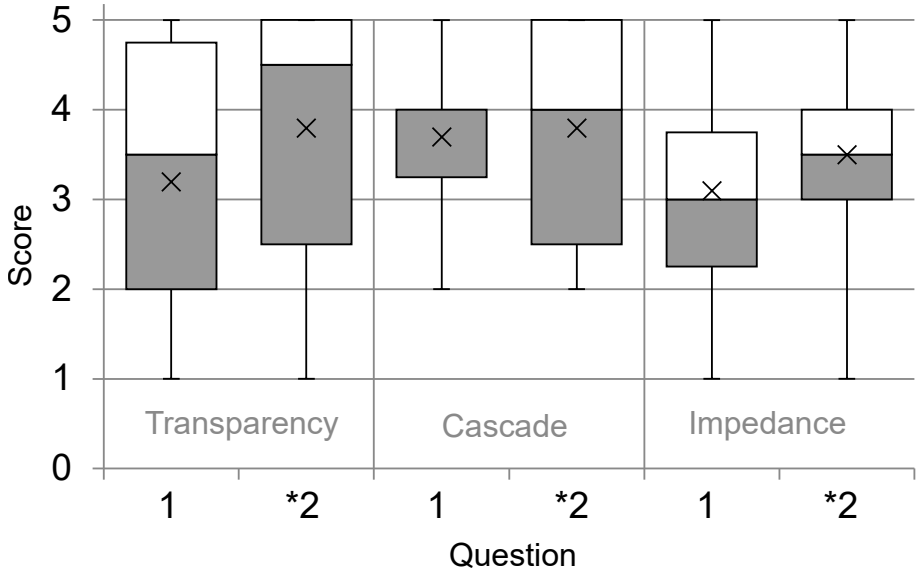

Source: Author (2021).

feelings. This is noted both in Fig. 46, where the spectrum is centered around zero, and in Fig. 47, where the median is exactly 3 and the mean slightly above it. With respect to the second question, most subjects could not agree that robot resistance was absent, which resulted in a slight offset to the right in Fig. 46, and in a mean score and median of 3.5 in Fig. 47.

In general, the reason behind this ambiguity is due the moments of lack of synchronization between robot and subject. All subjects stated that the robot was resisting to their movement when they were out of synchrony with it; but, if the robot was in synchrony, the perception of resistance was diminished. Here, the lack of synchrony is caused by the hard-coded desired trajectory that the robot follows. Regardless of the gait of the user, the robot imposes a trajectory, to which the healthy subject must adapt, until the two of them move at the same pace, and the assistance is in fact delivered.

For haptic assistance purposes while walking on a treadmill, to constrain the knee joint to a pre-recorded trajectory with high gains may not be the best approach to provide assistance and obtain a smoother walk. Though it may assist the user to perform the movement, it still offers some resistance. It has been noted in previous studies that healthy subjects, when subjected to constant high-gain impedance controllers, tend to anticipate the movement and get out of synchrony with the robotic device, which as a consequence deteriorates user performance inside VR (BERNARDONI *et al.*, 2019). Adaptive or real-time computed optimal impedance gains are an alternative to handle this issue (SANTOS; SIQUEIRA, 2019).

5.3.1.2 Cascade Controller

Regarding the cascade controller, which provided both haptic feedback and assistance, there seems to be an agreement about the perception of the controller among the subjects, which can be noted by an offset to the right in the answers to both questions, as in Fig. 46, and in an answer distribution closer to 4 in Fig. 47. Most subjects agreed that the robot was offering resistance to their movements. The synchrony issue described for the impedance controller was also perceived in this case, however with less intensity.

In overall, there seemed to be a greater agreement on the behavior of the robot in this case. And, even though more resistance was felt, the subjects stated that the robot was in general more comfortable, mainly because they could synchronize and adapt better to the robot movements.

5.3.1.3 Transparency controller

With respect to the transparency controller, which simply followed the user movements based on feedback signals, not providing any sort of haptic feedback or assistance, there were, again, distinct opinions, likewise the impedance controller. In general, most subjects stated that some sort of resistance was being placed by the robot deliberately, which can be seen by an offset to the right for the answers given to both questions in Fig. 46, and a mean and median of 3.2 and 3.5, respectively, as in Fig. 47. Most subjects also could not agree that there was no resistance, which can be seen by a mean and median of 3.8 and 4.5, respectively, in the same figure. The transparency controller presented the greatest median values, i.e., it was the controller mostly perceived as resisting, while it was not.

Compared with the other controllers, there seemed to be a greater agreement between the first and second statements in the case of the transparency controller, i.e., subjects who agreed with the first statement disagreed with the second and those who disagreed with the first, agreed with the second. Though it may not be clear to the user the role that the robot plays in this case, the behavior of the robot was not conditional or ambiguous, as with the impedance controller due to the moments of lack of synchrony and the fact that the robot was imposing a pre-recorded desired trajectory.

In general, even though no resistance was being deliberately applied to the subject's movement, many subjects felt some resistance, because the transparency of the robot could only be achieved to a certain extent. The subjects, in this case, had to dictate the movement to be done by the robot, which responded by means of a feedback controller, based on zero-torque reference. Because the robot responded only through feedback signals, there was some delay between the robot action and the user movement, which generated the interaction force, considered as a disturbance in the inner torque control loop of the impedance control scheme. Until the robot could address this error and drive it to zero,

Figure 48 – Answers given to the MSSQ. The closer to the right, the more often motion sickness was felt in these situations.

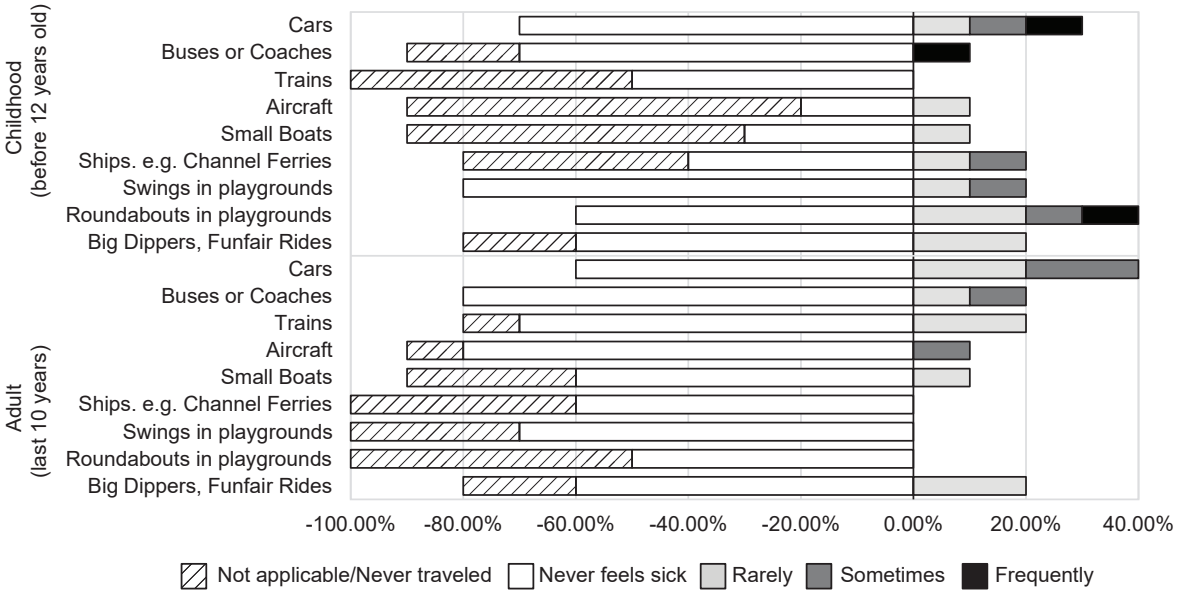

Source: Author (2021).

the subject felt the robot inertia.

A feedforward compensation may be able to enhance transparency, in this case, as it would improve the robot response to the human disturbance. In that sense, the lack of any compensation may function, to a certain degree, as a haptic feedback opposite to the subject's movements.

5.3.2 Motion Sickness Susceptibility Questionnaire (MSSQ)

Figure 48 shows the percentage score with respect to each MT regarding the experiences that happened during the childhood (C) of the subjects, i.e., before 12 years old, and during the adult phase (A), i.e., during their last ten years. The score regarding each MT for childhood (C) and adult phase (A) are given by Table 3.

The subjects presented a mean score as a child of 4.89 ± 8.20, maximum score of 20.57, showed by S9 (S7 also presented an elevated score of 19.8, the second highest one). Subjects presented a mean score of 1.96 ± 2.51 as an adult, maximum score of 6.43, also showed by S9, as well as by S7. The overall score was 6.85 ± 10.60. The maximum score was 27.00, presented by S9. The second highest total score was shown by S7, who scored 26.23.

With respect to the background questions of the subjects, all were undergraduate or graduate students. Most of them were only conducting their studies. S6 and S9 were also working in the industry, respectively as embedded software developer and R&D developer. No subject reported to possess pre-existing medical conditions which could make them

Table 3 – Total score regarding each MT for childhood (C) and adult phase (A).

	Not applicable/ Never traveled	Never feels sick	Rarely feels sick	Sometimes feels sick	Frequently feels sick
Cars (C)	–	7	1	1	1
Buses or Coaches (C)	2	7	–	–	1
Trains (C)	5	5	–	–	–
Aircraft (C)	7	2	1	–	–
Small Boats (C)	6	3	1	–	–
Ships. e.g., Channel Ferries (C)	4	4	1	1	–
Swings in playgrounds (C)	–	8	1	1	–
Roundabouts in playgrounds (C)	–	6	2	1	1
Big Dippers, Funfair Rides (C)	2	6	2	–	–
Cars (A)	–	6	2	2	–
Buses or Coaches (A)	–	8	1	1	–
Trains (A)	1	7	2	–	–
Aircraft (A)	1	8	–	1	–
Small Boats (A)	3	6	1	–	–
Ships. e.g., Channel Ferries (A)	4	6	–	–	–
Swings in playgrounds (A)	3	7	–	–	–
Roundabouts in playgrounds (A)	5	5	–	–	–
Big Dippers, Funfair Rides (A)	2	6	2	–	–

Source: Author (2021).

more prone to feel motion sickness. Most subjects exercised, except S1, S6 and S10. Among the ones who exercised, 2 stated that performed mostly resistance exercises (S2 and S9), 3 stated that performed mostly aerobic exercises (S4, S5 and S8), and S3 and S7 stated that performed both types of exercises. One subject possessed a pre-existing medical condition that affects physical performance. However the subject stated that the experiments would not aggravate the condition.

With respect to their self perception about MS susceptibility, all subjects stated that they did not find themselves prone to feel motion sickness, except S7 and S9, who defined themselves as strongly prone to feel it, i.e., they marked the highest option in the scale provided.

The MSSQ score of each subject is shown in Fig. 49, along with their SSQ score (explained further). Subjects who did not score in the MSSQ and SSQ (S1, S4 and S8) were suppressed.

According to Fig. 49, in general, the scores of most subjects were lower than the average scores presented by Golding (2006), with exception of S7 and S9. It was common as well that subjects scored nothing, e.g., S1, S2, S4, S8. This means that these subjects were considerably less prone to MS during the VR experience, which was later confirmed

Figure 49 – MSSQ score compared against the SSQ score.

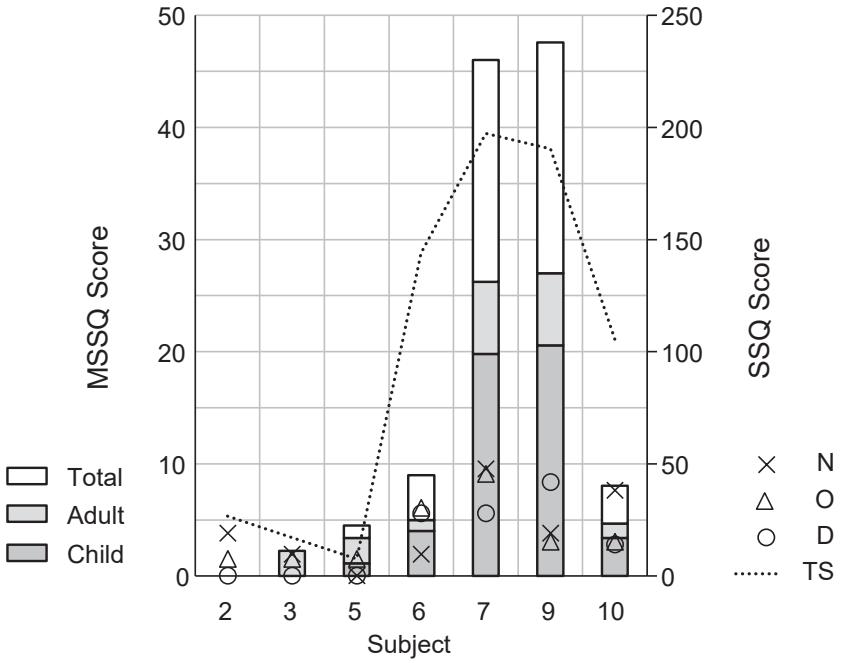

Source: Author (2021).

Table 4 – Matrix of Pearson coefficients among questionnaire scores. Despite the diagonal, darker colors denote greater coefficients, in a heat map fashion.

	MSSQ	GVRFQ	SSQ	PQ
MSSQ	1	-	-	-
GVRFQ	-0.193	1	-	-
SSQ	0.878	-0.041	1	-
PQ	-0.391	-0.294	-0.552	1

Source: Author (2021).

and stated in Section 5.3.4. Nonetheless, all subjects who scored low did not feel relevant side effects after the experience. Two subjects, S6, whose score was particularly low, and S7, whose score was high and, as anticipated, was prone to feel MS, reported to feel strong side effects symptoms associated with the experience. Particularly, the side effects felt by S6 were likely caused by the absence of eyeglasses during the experiment. S7 reported a slight dizziness throughout the day, after the experiments in the morning, which, however, disappeared in the next day. The symptoms were probably caused based on the lack of familiarity with gaming and VR stated by this subject. S9, though presented the highest total score, did not report to feel side effects after the experience, like S6, probably due to the familiarity with gaming reported by the subject.

Nonetheless, it is noticeable that the score was still significantly low and showed great variance. A reason to this may be the geographic, cultural and temporal differences

between the sample used by Golding (2006) and the sample used in this work. However, the greatest impact must have been due to the sample size. Golding (2006) validated the short-form of his questionnaire by collecting answers from 257 university students. The long-form of his questionnaire, which places identical questions as the short-form, but in a more extended version, was applied to two samples: a first sample of 147 university students; and a second sample of 101 patients undergoing chemotherapy. Henriques *et al.* (2014) performed a study on school children and applied the same questionnaire with a sample of 851 children. Besides that, their questionnaire was also adjusted: some modes of transportation were changed, when compared with the ones proposed by Golding (2006) originally.

The present work has a sample significantly smaller than the ones used by the previous authors. As expected, the sample of this work cannot be as large as the samples utilized by the aforementioned studies, since the intent of the present work is focused on the evaluation of the multisensory feedback interface for rehabilitation purposes, not on the study of the susceptibility to MS of a population. Therefore, it is difficult to confirm whether the questionnaire presented by Golding (2006) is suitable to identify and diagnose individuals prone to MS while performing exercises in VR, since it was purposed mainly to study the MS of large samples that represented a specific population under analysis, e.g., school children, people undergoing medical treatment, elderly, whereas here it is employed to study each person, individually. Still, the MSSQ, together with the other questionnaires worked more as a way of anticipating people with high probability of feeling sick after the experience, than studying the susceptibility of a population. In this study, the questionnaire alone would have failed in identifying the reasons behind the sickness and other side effects felt after the experience. Here, the causes of the reported side effects could be mostly identified based on an analysis of each individual, which was possible due to the small size of the sample and protocol, rather than by analyzing the subject's MSSQ score only.

5.3.3 Gaming and Virtual Reality Familiarity Questionnaire (GVRFQ)

90% of the subjects had already had experiences with non-VR gaming; 10% had not (S7). With respect to non-VR gaming frequency, answers are summarized in Fig. 50. Many stated that only played video games while they were younger or reported that played rarely. When no recent experience was available, they stated the gaming frequency based on past experiences. Only S5 reported familiarity with VR (three hours per week). No familiarity with the VR equipment used in the experiment was reported. Regarding the platforms utilized by the subjects, 45% were used to PC games, followed by video game consoles (20%) and mobile games (20%). These accounted for 85% of all reported platforms.

Figure 50 – Hours spent per week by each subject. The black horizontal line denotes the mean (8.5 h).

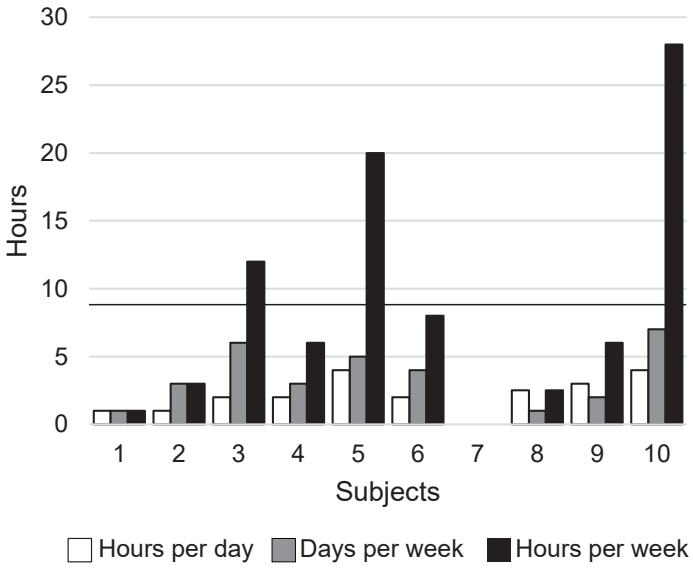

Source: Author (2021).

Figure 50 shows the hours played per day, days per week and total hours per week by each subject. S3, who reported to be recently involved with games in general, except for VR, stated disappointment with respect to the screen resolution of the HMD. According to S3, one could be able to see the pixels of the screen, which was frustrating. S10, who was the most involved with non-VR games, also stated disappointment with respect to the graphics of the VR experience. These statements suggest that VR is still something inaccessible to most people, and those interested in it set high expectations with regards to the technical quality of the experience.

As anticipated in Section 5.3.2, and later elaborated in Section 5.3.4, S7, the only one who reported to not possess familiarity with gaming, presented the second highest MSSQ score, the highest SSQ score, and was the only subject who reported to feel slight dizziness side effects throughout the day a few hours after the experiment.

5.3.4 Simulator Sickness Questionnaire (SSQ)

Table 5 shows the intensity of the reported symptoms by to each subject. The overall score for each group of symptom is observed in Table 6. Figure 51 summarizes the symptoms reported in Table 5. According to Fig. 51, the most reported symptoms were fatigue (31.8%), sweating (22.7%), followed by difficulty concentrating (9.1%) and stomach awareness (9.1%), which sum up to 72.2% of the reported symptoms. All other reported symptoms accounted for 4.5% each of them. Some symptoms were not reported at all, as can be noted in Table 5, e.g., headache, eyestrain, fullness of head, blurred vision and burping.

Table 5 – Symptoms reported by each subject and their severity (blank, not-reported symptom; the symptoms could be reported based on a 3-point severity: 1, slight; 2, moderate; 3, severe).

	Subject									
	1	2	3	4	5	6	7	8	9	10
General discomfort	–	–	–	–	–	–	1	–	–	–
Fatigue	–	1	1	–	1	2	3	–	1	2
Headache	–	–	–	–	–	–	–	–	–	–
Eyestrain	–	–	–	–	–	–	–	–	–	–
Difficulty focusing	–	–	–	–	–	2	–	–	–	–
Increased salivation	–	–	–	–	–	–	–	–	–	1
Sweating	–	2	1	–	–	1	1	–	–	2
Nausea	–	–	–	–	–	–	–	–	1	–
Difficulty concentrating	–	–	–	–	–	–	2	–	1	–
Fullness of head	–	–	–	–	–	–	–	–	–	–
Blurred vision	–	–	–	–	–	–	–	–	–	–
Dizzy (eyes open or closed)	–	–	–	–	–	–	1	–	–	–
Vertigo	–	–	–	–	–	–	–	–	2	–
Stomach awareness	–	–	–	–	–	–	1	–	–	1
Burping	–	–	–	–	–	–	–	–	–	–

Source: Author (2021).

According to Table 6, it can be noted that the scores were significantly low and showed great variance among subjects. At the end of the test, the subjects were asked why they picked those symptoms to describe what they felt. Regarding fatigue and sweat, all subjects clarified that the exercising, i.e., walking on the treadmill for about 10 minutes carrying partially the weight of the robotic exoskeleton, made them feel these symptoms, not the VR experience. Kennedy *et al.* (1993) states that the sort of fatigue and sweat, to which the symptoms made reference, regarded to the oculomotor system and nausea-related symptoms. The subjects clarified that they did not feel the sweetness and fatigue like when they feel sick or nauseated, but strictly due to exercise. Likewise, the subjects who reported to feel difficulty concentrating explained that the symptom was caused due to the stimuli from the VE, and not because they felt nauseated or MS-related symptoms. The stomach awareness reported by some subjects also was not related to MS: subjects explained that the belt used to attach the exoskeleton to their torsos was slightly too tight, and it was upsetting their bellies, not their stomachs per se.

Despite sweat and fatigue symptoms, S6 stated that there was difficulty focusing, because the subject chose to undergo the tests without wearing glasses, and later clarified that this was the main reason why the difficulty focusing was felt.

Table 6 – Subject's scores with respect to each group of symptom (N, O, D) and the total severity score (TS).

Subject	n	o	d	N	O	D	TS
1	0	0	0	0	0	0	0
2	2	1	0	19.08	7.58	0	26.66
3	1	1	0	9.54	7.58	0	17.12
4	0	0	0	0	0	0	0
5	0	1	0	0.00	7.58	0	7.58
6	1	4	2	9.54	30.32	27.84	143.98
7	5	6	2	47.70	45.48	27.84	197.30
8	0	0	0	0	0	0	0
9	2	2	3	19.08	15.16	41.76	190.42
10	4	2	1	38.16	15.16	13.92	105.38
			Mean	13.88	12.40	10.12	64.14
			σ	16.17	14.09	15.36	79.45

Source: Author (2021).

Besides these four symptoms, whose occurrence could be explained, the other reported symptoms, e.g., dizzy (S7), increased salivation (S10), general discomfort (S7), vertigo (S9) and nausea (S9), were reported only once by the aforementioned subjects, some of whom (S7 and S9) presented the highest MSSQ scores. It is safe to admit, with respect to the age group that composed the sample, that the setup is safe and not prone to upset the subject's bodies with severe MS and related side effects. However, the subjects may feel some effects due to the exercise (treadmill walking with the exoskeleton) with

Figure 51 – Symptoms occurrence among subjects.

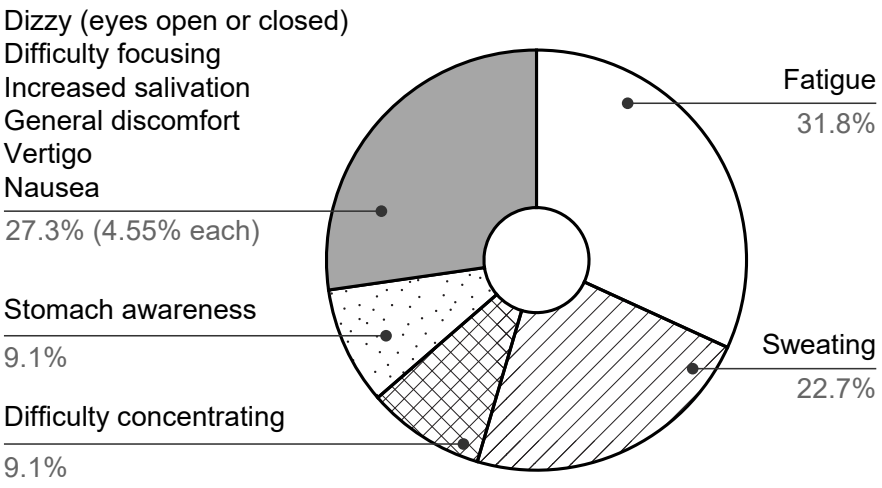

Source: Author (2021).

Figure 52 – Summary of answers given to the PQ.

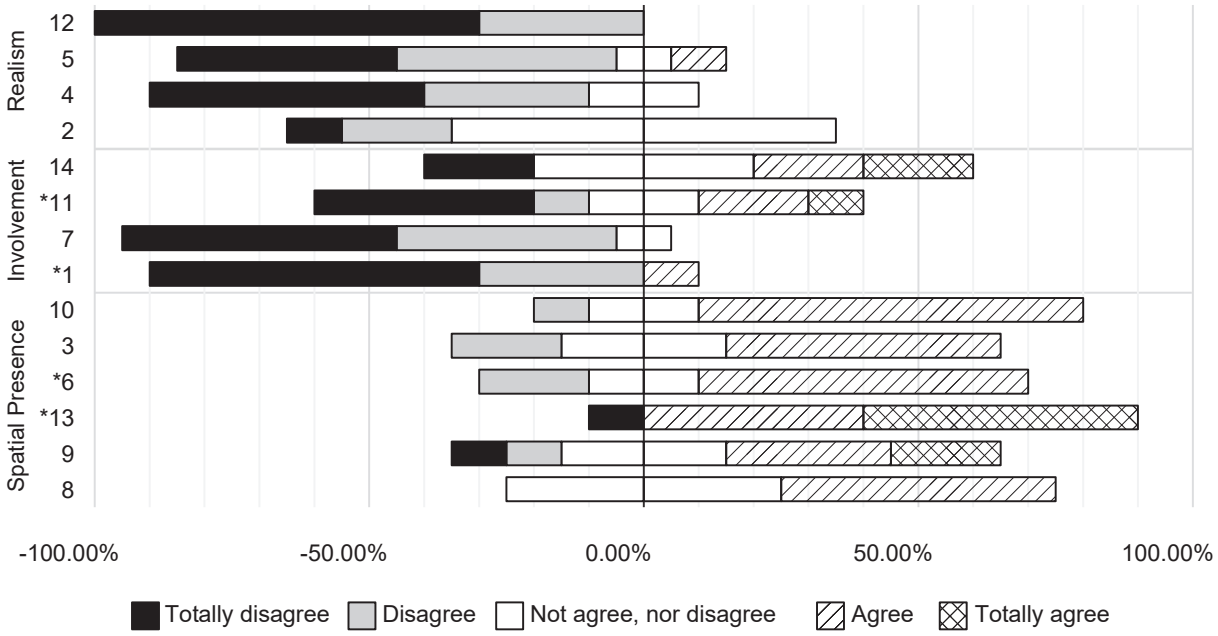

Source: Author (2021).

more intensity than VR side effects.

5.3.5 Presence Questionnaire (PQ)

Figure 52 shows the answers, in percentage, given to the presence questionnaire. Questions 3, *6, 8, 9, 10 and *13 and 10 measure the spatial presence felt by the users; questions *1, 7, *11 and 14 measure their degree of involvement; questions 2, 4, 5 and 12 measure the realness of the experience. The asterisk (*) denotes that the user felt more present the more they disagreed with the proposed statement, so their answers needed to be inverted for the analysis.

Figure 52 suggests that the subjects felt a strong feeling of spatial presence during the experience in the VE; that the subjects had mixed feelings with respect to the involvement aspect of the feeling of presence; and that the subjects were convinced that the experience was not as realistic as corresponding experiences in the real world.

The strong feeling of spatial presence is possibly due to the immersive VR experience, i.e., the VE involved most of the FOV of the subjects. The fact that the subject's lower limbs were being tracked also contributed to this feeling, as there is a well-known relation between embodiment and the feeling of spatial presence (TOET *et al.*, 2020).

Regarding the involvement of the subjects, there seems to be an agreement for question *1, 7 and 14, whose answers tended mostly to one side of the spectrum only. In question *11, "I still paid attention to the real environment", though there is no common ground to the answers, most subjects stated that there were a few moments of distraction

and full immersion, but they were constantly reminded of the physical space where they were, i.e., there were many moments of break-in-presence (BIP).

Here, however, the BIP was somewhat desirable, in order to ensure user comfort and safety. First, the subjects were constantly sharing their impressions and being warned about what they were going to experience next. For instance, they were told when to pose still, in order to calibrate the robot, as well as when the treadmill was going to be turned on and off. The author, who conducted the tests, was also asking whether there was some discomfort, in order to ensure the well-being of the subjects. Conversely, they were answering and also providing feedback during the experiment, as if the contact with someone outside, under control of the situation, ensured them more safety. Naturally, this communication prevented the users from using the earplugs during the experiment, so the auditory feedback, which was plainly background sounds, was neglected by the subjects voluntarily.

Second, another reason why the bond with the physical world had to be maintained is related with the fact that the subjects were walking on a treadmill and, in order to prevent stepping out of the treadmill belt limits, they asked deliberately that the HMD camera was enabled, so that they could see their physical feet position during the experiment. The subjects also held firmly to the treadmill handrails, sometimes only the left one, sometimes both, whereas in VR their hands were free, floating in the VE, and not being tracked, due to the lack of tracking devices to track all limbs. To hold onto the treadmill handrails also may have contributed to constantly remind the subjects about the physical world surrounding them.

Therefore, it was expected that the answers for these questions yielded a low degree of involvement. In that sense, one way of improving the configuration to score better at these questions could be to develop an avatar for the person outside the VE (e.g., the supervisor, the person conducting the experiment), so that the communication can flow between his or her avatar and the subject's avatar, instead of between the person in the physical world and the subject in the VE. Rather than the avatar, a virtual window with the camera view of the person outside the VE could be placed as well, as if the avatar of the subject was using augmented reality glasses that could project into the avatar's FOV a computer window depicting someone's camera.

Moreover, to track all limbs and the torso may help to enhance this involvement, or presence in general, since full embodiment is proven to deliver a stronger feeling of presence.

Finally, some subjects stated that they felt more comfortable when they could see and hear the robot and its actuator, because they then knew the moment the robot was going to drive their limbs, and they wanted to grasp this information so that they could synchronize with the robot movement. Again, the lack of synchrony between the subject

and the robot hampered the experience and prevented it from being conducted seamlessly inside VR.

With respect to the questions regarding the realness of the experience, it is observed much hesitation in the answers given to question 2, whereas the answers given to questions 4, 5 and 12 seem much more definite. These questions evaluate to which degree the virtual experience is considered about as realistic (or even more) to the correspondent experience in the physical world. The subjects stated that the most realistic feature was the virtual sky. The other elements in the scene, e.g., the birds, the ocean, the island and the sand, did not seem as realistic, but all subjects stated that, even though they lack realism, these features serve well as stimuli and distraction. Regarding the action taking place in the VE, S5 stated that the pace of the avatar did not match the pace on the treadmill: while on the treadmill the subject walked continuously, the avatar seemed to walk in steps, as if the avatar only walked forward during some time samples of the simulation. Unfortunately, the approach employed to estimate the linear velocity of the avatar may has caused this impression.

The IPQ places realism as an attribute strongly linked to the feeling of presence and studies show that an increase in the realism does cause an increase the feeling of presence (SLATER *et al.*, 2009; SLATER, 2009b; BERKMAN; AKAN, 2019; GISBERGEN *et al.*, 2019). However, the enhancement in realism performed between experiments is relative.

Slater *et al.* (2009) performed two experiments: in one scene, there were dynamic shadows generated by full real-time global-illumination (or ray-casting), as well as a virtual mirror, on which the subjects inside VR could see their own avatar (in this case, a cuboid humanoid avatar); the other scene was absent of these features and contained only static ray-casting. A total of 33 subjects were present: 17 underwent the experience in the first virtual scene, 16 in the second scene. It was noted that the first room, with more features, delivered a greater experienced realism, thus, feeling of presence. Nonetheless, both features mentioned as ways of increasing the realism are already present in the VE of this work and, notoriously, if they were absent, the realism of the experience would be even weaker.

A more recent study, with graphics that resemble commercial VR games, was performed by Hvass *et al.* (2017), with a sample of 50 individuals. In the study, it was noted as well that greater realism, in this case the rendering resolution of the VE and game objects, led to an increase in the experience realism as well. The study concludes this through a SUS questionnaire (some questions of the SUS questionnaire compose the IPQ used in this work), as well as the results of a specific questionnaire, intended to measure the fear felt by the subjects. The objective was to study the interplay among presence, fear and realism. They concluded that in some cases an enhance in the perceived realism does not lead to an increase in the feeling of presence. The reasons vary, but the most prominent one is the purpose of the application and the task being performed inside VR.

Gisbergen *et al.* (2019) studied the effect of realism on user experience and behaviour, with a sample of 72 participants, Bachelor's and Master's students from Breda University of Applied Science, and noticed that many variables exist that can interfere in the experience, in such way that the effects of realism are obliterated, so it is difficult to isolate the effects of the attributes that enhance realism. Furthermore, by increasing the realism of a single element, the experience is not necessarily enhanced by the same degree. There must be an overall increase of different elements in the scene in order to achieve greater experience realism, an approach employed by Hvass *et al.* (2017). Gisbergen *et al.* (2019) highlight as well that the user expectations influence the experience (e.g., their familiarity with gaming), along with the application performance (latency or delay), and the study concludes that it is not always necessary to invest more effort and costs to obtain greater visual realism.

In summary, though the subscales of spatial presence, involvement and realism are treated as separated features of the VR experience, there is an interplay among them. Therefore, it is expected, when the involvement or the realness is hampered, that the spatial feeling of presence during the experience is affected as well. Nonetheless, the spatial presence (as well as the other aspects) retain some independence from one another, which explains why there is still spatial presence, even though almost no realness was experienced.

6 CONCLUSIONS

Having in mind the worldwide increase in average life expectancy and world population, technology plays a fundamental role in order to improve the recovery of patients in need of physiotherapy. As a means of achieving this, rehabilitation robotics along with virtual reality (VR) have been extensively employed over the last decades.

The main objective of this work was to develop a setup capable of integrating the existing robotic devices at EESC-USP with VR. The robotic device chosen was the lower limbs exoskeleton ExoTao and the VR equipment consisted of the HTC Vive. A multisensory feedback system was designed, by employing the robot as a haptic interface and the VR equipment as the source of auditory and visual stimuli. The greatest challenge relied on the design of a controller architecture that would adapt the lower limbs exoskeleton to function as haptic interface device, at the same time it would be capable of delivering assistance to perform movements.

To accomplish these aforementioned objectives, a broad review on the role of VR in rehabilitation robotics, followed by a review on haptic feedback and ways to achieve it for the implementation of multisensory feedback systems was carried out. Further, details regarding the haptic feedback interface design were provided.

The haptic feedback was delivered by the lower limbs exoskeleton ExoTao, developed at EESC-USP. Though the exoskeleton was not designed primarily for haptic feedback purposes, it was expected that the control architecture was capable of compensating partially for eventual hardware deficiencies.

Impedance control was already utilized with the exoskeleton device, therefore it was the first approach utilized to adapt the robot to function as a haptic interface. The impedance controller handled the interactions with stiff environments but showed limitations when resistive environment forces were present, especially when coupled to the human. A control architecture based on an outer admittance controller loop followed by an inner impedance controller loop presented itself as an alternative to handle resistive environments and human disturbance. The proposed cascade controller comprises the impedance controller already employed with the exoskeleton, guaranteeing compliance and safety during human-robot interaction, alongside the soft joints of the robot; furthermore, it has the advantage of being capable of dealing with interaction forces arising from virtual resistive environments, as long as a desired trajectory is provided beforehand.

Both cascade and impedance control architectures presented the same performance with respect to trajectory tracking, since the impedance controller gains are the same for both. As mentioned, the cascade, however, was capable of dealing of highly resistive

environments. The performance of both architectures with respect to rigid environments has room for improvement.

Once the controllers of the haptic interface were designed, tuned and tested in the robot, tests with healthy human subjects were carried out. The tests intended to measure the robot performance with the human disturbance and, specially, the user experience under influence of the robotic device and the virtual environment.

Ten healthy subjects participated in the study. Before the tests were initiated, they answered two questionnaires, the MSSQ and the GVRFQ. The first questionnaire intended to measure their susceptibility to feel motion sickness during the experiment; the second, intended to measure their familiarity with gaming and VR. The tests were conducted three times; each time, the subjects walked approximately two minutes wearing the VR equipment and the lower limbs exoskeleton robotic device with a specific controller, assigned in a pseudo-random order. The controllers could deliver haptic assistance only (impedance controler), both haptic assistance and feedback (cascade controller) or simply follow the movement of the subjects (transparency controller). In between, the subjects rested and answered the HFQ. In the end of the experiment, the subjects answered two more questionnaires: the SSQ and the IPQ, which intended to assess the motion sickness-related side effects felt by the subjects after the virtual experience, as well as measure their feeling of presence, divided into three different aspects: spatial presence, involvement and realism.

Results suggest that the test protocol is safe, even for those who presented susceptibility of being affected by motion sickness. Gaming familiarity influenced the experience to a certain extent: subjects familiar with electronic games were most skeptical and critical about the experience, and those who were not familiar at all presented slight dizziness after the experience. Furthermore, most symptoms reported by the subjects in the SSQ were related to the exercising experience, rather than motion sickness side effects. Finally, the experience could deliver a strong feeling of spatial presence; the bond with the physical world was deliberately maintained by the subjects: this bond prevented them from stumbling and falling out of the treadmill limits, as well as observing the robot behavior to be more in synchrony with it. The bond was also crucial to keep constant contact with the subjects and to collect free-form feedback from them. In general, this decision enhanced their comfort and safety, at the same time the involvement aspect of the feeling of presence deteriorated. Finally, the general experience lacked realism, from the point of view of the users. However, not always a more realistic representation of virtual objects leads to a stronger feeling of experienced realism and, thus, presence. The overall protocol must be reviewed in order to address these issues.

6.1 Study limitations and future works

The task chosen for this work presented itself as much more complex when VR was inserted in the tests. The fact that the users felt much more comfortable and safe while they could still see the treadmill and the robot attached to their legs was not considered and most users decided to keep paying attention to the physical world, since there was the risk of stumbling or falling out of the treadmill limits, as well as not being able to synchronize with the robot movement, once the device could not be either seen or listened.

The cascade controller architecture ensured motion tracking performance as the impedance controller, with the advantage of it being able to handle interaction with resistive environments. However, the stability analysis must be carried out, in order to ensure the range of environment and interaction forces it can handle safely.

Though it was a complex task, most individuals did not suffered from motion sickness symptoms, even those who were prone to feel it. The time exposure to VR was short. A longer treadmill walking session with just one controller can ellicit better if the experience is safe for longer periods of exposure and exercises.

In general, the MSSQ and SSQ questionnaires could not account for the particularities of this experience. Most users could not relate to the experiences and modes of transportation in the MSSQ. If the MSSQ is applied to future tests, it is suggested that the modes of transportation are changed so that people can identify better experiences in which they suffered from motion sickness, along with daily life situations. For example, elevators, reading and checking your phone in the transportation, escalators, all these modes of transportation and situations could be added. Regarding the SSQ, most subjects misunderstood the motion sickness-related symptoms with what they were feeling due to the exercising nature of the task. The author decided not to intervene while the users answered to the questions. However, perhaps the exercising side effects stood out to the point that the subject could not ignore them and decided to report them, even though they were not related to motion sickness.

The IPQ was suitable, even though in the end, to understand the perception of the haptic feedback, a new short haptic questionnaire was proposed and applied in between tests.

The tests performed here highlighted that many aspects must still be improved, before the subjects can feel truly immersed inside the virtual environment (VE) while walking. First, the link with the physical environment shall be ceased. Second, the human-robot synchronization problem shall be addressed, if the impedance and cascade control architectures are used as haptic interfaces. Third, the realism of the experience must be enhanced, i.e., the VE should accommodate features that are more visually appealing, without overwhelming the user with too many stimuli. To address the first problem, if a

wider body tracking system is implemented, a more accurate position of the subject in the real world can be transmitted to the VE; once this is achieved, a virtual representation of the treadmill limits can be implemented, so that the users can guide themselves without the need of keeping monitoring their own position in the real world through the real-world window inside VR. The second problem can be approached by different means: a new control architecture, based only in adaptive force controller gains, can be used to achieve different robot behaviors according to different environment characteristics; in that sense, the robot compensation can vary, so that less compensation is perceived as a greater resistance to the subject's movement, and more compensation is perceived as less resistance, i.e., more transparency.

In summary, to impose a desired trajectory to a healthy subject augments the lack of synchronization, which hampers the experience. However, motor-impaired people may benefit more from controllers that provides a reference trajectory to their joints. These subjects, though, would only be able to walk safely in the current setup and let the robot drive their legs to the desired position if a structure that could sustain the subject's body weight existed. This is a requirement because the motor-impaired subjects, even when assisted, may not be able to contend against the treadmill speed. In fact, with the tests performed with healthy subjects already, some stated that 1 km/h was still too fast for the cascade and transparency controllers to provide a convincing feedback response.

REFERENCES

ALBU-SCHAFFER, A.; OTT, C.; FRESE, U.; HIRZINGER, G. Cartesian impedance control of redundant robots: recent results with the dlr-light-weight-arms. *In*: **2003 IEEE International Conference on Robotics and Automation (Cat. No.03CH37422)**. [*S.l.: s.n.*], 2003. v. 3, p. 3704–3709 vol.3.

AYAD, S.; AYAD, M.; MEGUENI, A.; SCHIOLER, H.; LOTTE, N.; STRUIJK, A. Unity3d based control method for a robotic ground walking platform in a virtual reality environment. *In*: . [*S.l.: s.n.*], 2018. p. 1236–1241.

AZMANDIAN, M.; HANCOCK, M.; BENKO, H.; OFEK, E.; WILSON, A. Haptic retargeting: Dynamic repurposing of passive haptics for enhanced virtual reality experiences. *In*: . [*S.l.: s.n.*], 2016. p. 1968–1979.

BALACHANDRAN, R.; KOZLOVA, N.; OTT, C.; ALBU-SCHäEFFER, A. Non-linear local force feedback control for haptic interfaces. **IFAC-PapersOnLine**, v. 51, p. 486–492, 01 2018.

BARTYś, M.; HRYNIEWICKI, B. The trade-off between the controller effort and control quality on example of an electro-pneumatic final control element. **Actuators**, v. 8, p. 23, 03 2019.

BENNETT, D. R.; BLACKBURN, J. T.; BOLING, M. C.; MCGRATH, M.; WALUSZ, H.; PADUA, D. A. The relationship between anterior tibial shear force during a jump landing task and quadriceps and hamstring strength. **Clinical Biomechanics**, v. 23, n. 9, p. 1165–1171, 2008. ISSN 0268-0033. Available at: <https://www.sciencedirect.com/science/article/pii/S0268003308001988>.

BERKMAN, M. I.; AKAN, E. Presence and immersion in virtual reality. *In*: _____. **Encyclopedia of Computer Graphics and Games**. Cham: Springer International Publishing, 2019. p. 1–10. ISBN 978-3-319-08234-9. Available at: <https://doi.org/10.1007/978-3-319-08234-9_162-1>.

BERNARDONI, F.; ÖZEN, Ö.; BUETLER, K.; MARCHAL-CRESPO, L. Virtual reality environments and haptic strategies to enhance implicit learning and motivation in robot-assisted training. *In*: **2019 IEEE 16th International Conference on Rehabilitation Robotics (ICORR)**. [*S.l.: s.n.*], 2019. p. 760–765. ISSN 1945-7898.

BOEING, A.; BRAUNL, T. Evaluation of real-time physics simulation systems. *In*: . [*S.l.: s.n.*], 2007. p. 281–288.

BURDEA, G. C.; COIFFET, P. **Virtual Reality Technology**. 2. ed. USA: John Wiley & Sons, Inc., 2003. ISBN 0471360899.

CALANCA, A.; MURADORE, R.; FIORINI, P. A review of algorithms for compliant control of stiff and fixed-compliance robots. **IEEE/ASME Transactions on Mechatronics**, v. 21, n. 2, p. 613–624, 04 2016. ISSN 1941-014X.

CARVALHO, M. R. d.; COSTA, R. T. d.; NARDI, A. E. Simulator Sickness Questionnaire: tradução e adaptação transcultural. **Jornal Brasileiro de Psiquiatria**, scielo, v. 60, p. 247 – 252, 00 2011. ISSN 0047-2085. Available at: <http://www.scielo.br/scielo.php?script=sci_arttext&pid=S0047-20852011000400003&nrm=iso>.

CLOVER, C. L. A control-system architecture for robots used to simulate dynamic force and moment interaction between humans and virtual objects. **IEEE Transactions on Systems, Man, and Cybernetics, Part C (Applications and Reviews)**, v. 29, n. 4, p. 481–493, 11 1999. ISSN 1558-2442.

CLOVER, C. L.; LUECKE, G. R.; TROY, J. J.; MCNEELY, W. A. Dynamic simulation of virtual mechanisms with haptic feedback using industrial robotics equipment. *In*: **Proceedings of International Conference on Robotics and Automation**. [*S.l.: s.n.*], 1997. v. 1, p. 724–730 vol.1.

CRAIG, J. **Introduction to Robotics: Mechanics and Control**. Pearson, 2018. ISBN 9780133489798. Available at: <https://books.google.com.br/books?id=JblZuwAACAAJ>.

CROCETTA, T.; ARAúJO, L.; GUARNIERI, R.; MASSETTI, T.; FERREIRA, F.; ABREU, L.; MONTEIRO, C. Virtual reality software package for implementing motor learning and rehabilitation experiments. **Virtual Reality**, 09 2017.

EISAPOUR, M.; CAO, S.; DOMENICUCCI, L.; BOGER, J. Virtual reality exergames for people living with dementia based on exercise therapy best practices. **Proceedings of the Human Factors and Ergonomics Society Annual Meeting**, v. 62, n. 1, p. 528–532, 2018. Available at: <https://doi.org/10.1177/1541931218621120>.

FRISOLI, A.; BORELLI, L.; MONTAGNER, A.; MARCHESCHI, S.; PROCOPIO, C.; SALSEDO, F.; BERGAMASCO, M.; CARBONCINI, M. C.; TOLAINI, M.; ROSSI, B. Arm rehabilitation with a robotic exoskeleleton in virtual reality. *In*: **2007 IEEE 10th International Conference on Rehabilitation Robotics**. [*S.l.: s.n.*], 2007. p. 631–642.

FROST, R.; SKIDMORE, J.; SANTELLO, M.; ARTEMIADIS, P. Sensorimotor control of gait: a novel approach for the study of the interplay of visual and proprioceptive feedback. **Frontiers in Human Neuroscience**, v. 9, p. 14, 2015. ISSN 1662-5161. Available at: <https://www.frontiersin.org/article/10.3389/fnhum.2015.00014>.

GISBERGEN, M.; KOVACS, M.; CAMPOS, F.; HEEFT, M.; VUGTS, V. What we don't know. the effect of realism in virtual reality on experience and behaviour. *In*: _____. [*S.l.: s.n.*], 2019. p. 45–59. ISBN 978-3-030-06245-3.

GOLDING, J. F. Motion sickness susceptibility questionnaire revised and its relationship to other forms of sickness. **Brain Research Bulletin**, v. 47, n. 5, p. 507 – 516, 1998. ISSN 0361-9230. Available at: <http://www.sciencedirect.com/science/article/pii/S0361923098000914>.

GOLDING, J. F. Predicting individual differences in motion sickness susceptibility by questionnaire. **Personality and Individual Differences**, v. 41, n. 2, p. 237 – 248, 2006. ISSN 0191-8869. Available at: <http://www.sciencedirect.com/science/article/pii/S0191886906000602>.

HAMZEHEINEJAD, N. [DC] VR Simulation as a Motivator in Gait Rehabilitation. *In*: **2019 IEEE Conference on Virtual Reality and 3D User Interfaces (VR)**. [*S.l.: s.n.*], 2019. p. 1383–1384. ISSN 2642-5246.

HAMZEHEINEJAD, N.; STRAKA, S.; GALL, D.; WEILBACH, F.; LATOSCHIK, M. E. Immersive robot-assisted virtual reality therapy for neurologically-caused gait impairments. *In*: **2018 IEEE Conference on Virtual Reality and 3D User Interfaces (VR)**. [*S.l.: s.n.*], 2018. p. 565–566.

HENRIQUES, I. F.; OLIVEIRA, D. W. D. D.; OLIVEIRA-FERREIRA, F.; ANDRADE, P. M. Motion sickness prevalence in school children. **European journal of pediatrics**, Springer, v. 173, n. 11, p. 1473–1482, 2014.

HOBBS, B.; ARTEMIADIS, P. A review of robot-assisted lower-limb stroke therapy: Unexplored paths and future directions in gait rehabilitation. **Frontiers in Neurorobotics**, v. 14, p. 19, 2020. ISSN 1662-5218.

HOCOMA. **Lokomat®**. 2020. Retrieved May, 2020. Available at: <https://www.hocoma.com/de/losungen/lokomat/>.

HOGAN, N. Impedance Control: An Approach to Manipulation: Parts I, II and III. **Journal of Dynamic Systems, Measurement, and Control**, v. 107, n. 1, p. 1–24, 03 1985. ISSN 0022-0434. Available at: <https://%doi.org/10.1115/1.3140701>.

HTC CORPORATION. **HTC Vive User Guide**. 2016. HTC Corporation Website.

HVASS, J.; LARSEN, O.; VENDELBO, K.; NILSSON, N.; NORDAHL, R.; SERAFIN, S. Visual realism and presence in a virtual reality game. *In*: **2017 3DTV Conference: The True Vision - Capture, Transmission and Display of 3D Video (3DTV-CON)**. [*S.l.: s.n.*], 2017. p. 1–4.

JERALD, J. **The VR Book: Human-Centered Design for Virtual Reality**. 1st. ed. New York, NY: Association for Computing Machinery and Morgan; Claypool, 2016.

KENNEDY, R. S.; LANE, N. E.; BERBAUM, K. S.; LILIENTHAL, M. G. Simulator sickness questionnaire: An enhanced method for quantifying simulator sickness. **The International Journal of Aviation Psychology**, Taylor & Francis, v. 3, n. 3, p. 203–220, 1993. Available at: <https://doi.org/10.1207/s15327108ijap0303_3>.

KERN, F.; WINTER, C.; GALL, D.; KäTHNER, I.; PAULI, P.; LATOSCHIK, M. E. Immersive virtual reality and gamification within procedurally generated environments to increase motivation during gait rehabilitation. *In*: **2019 IEEE Conference on Virtual Reality and 3D User Interfaces (VR)**. [*S.l.: s.n.*], 2019. p. 500–509. ISSN 2642-5246.

KIRTLEY. **CGA Normative Gait Database**. 2006. Hong Kong Polytechnic University, Available at: http://www.clinicalgaitanalysis.com/.

KOLANKIEWICZ, A. C. B.; DOMENICO, E. B. L. D.; LOPES, L. F. D.; MAGNAGO, T. S. B. d. S. Portuguese validation of the Symptom Inventory of the M.D. Anderson Cancer Center. **Revista da Escola de Enfermagem da USP**, scielo, v. 48, p. 999 – 1005, 12 2014. ISSN 0080-6234. Available at: <http://www.scielo.br/scielo.php?script=sci_arttext&pid=S0080-62342014000600999&nrm=iso>.

KONG, K.; MOON, H.; JEON, D.; TOMIZUKA, M. Control of an exoskeleton for realization of aquatic therapy effects. **IEEE/ASME Transactions on Mechatronics**, v. 15, n. 2, p. 191–200, 2010.

KUKA AG. **Healthcare**. 2020. Retrieved May, 2020. Available at: <https://www.kuka.com/de-de/branchen/healthcare>.

LEWIS, F.; DAWSON, D.; ABDALLAH, C. **Robot Manipulator Control: Theory and Practice**. [*S.l.: s.n.*]: CRC Press, 2003. (Automation and Control Engineering). ISBN 9780203026953.

LUECKE, G.; CHAI, Y.-H. Haptic interaction using a puma560 and the isu force reflecting exoskeleton system. *In*: . [*S.l.: s.n.*], 1997. p. 106 – 111 vol.1. ISBN 0-7803-3612-7.

LUECKE, G. R.; EDWARDS, J. C. Virtual cooperating manipulators as a virtual reality haptic interface. *In*: **Proceedings Third Annual Symposium on Human Interaction with Complex Systems. HICS'96**. [*S.l.: s.n.*], 1996. p. 133–140.

LYNCH, K.; PARK, F. **Modern Robotics: Mechanics, Planning, and Control**. [*S.l.: s.n.*]: Cambridge Univeristy Press, 2017. ISBN 978-1107156302.

MARCHAL-CRESPO, L.; BAUMANN, T.; IMOBERSTEG, M.; MAASSEN, S.; RIENER, R. Experimental evaluation of a mixed controller that amplifies spatial errors and reduces timing errors. **Frontiers in Robotics and AI**, v. 4, p. 19, 06 2017.

MARTELLI, D.; XIA, B.; PRADO, A.; AGRAWAL, S. Gait adaptations during overground walking and multidirectional oscillations of the visual field in a virtual reality headset. **Gait & Posture**, v. 67, 10 2018.

MATSANGIDOU, M.; ANG, C. S.; MAUGER, A.; INTARASIRISAWAT, J.; OTKHMEZURI, B.; AVRAAMIDES, M. Is your virtual self as sensational as your real? virtual reality: The effect of body consciousness on the experience of exercise sensations. **Psychology of Sport and Exercise**, v. 41, p. 218–224, 03 2019.

MERRIAM-WEBSTER. **Definition of Virtual Reality**. 2020. Retrieved March, 2020. Available at: <https://www.merriam-webster.com/dictionary/virtual\%20reality>.

MICROSOFT. **Get started with Mixed Reality**. 2019. Microsoft Mixed Reality Documentation. Available at: <https://docs.microsoft.com/en-us/windows/mixed-reality/>.

MILGRAM, P.; KISHINO, F. A taxonomy of mixed reality visual displays. **IEICE Trans. Information Systems**, vol. E77-D, no. 12, p. 1321–1329, 12 1994.

MOGUILLANSKY, C. V.; O'REGAN, J.; PETITMENGIN, C. Exploring the subjective experience of the "rubber hand" illusion. **Frontiers in Human Neuroscience**, v. 7, p. 659, 2013. ISSN 1662-5161. Available at: <https://www.frontiersin.org/article/10.3389/fnhum.2013.00659>.

MORI, M.; MACDORMAN, K. F.; KAGEKI, N. The uncanny valley [from the field]. **IEEE Robotics Automation Magazine**, v. 19, n. 2, p. 98–100, 2012.

NIESEN, M. R.; LUECKE, G. R. Virtual dynamic prototyping for operator interface design. *In*: **8th IEEE International Workshop on Robot and Human Interaction. RO-MAN '99 (Cat. No.99TH8483)**. [*S.l.: s.n.*], 1999. p. 357–361.

NVIDIA. **Rigid Body Dynamics: NVIDIA PhysX SDK**. 2019. NVIDIA PhysX SDK Documentation. Available at: <https://documentation.help/NVIDIA-PhysX-SDK-Guide/RigidDynamics.html>.

ORGANIZATION, W. H. **World report on disability**. 2011. World Health Organization Website. Retrieved March, 2021. Available at: <https://www.who.int/disabilities/world_report/2011/en/>.

OSTAN, I.; SIQUEIRA, A. A. G. Incorporação de membros inferiores através do algoritmo ccd para prática de terapia física com realidade virtual. *In*: **IV Simpósio do Programa e Pós-Graduação em Engenharia Mecânica da EESC-USP**. São Carlos, SP: [*S.l.: s.n.*], 2019. ISSN 2674-8452.

OSTAN, I.; SIQUEIRA, A. A. G. Motion capture of a lower limbs exoskeleton for virtual reality application with a treadmill. *In*: **25th International Congress of Mechanical Engineering**. [*S.l.: s.n.*], 2019.

OTT, C.; ALBU-SCHAFFER, A.; KUGI, A.; HIRZINGER, G. On the passivity-based impedance control of flexible joint robots. **IEEE Transactions on Robotics**, v. 24, n. 2, p. 416–429, 2008.

OTT, C.; MUKHERJEE, R.; NAKAMURA, Y. Unified impedance and admittance control. *In*: **2010 IEEE International Conference on Robotics and Automation**. [*S.l.: s.n.*], 2010. p. 554–561. ISSN 1050-4729.

OTT, C.; NAKAMURA, Y. Base force/torque sensing for position based cartesian impedance control. *In*: **2009 IEEE/RSJ International Conference on Intelligent Robots and Systems**. [*S.l.: s.n.*], 2009. p. 3244–3250.

PARISI, T. **Learning Virtual Reality: Developing Immersive Experiences and Applications for Desktop, Web, and Mobile**. Sebastopol, CA: O'Reilly Media, 2015. ISBN 9781491922828.

PARK, D.; CHANG, J.; CHENG, H.; ASHSIDDIQUE, M.; HAUK, B. M. O.; YU, H. Development and evaluation of a novel passive wrist bilateral rehabilitation device paired with virtual reality: A feasibility study. *In*: **2019 IEEE 16th International Conference on Rehabilitation Robotics (ICORR)**. [*S.l.: s.n.*], 2019. p. 282–287. ISSN 1945-7898.

PARK, H.; CHAE, S. H.; YOON, J. W.; KIM, J.; SUDDUTH, A.; STANLEY, C. Implementing overground turning on a linear treadmill. *In*: **2015 12th International Conference on Ubiquitous Robots and Ambient Intelligence (URAI)**. [*S.l.: s.n.*], 2015. p. 390–391.

PEREZ-MARCOS, D. Virtual reality experiences, embodiment, videogames and their dimensions in neurorehabilitation. **Journal of NeuroEngineering and Rehabilitation**, v. 15, 12 2018.

PIGGOTT, L.; WAGNER, S.; ZIAT, M. Haptic neurorehabilitation and virtual reality for upper limb paralysis: A review. **Critical Reviews in Biomedical Engineering**, v. 44, 01 2016.

PONS, J. L. **Wearable Robots: Biomechatronic Exoskeletons**. 1st edition. ed. West Sussex: John Wiley & Sons, 2008.

RILEY, P. O.; PAOLINI, G.; Della Croce, U.; PAYLO, K. W.; KERRIGAN, D. C. A kinematic and kinetic comparison of overground and treadmill walking in healthy subjects. **Gait & Posture**, v. 26, n. 1, p. 17–24, 2007. ISSN 0966-6362. Available at: <https://www.sciencedirect.com/science/article/pii/S0966636206001457>.

SALISBURY, K.; CONTI, F.; BARBAGLI, F. Haptic rendering: introductory concepts. **IEEE Computer Graphics and Applications**, v. 24, n. 2, p. 24–32, 2004.

SANTOS, W. M. dos; CAURIN, G. A.; SIQUEIRA, A. A. Design and control of an active knee orthosis driven by a rotary series elastic actuator. **Control Engineering Practice**, v. 58, p. 307–318, 2017. ISSN 0967-0661. Available at: <https://www.sciencedirect.com/science/article/pii/S0967066115300198>.

SANTOS, W. M. dos; NOGUEIRA, S. L.; OLIVEIRA, G. C. de; PEñA, G. G.; SIQUEIRA, A. A. G. Design and evaluation of a modular lower limb exoskeleton for rehabilitation. *In*: **2017 International Conference on Rehabilitation Robotics (ICORR)**. [*S.l.: s.n.*], 2017. p. 447–451. ISSN 1945-7901.

SANTOS, W. M. dos; SIQUEIRA, A. A. Impedance control of a rotary series elastic actuator for knee rehabilitation. **IFAC Proceedings Volumes**, v. 47, n. 3, p. 4801 – 4806, 2014. ISSN 1474-6670. 19th IFAC World Congress. Available at: <http://www.sciencedirect.com/science/article/pii/S1474667016423578>.

SANTOS, W. M. dos; SIQUEIRA, A. A. Optimal impedance via model predictive control for robot-aided rehabilitation. **Control Engineering Practice**, v. 93, p. 104177, 2019. ISSN 0967-0661. Available at: <http://www.sciencedirect.com/science/article/pii/S0967066119301674>.

SCHUBERT, T.; FRIEDMANN, F.; REGENBRECHT, H. The experience of presence: Factor analytic insights. **Presence**, v. 10, p. 266–281, 06 2001.

SCHULZE, J. P. **Protein Data Bank Visualization**. 2006. Retrieved May, 2020. Available at: <https://www.nsf.gov/news/mmg/mmg_disp.jsp?med_id=62893>.

SCHWIND, V.; KNIERIM, P.; HAAS, N.; HENZE, N. Using presence questionnaires in virtual reality. *In*: . [*S.l.: s.n.*], 2019.

SICILIANO, B.; KHATIB, O. **Springer Handbook of Robotics**. 1st edition. ed. [*S.l.: s.n.*]: Springer-Verlag Berlin Heidelberg, 2008. 1611 p.

SKIDMORE, J.; BARKAN, A.; ARTEMIADIS, P. Variable stiffness treadmill (vst): System development, characterization, and preliminary experiments. **IEEE/ASME Transactions on Mechatronics**, v. 20, n. 4, p. 1717–1724, 2015.

SLATER, M. Place illusion and plausibility can lead to realistic behaviour in immersive virtual environments. **Philosophical transactions of the Royal Society of London. Series B, Biological sciences**, v. 364, p. 3549–57, 12 2009.

SLATER, M. Place illusion and plausibility can lead to realistic behaviour in immersive virtual environments. **Philosophical transactions of the Royal Society of London. Series B, Biological sciences**, v. 364, n. 1535, p. 3549–3557, 2009.

SLATER, M.; KHANNA, P.; MORTENSEN, J.; YU, I. Visual realism enhances realistic response in an immersive virtual environment. **IEEE Computer Graphics and Applications**, v. 29, n. 3, p. 76–84, 2009.

SLATER, M.; STEED, A. A virtual presence counter. **Presence**, v. 9, p. 413–434, 10 2000.

SLATER, M.; USOH, M.; STEED, A. Depth of presence in virtual environments. **Presence: Teleoper. Virtual Environ.**, MIT Press, Cambridge, MA, USA, v. 3, n. 2, p. 130–144, 01 1994. ISSN 1054-7460. Available at: <https://doi.org/10.1162/pres.1994.3.2.130>.

SLATER, M.; WILBUR, S. A framework for immersive virtual environments five: Speculations on the role of presence in virtual environments. **Presence: Teleoper. Virtual Environ.**, MIT Press, Cambridge, MA, USA, v. 6, n. 6, p. 603–616, dez. 1997. ISSN 1054-7460. Available at: <https://doi.org/10.1162/pres.1997.6.6.603>.

STEUER, J. Defining virtual reality: Dimensions determining telepresence. **JOURNAL OF COMMUNICATION**, v. 42, p. 73–93, 1992.

SUN, Q.; KAUFMAN, A.; PATNEY, A.; WEI, L.-Y.; SHAPIRA, O.; LU, J.; ASENTE, P.; ZHU, S.; MCGUIRE, M.; LUEBKE, D. Towards virtual reality infinite walking: Dynamic saccadic redirection. **ACM Transactions on Graphics**, v. 37, p. 1–13, 07 2018.

SVEISTRUP, H. Motor rehabilitation using virtual reality. **Journal of neuroengineering and rehabilitation**, v. 1, p. 10, 01 2005.

TECHNOLOGIES, I. **WorksiteVR™ Quest**. 2020. Retrieved May, 2020. Available at: <https://www.immersivetechnologies.com/products/WorksiteVR.htm>.

TOET, A.; KULING, I. A.; KROM, B. N.; ERP, J. B. F. van. Toward enhanced teleoperation through embodiment. **Frontiers in Robotics and AI**, v. 7, p. 14, 2020. ISSN 2296-9144. Available at: <https://www.frontiersin.org/article/10.3389/frobt.2020.00014>.

UNITY TECHNOLOGIES. **Unite Berlin 2018 - An Introduction to CCD IK and How to use it**. 2018. Unity YouTube Channel. Available at: <https://www.youtube.com/watch?v=MA1nT9RAF3k>.

UNITY TECHNOLOGIES. **Game engines — how do they work?** 2019. Unity Documentation <https://unity3d.com/what-is-a-game-engine>.

VALVE CORPORATION. **STEAM Store**. 2020. Available at: <https://store.steampowered.com/>.

VASCONCELOS-RAPOSO, J.; BESSA, M.; MELO, M.; BARBOSA, L.; RODRIGUES, R.; TEIXEIRA, C. M.; CABRAL, L.; SOUSA, A. A. Adaptation and validation of the igroup presence questionnaire (ipq) in a portuguese sample. **Presence: Teleoperators and Virtual Environments**, v. 25, n. 3, p. 191–203, 2016. Available at: <https://doi.org/10.1162/PRES_a_00261>.

VILLAMIZAR, J. Y. M.; OSTAN, I.; ORTEGA, D. A. E.; SIQUEIRA, A. A. G. Remote control architecture for virtual reality application for ankle therapy. *In*: **XXVI Brazilian Congress on Biomedical Engineering, CBEB**. [*S.l.: s.n.*], 2020.

WANG, L. . T.; CHEN, C. C. A combined optimization method for solving the inverse kinematics problems of mechanical manipulators. **IEEE Transactions on Robotics and Automation**, v. 7, n. 4, p. 489–499, 08 1991.

WEISS, P. L.; KESHNER, E. A.; LEVIN, M. F. Virtual reality for physical and motor rehabilitation. *In*: . [*S.l.: s.n.*], 2014.

WENK, N.; Penalver-Andres, J.; Palma, R.; Buetler, K. A.; Müri, R.; Nef, T.; Marchal-Crespo, L. Reaching in several realities: Motor and cognitive benefits of different visualization technologies. *In*: **2019 IEEE 16th International Conference on Rehabilitation Robotics (ICORR)**. [*S.l.: s.n.*], 2019. p. 1037–1042. ISSN 1945-7898.

WITMER, B. G.; SINGER, M. J. Measuring presence in virtual environments: A presence questionnaire. **Presence: Teleoper. Virtual Environ.**, MIT Press, Cambridge, MA, USA, v. 7, n. 3, p. 225–240, 06 1998. ISSN 1054-7460. Available at: <https://doi.org/10.1162/105474698565686>.

WÜRZBURG, J.-M.-U. **iLAST: Immersive Leg Coordination and Strength Therapy**. 2018. Retrieved May, 2020. Available at: <https://emlab.hci.uni-wuerzburg.de/>.

YATES, A. **Advanced Integration of VR in Physical Therapy**. 2020. Neuro Rehab VR Website. Retrieved June, 2021. Available at: <https://www.neurorehabvr.com/blog/advanced-vr-into-physical-therapy>.

ZELTZER, D. Autonomy, interaction, and presence. **Presence: Teleoperators and Virtual Environments**, v. 1, n. 1, p. 127–132, 1992.

APPENDIX

APPENDIX A – COMPLEMENTARY DATA

Table 7 – Subject's age, mass, height and sex.

Subject	Age (years)	Mass (kg)	Height (cm)	Sex
1	34	70	173	M
2	35	66	177	F
3	26	93	182	M
4	30	80	177	M
5	22	74	174	M
6	23	62	175	M
7	21	79	175	M
8	25	51	153	F
9	22	75	183	M
10	23	110	173	M
$\bar{x} \pm \sigma$	26.10 ± 5.13	76.00 ± 16.44	174.20 ± 8.22	8 M, 2 F

Source: Author (2021).

Table 8 – Controllers order assigned to each subject.

Subject	Controller #1	Controller #2	Controller #3
1	Transparent	Impedance	Cascade
2	Impedance	Cascade	Transparent
3	Cascade	Impedance	Transparent
4	Transparent	Cascade	Impedance
5	Transparent	Cascade	Impedance
6	Cascade	Impedance	Transparent
7	Impedance	Transparent	Cascade
8	Impedance	Cascade	Transparent
9	Cascade	Transparent	Impedance
10	Cascade	Impedance	Transparent

Source: Author (2021).

Table 9 – Haptic feedback questionnaire answers by each subject.

Subject	1 (TC)	*2(TC)	1 (AC)	*2(AC)	1 (IC)	*2 (IC)
1	5	5	5	5	1	3
2	1	2	2	2	3	4
3	4	4	4	4	5	1
4	1	1	3	2	3	3
5	3	2	5	5	3	3
6	5	5	4	5	3	3
7	5	5	4	4	5	5
8	2	4	2	4	2	4
9	2	5	4	5	2	5
10	4	5	4	2	4	4

Source: Author (2021).

Table 10 – Discarded steps of each subject for the tests with the impedance and cascade controllers.

Subject	Cascade	Impedance
1	1, 2	1, 2, 3, 4
2	1, 2, 3, 4, 5, 6	1, 2
3	1, 2, 3, 4	1, 2
4	1, 2, 3, 4	1, 2, 3
5	1, 2, 3, 4, 5, 6, 7, 8	1, 2, 3, 4
6	1, 2, 3	1, 2, 3, 50, 51
7	1, 2, 3	1 to 12
8	1, 2, 3, 31 to 51	1, 2, 3, 32 to 51
9	1, 2	1, 2, 3, 4, 5, 6
10	1, 2, 3, 4	1, 2, 21, 22, 30, 31, 37, 39, 50, 51

Source: Author (2021).

APPENDIX B – MOTION SICKNESS SUSCEPTIBILITY QUESTIONNAIRE (PORTUGUESE TRANSLATION)

Questionário de Suscetibilidade à Cinetose

1. Preencha com sua idade (anos):_____

2. * Preencha com seu peso (kg): _____

3. * Preencha com sua altura (m):_____

4. Preencha com seu sexo: *Marque apenas uma opção*

   ☐ Feminino

   ☐ Masculino

   ☐ Prefiro não declarar

   ☐ Outro:_____

5. Preencha com sua atual ocupação/profissão:_____

6. Você se considera propenso a sentir enjoo de movimento (cinetose)? *Marque apenas uma opção*

   ☐ Não

   ☐ Um pouco

   ☐ Moderadamente

   ☐ Bastante

7. * Você possui alguma condição médica que lhe torna mais suscetível à cinetose? *Marque apenas uma opção*

   ☐ Sim

   ☐ Não

   ☐ Prefiro não revelar

8. * Você se exercita com frequência? (pelo menos duas vezes por semana) *Marque apenas uma opção*

   ☐ Sim, geralmente exercícios aeróbicos

   ☐ Sim, geralmente exercícios de resistência

   ☐ Não

   * Você se enquadra em alguma situação das seguintes descrições: possuo condição médica pré-existente que afeta meu desempenho físico; possui condição psicológica/psiquiátrica pré-existente que afeta meu desempenho físico e/ou cognitivo; estou grávida; sinto-me doente, fatigado, sob efeito de alguma droga ou indisposto fisicamente; possuo histórico de epilepsia; possuo marca-passo ou algum implante eletrônico? *Marque apenas uma opção*

   ☐ Sim

   ☐ Não

Este questionário busca mensurar a suscetibilidade à cinetose e quais são suas principais causas. Aqui, enjoo significa sentir-se com náuseas ou de fato haver vomitado. Para cada meio de transporte ou entretenimento abaixo, preencha. Caso não tenha utilizado algum meio, marque a primeira coluna (Nunca utilizei). Apenas marque as seguintes colunas caso tenha utilizado.

9. Quando criança (até 12 anos), com que frequência você se sentiu nauseado ou enjoado nos meios abaixo? *Marque apenas um círculo por linha*

	Nunca utilizei	Nunca	Raramente	Às vezes	Frequentemente
Carros	○	○	○	○	○
Ônibus/Vans	○	○	○	○	○
Trens/Metrôs	○	○	○	○	○
Aviões	○	○	○	○	○
Barcos	○	○	○	○	○
Navios, barcas	○	○	○	○	○
Balanços	○	○	○	○	○
Gira-giras	○	○	○	○	○
Montanhas-russas	○	○	○	○	○
	t	0	1	2	3

10. Nos últimos 10 anos (aproximadamente), com que frequência você se sentiu nauseado ou enjoado nos meios abaixo? *Marque apenas um círculo por linha*

	Nunca utilizei	Nunca	Raramente	Às vezes	Frequentemente
Carros	○	○	○	○	○
Ônibus/Vans	○	○	○	○	○
Trens/Metrôs	○	○	○	○	○
Aviões	○	○	○	○	○
Barcos	○	○	○	○	○
Navios, barcas	○	○	○	○	○
Balanços	○	○	○	○	○
Gira-giras	○	○	○	○	○
Montanhas-russas	○	○	○	○	○
	t	0	1	2	3

APPENDIX C – GAMING AND VIRTUAL REALITY FAMILIARITY QUESTIONNAIRE (PORTUGUESE TRANSCRIPTION)

Questionário de Familiaridade com Jogos e Realidade Virtual

1. Você joga jogos (com exceção de jogos de realidade virtual)? *Marque apenas uma opção*

   ☐ Sim *(Ir para a questão 2)*

   ☐ Não *(Ir para a questão 5)*

2. Quantas horas por dia?_____

3. Quantas dias por semana?_____

4. Quais plataformas você utiliza? *Marque todas que se aplicam*

   ☐ PC

   ☐ Xbox 360/Xbox One/ Xbox One X

   ☐ Playstation 4/Playstation 5

   ☐ Wii/WiiU/Switch

   ☐ Dispositivos móveis (Celular, Nintendo DS/3DS, PSVita , i.e. outros consoles móveis)

   ☐ Outro (por favor especifique):_____

   Ir para questão 5

5. Você joga jogos de realidade virtual? *Marque apenas uma opção*

   ☐ Sim *(Ir para questão 6)*

   ☐ Não *(Fim do questionário)*

6. Quantas horas por dia?_____

7. Quantos dias por semana?_____

8. Quais plataformas você utiliza? *Marque todas que se aplicam*

   ☐ Playstation VR

   ☐ HTC Vive

   ☐ Oculus Rift

   ☐ Google Cardboard

   ☐ Samsung Gear VR

   ☐ Outro (por favor especifique):_____

APPENDIX D – SIMULATOR SICKNESS QUESTIONNAIRE (VALIDATED PORTUGUESE TRANSLATION)

Questionário de Cinetose em Simuladores

	(0) Nenhum	**(1) Leve**	**(2) Moderado**	**(3) Grave**
Mal-estar generalizado	○	○	○	○
Cansaço	○	○	○	○
Dor de cabeça	○	○	○	○
Vista cansada	○	○	○	○
Dificuldade em manter o foco	○	○	○	○
Aumento de salivação	○	○	○	○
Sudorese	○	○	○	○
Náusea	○	○	○	○
Dificuldade de concentração	○	○	○	○
“Cabeça pesada”	○	○	○	○
Vista embaçada	○	○	○	○
Tontura com olhos abertos ou fechados	○	○	○	○
Vertigem	○	○	○	○
Desconforto Abdominal	○	○	○	○
Arroto	○	○	○	○

APPENDIX E – IGROUP PRESENCE QUESTIONNAIRE (ENGLISH TRANSCRIPTION)

This questionnaire aims at evaluating the feeling of presence felt during the virtual reality experience after the experience is finished. For each of the following statements, please indicate how true it is for you, using their respective scales.

1. In the computer generated world I had a sense of "being there".

	1	2	3	4	5	
Not at all	○	○	○	○	○	Very much so

2. Somehow I felt that the virtual world surrounded me.

	1	2	3	4	5	
Fully disagree	○	○	○	○	○	Fully agree

3. I felt like I was just perceiving pictures.

	1	2	3	4	5	
Fully disagree	○	○	○	○	○	Fully agree

4. I did not feel present in the virtual space.

	1	2	3	4	5	
Did not feel	○	○	○	○	○	Felt present

5. I had a sense of acting in the virtual space, rather than operating something from outside.

	1	2	3	4	5	
Fully disagree	○	○	○	○	○	Fully agree

6. I felt present in the virtual space.

	1	2	3	4	5	
Fully disagree	○	○	○	○	○	Fully agree

7. How aware were you of the real world surrounding while navigating in the virtual world (e.g. sounds, room temperature, other people, etc.).

	1	2	3	4	5	
Extremely aware	○	○	○	○	○	Not aware at all

8. I was not aware of my real environment.

	1	2	3	4	5	
Fully disagree	○	○	○	○	○	Fully agree

9. I still paid attention of the real environment.

	1	2	3	4	5	
Fully disagree	○	○	○	○	○	Fully agree

10. I was completely captivated by the virtual world.

	1	2	3	4	5	
Fully disagree	○	○	○	○	○	Fully agree

11. How real did the virtual world seem to you?

	1	2	3	4	5	
Completely real	○	○	○	○	○	Not real at all

12. How much did your experience in the virtual environment seem consistent with your real world experience.

	1	2	3	4	5	
Not consistent	○	○	○	○	○	Very consistent

13. How real did the virtual world seem to you?

	1	2	3	4	5	
As real as an imagined world	○	○	○	○	○	Indistinguishable from reality

14. The virtual world seemed more realistic than the real world.

	1	2	3	4	5	
Fully disagree	○	○	○	○	○	Fully agree

APPENDIX F – HAPTIC FEEDBACK QUESTIONNAIRE (PORTUGUESE TRANSLATION)

Questionário sobre Feedback Háptico

Responda ao final de cada caminhada em relação à experiência com os respectivos controladores: (I) Impedância; (A) Cascata admitância-impedância; (T) Transparência.

1. (I) Eu senti que o ambiente/robô agia contra mim/meu movimento

	1	2	3	4	5	
Discordo Totalmente	○	○	○	○	○	Concordo Totalmente

2. (I) Eu não senti a resistência do ambiente/robô

	1	2	3	4	5	
Discordo Totalmente	○	○	○	○	○	Concordo Totalmente

3. (A) Eu senti que o ambiente/robô agia contra mim/meu movimento

	1	2	3	4	5	
Discordo Totalmente	○	○	○	○	○	Concordo Totalmente

4. (A) Eu não senti a resistência do ambiente/robô

	1	2	3	4	5	
Discordo Totalmente	○	○	○	○	○	Concordo Totalmente

5. (T) Eu senti que o ambiente/robô agia contra mim/meu movimento

	1	2	3	4	5	
Discordo Totalmente	○	○	○	○	○	Concordo Totalmente

6. (T) Eu não senti a resistência do ambiente/robô

	1	2	3	4	5	
Discordo Totalmente	○	○	○	○	○	Concordo Totalmente